Electronic Conduction and Noise in Strongly Correlated Systems

by

Cláudio de Carvalho Chamon

B.S. Aeronautics and Astronautics, MIT (1989)
M.S. Electrical Engineering and Computer Science, MIT (1991)

Submitted to the Department of Physics
in partial fulfillment of the requirements for the degree of

Doctor of Philosophy

at the

MASSACHUSETTS INSTITUTE OF TECHNOLOGY

June 1996

Author .....
Department of Physics
May 3, 1996

Certified by .....
Xiao-Gang Wen
Assistant Professor
Thesis Supervisor

Accepted by .....
George F. Koster
Chairman, Departmental Committee on Graduate Students

Electronic Conduction and Noise in Strongly Correlated Systems

by

Cláudio de Carvalho Chamon

B.S. Aeronautics and Astronautics, MIT (1989)

M.S. Electrical Engineering and Computer Science, MIT (1991)

Submitted to the Department of Physics
on May 3, 1996, in partial fulfillment of the
requirements for the degree of
Doctor of Philosophy

Abstract

This thesis presents a study of the tunneling current between chiral Luttinger liquids, which are physically realizable on the edges of fractional quantum Hall (FQH) states. The work focuses on both the tunneling conductance and the noise spectrum of the tunneling current, which can be used as probes of the strongly correlated chiral Luttinger liquid states.

The electron and quasiparticle propagators in chiral Luttinger liquids have anomalous exponents g, which are quantum numbers associated with the bulk FQH state. These anomalous exponents in the propagators are responsible for the characteristic nonlinear dependence of the tunneling current on the applied voltage and on the temperature. The tunneling current scales with the applied voltage as $I_t \propto V^{2g-1}$ at zero temperature, and the linear conductance σ scales with the temperature as $\sigma \propto T^{2(g-1)}$.

The noise spectrum of the tunneling current contains interesting features that come from the strongly correlated properties of chiral Luttinger liquids, such as fractional charge and statistics. In this thesis, a framework for the study of equilibrium and non-equilibrium noise in these systems is introduced. A Coulomb gas expansion of tunneling events on a Keldysh contour is developed. The charges tend to reorganize in a dipole gas, which provides a unified description of the low and high frequency noise: correlations between different dipoles define the structure of the noise near zero frequency, whereas correlations between the two charges within the dipole should contribute to the noise near the "Josephson" frequency $\omega_J = e^*V/\hbar$. This interpretation is justified using formal diagrammatic techniques, and, for integer g, exact answers for the form of the singularity in the equilibrium case are obtained.

For electron tunneling, an algebraic singularity at the electron frequency $\omega_J = eV/\hbar$ is present to all orders in perturbation theory. For quasiparticle tunneling, to lowest order in perturbation theory, the singularity is located at the frequency $\omega_J = e^*V/\hbar$. The two cases are related by a strong-weak coupling duality, so that one must find the mechanism through which the singularity moves from the quasiparticle frequency to the electron frequency. These matters are resolved in this thesis, where it is shown non-perturbatively for an exactly solvable case that the singularity at the quasiparticle frequency exists only in the limit of zero quasiparticle tunneling, whereas the electron singularity is present for all coupling. The structure near the quasiparticle frequency is no longer singular; the original singularity is smeared over a finite width controlled by the coupling strength. Finite quasiparticle tunneling destroys the perfectly quantized Hall conductance, so that this mechanism suggests that the quasiparticle singularity in the noise spectrum is destroyed concomitantly with the quantized conductance. The smearing of the quasiparticle singularity in the noise spectrum can be interpreted as the acquisition by the quasiparticle of a finite life-time.

Thesis Supervisor: Xiao-Gang Wen
Title: Assistant Professor

Acknowledgments

I believe that, regardless how much I try, I will not be able to write an acknowledgment that will make justice to my advisor Xiao-Gang Wen. Xiao-Gang is a model to be followed by the faculty of any institution. I feel very fortunate to have had him as my mentor during my doctorate, for many reasons.

I cannot remember a single time when Xiao-Gang would not receive me in his office. There were times when we would meet every day of the week, for several hours. These visits to his office were sources of great intellectual pleasure, and I will remember his office as the site of most delightful scientific conversations.

Xiao-Gang has oriented me well to be open-minded when approaching scientific problems. He inspired me not to focus on specific methodologies, but to develop creative solutions to each individual problem. He also motivated me to try to collaborate with other faculty members, from which I learned a great deal. I do appreciate the freedom and the flexibility he gave me, even when these outside collaborations took me away from his main research for some time.

Besides, his personality has made it very pleasant to interact with him. In addition to being an outstanding scientist and advisor, he is an excellent human being. He is modest, fair and polite. Many times I would feel more comfortable saying something wrong over a scientific discussion in front of my advisor than of a fellow student, for he would correct me in a way that would make me aware of the error, but not make me refrain from voicing further ideas out of fear of sounding ridiculous. This way, it was very comfortable for me to build confidence, and to learn that some of the best ideas can evolve from some of the worst.

Xiao-Gang unquestionably performed the role of mentor at its highest possible standards. I believe the greatest challenge in my scientific career will be, when mentoring my own students, to attempt to match what he has done for me.

Besides my advisor, I would also like to thank Mark Kastner and his group for giving me the opportunity to collaborate closely with them. I am fortunate, as a theoretician, to have been able to work with outstanding experimental physicists.

This collaboration was unquestionably of fundamental importance to my education. I am particularly thankful to Olivier Klein, whose friendship, acquired during this collaboration, was a great gift to me.

I also wish to thank those with whom I spent an enjoyable time working: Denise Freed, for her collaboration in several projects, as well as for her pleasant company; my present officemate and collaborator, Christopher Mudry, with whom I had endless conversations; Yong-Baek Kim, my previous officemate, whose company I enjoyed for four years. He demonstrated an honest concern and support on my search for a Postdoctoral position, which I appreciate very much.

I also have to thank Barton Zwiebach for his support when I switched from Engineering to Science. It would have been impossible to have done it without him. He explained that the difference between the two fields is that in Science there is less money, less jobs, and more competition, but that I should do what I loved most. He did not lie about the difference, and I do not regret a bit that I have changed.

Thanks for George Koster, for a miraculous phone call, letting me know that there was an opening for a TA position for my first year in the Physics Department. As I was originally admitted without funding, his offer was what made it possible for me to become a Scientist; this is a macroscopic example of a tunneling process.

I would like to thank my friend Marcos Fernandes, for only he can tell a ten year story.

Thanks to my parents, Nagib and Denise, for being always close to me, regardless of the physical distance separating us, and to my brothers, Jorge and Marcos, for bringing home closer to me.

Last, but not least, thanks to Flavia for understanding my madness, my irrationality, and my dreams, for coping with the difficult times and uncertainty about where we would be in the future, and finally, for just being there for me.

To Flavia

Contents

List of Figures

Chapter 1

Introduction

1.1 Background and Motivation

One of the many great successes of Physics this century is the application of Quantum Mechanics to the study of solids. The interest in the study of properties such as electrical and thermal conductance in metals gave birth to Solid State Physics. The importance of the underlying crystalline order in solids was understood, and then the study of the effects of the periodic potential due to the lattice structure on the electronic motion led to band structure theory. Knowing how the different electronic bands are occupied, one can identify whether a certain solid is a metal, an insulator, or a semiconductor. Applications of Solid State Physics came fast and far reaching, and, unquestionably, one can safely assert that its development is responsible for much of the technological progress in this century.

Together with the many answers provided by the theory of solids, many questions have also arisen. One of the deepest inquires has been on the effects of the interaction between electrons. The answers provided by band theory assumed independent or non-interacting electrons, *i.e.*, electrons only interact with the underlying periodic potential of the crystal lattice, but not among themselves. Still, the independent electron approximation seemed to give very good answers. The question was then how come the electronic interaction, which was not weak, could be neglected for most purposes.

A partial answer to the interacting electron problem came from the idea of screening; charge is redistributed so as to suppress the long range repulsion between two electrons. A better handle to the problem has come from Landau's theory of a Fermi Liquid, which takes as a starting point the free electron system: the spectrum of the interacting system flows adiabatically from the non-interacting system as the interaction strength is increased. Much has been construct over the seminal idea of Landau, and a great deal of progress has been made in terms of quantifying the Fermi liquid picture. Although Fermi liquid theory is 50 years old, it is still an open field, as a fully satisfying quantitative account of it has not yet been attained.

Maybe an even more interesting question than when Fermi liquid theory is applicable is when it is not. Several electronic systems present physical phenomena that cannot be understood in terms of the single particle behavior of non-interacting electrons. In this case, the underlying theory describing the interesting physics is in the strong coupling regime, and the physical properties are truly many body in nature. It is in this category, the so called non-Fermi liquids, that we find physical systems displaying striking properties such as superconductivity and the fractionally quantized Hall effect.

1.2 Luttinger liquids

Non-Fermi liquid behavior has been theoretically known to occur in one-dimensional (1D) systems, where the scattering processes due to the particle interactions destroy the Fermi singularity. The reduced dimensionality plays an essential role for non-Fermi liquid behavior. The ground state of the interacting system is a strongly correlated state. The description of the low energy excitations of the 1D system is termed Luttinger liquid, a concept introduced by Haldane [1] after the exactly solvable Luttinger model [2, 3].

The basis of the Luttinger liquid model is that the elementary excitation spectrum of interacting electrons can be described in terms of the elementary excitation spectrum of non-interacting bosons. In 1D it is possible to express both the kinetic energy

and the interaction energy of fermions as quadratic terms in the fermion density, and this is the reason why the model is exactly solvable through bosonization. Consider the case of spinless electrons. The electron operator can be written as a sum of left and right moving fermions:

$$\psi^\dagger(x) = e^{-ik_F x}\ \psi_L^\dagger(x)\ +\ e^{ik_F x}\ \psi_R^\dagger(x)\ , \tag{1.1}$$

where k_F is the Fermi momentum. The kinetic energy, or the free part of the Hamiltonian, can be written as

$$H_0 = \int dx\ v_F\ \left[\psi_L^\dagger i\partial_x\psi_L - \psi_R^\dagger i\partial_x\psi_R\right]\ . \tag{1.2}$$

One can study this model in terms of the density operators for right and left moving fermions

$$\rho_{R,L}(t,x) =: \psi_{R,L}^\dagger(t,x+\epsilon)\ \psi_{R,L}(t,x-\epsilon) :\ . \tag{1.3}$$

The definition above is a careful one, with the normal ordering and the introduction of point splitting. The densities satisfy the following (Kac-Moody) algebra:

$$\begin{aligned} [\rho_{R,L}(t,x)\ ,\ \rho_{R,L}(t,y)] &= \mp\frac{i}{2\pi}\delta'(x-y) \\ [\rho_R(t,x)\ ,\ \rho_L(t,y)] &= 0\ . \end{aligned} \tag{1.4}$$

The free part of the Hamiltonian can be rewritten in terms of the current operators as

$$H_0 = \pi v_F \int dx\ (\rho_L^2\ +\ \rho_R^2\ )\ , \tag{1.5}$$

which is quadratic in the currents. The electron operators can be also written in terms of the density operators as $\psi_{R,L} = \eta\ :\ e^{\pm i\phi_{R,L}}\ :$, where η is a cut-off dependent constant, and the fields $\phi_{R,L}$ are related to $\rho_{R,L}$ by $\rho_{R,L} = \frac{1}{2\pi}\partial_x\phi_{R,L}$. One can verify that the above definition is consistent with a charge 1 fermion, *i.e.*, that $[\rho_{R,L}(t,x)\ ,\ \Psi_{R,L}^\dagger(t,y)] = \Psi_{R,L}^\dagger(t,y)\delta(x-y)$. The correlation function for the bosonic

fields is obtained from the Hamiltonian and the commutation relations:

$$\langle \phi_{R,L}(t,x)\phi_{R,L}(0,0)\rangle = \ln(x \mp v_F t) \ , \tag{1.6}$$

and one can then calculate the correlations for the electron operators

$$\langle \psi_{R,L}(t,x)\psi_{R,L}(0,0)\rangle = (x \mp v_F t)^{-1} \ . \tag{1.7}$$

Adding an interaction is simple, since the Hamiltonian will remain quadratic in the densities. Consider, for example, a short range interaction $V(x) = \lambda\delta(x)$. The Hamiltonian becomes

$$H = \int dx \ \left[(\pi v_F + \lambda)\ (\rho_L^2 \ + \ \rho_R^2\ ) \ + 2\lambda\rho_L\ \rho_R\right] \ , \tag{1.8}$$

and can be diagonalized by the transformation

$$\tilde{\rho}_{R,L} = \cosh(\theta)\ \rho_{R,L} \ + \sinh(\theta)\ \rho_{L,R} \ , \tag{1.9}$$

with $\sinh(\theta) = \lambda/(\pi v_F + \lambda)$. The diagonal Hamiltonian is

$$H = \pi\tilde{v}_F \int dx\ (\tilde{\rho}_L^2 \ + \ \tilde{\rho}_R^2\ ) \ , \tag{1.10}$$

where the renormalized Fermi velocity is $\tilde{v} = (v_F + \lambda/\pi)\mathrm{sech}(2\theta)$. The densities $\tilde{\rho}_{R,L}$ so defined satisfy the same commutation relations as in Eq.(1.4). The electron operator can be expressed in terms of the rotated fields as

$$\psi_{R,L} = \eta : e^{\pm i[\cosh(\theta)\phi_{R,L} - \sinh(\theta)\phi_{L,R}]} : \ , \tag{1.11}$$

and the correlation functions are now given by

$$\langle \psi_{R,L}(t,x)\psi_{R,L}(0,0)\rangle = \frac{1}{(x \mp \tilde{v}_F t)(x^2 - \tilde{v}_F^2 t^2)^{\alpha}} \ , \tag{1.12}$$

where $\alpha = \sinh^2(\theta)$. Notice that the effect of the interactions is to mix left and right moving excitations, and that the electron correlations have now an anomalous exponent which depends on the interaction. This anomalous exponent is a signature of the Luttinger model with short range interactions.

A very important point to be made is that the most difficult step in the solution of the Luttinger model is not the inclusion of the interactions, which are obviously quadratic in the densities. It is indeed the fact that the kinetic energy of the fermions can be written as quadratic in the densities that is most notable. The linear dispersion for the fermions is necessary for the exactly solvability of the model. Haldane has shown that the low-energy structure of the the Luttinger model is preserved in the presence of a nonlinear fermion dispersion. In an analogy with Fermi liquid theory, where the structure of the low-lying excitations is preserved in the presence of interactions, the one-dimensional strongly correlated state was named Luttinger liquid.

Although the Luttinger liquid model is theoretically well understood, experimental realizations of 1D models that show Luttinger liquid behavior are extremely hard to obtain. The difficulty lies in that in 1D even the smallest amount of impurities are enough to cause localization of states, such that 1D wires will be insulators and not metallic as suggested by the Luttinger liquid state.

1.3 Chiral Luttinger liquids

One way to circumvent the problem of localization is to consider chiral systems, where the left and right moving excitations are separated, so that backscattering is suppressed. Such chiral Luttinger liquids exist on the edges or boundaries of quantum Hall (QH) fluids. The presence of the magnetic field causes excitations to move in a certain orientation set by the direction of the field, so that left and right moving excitations are spatially separated by the incompressible quantum Hall liquid, as shown in Figure 1-1.

That the edge excitations in the quantum Hall effect (QHE) are described by a

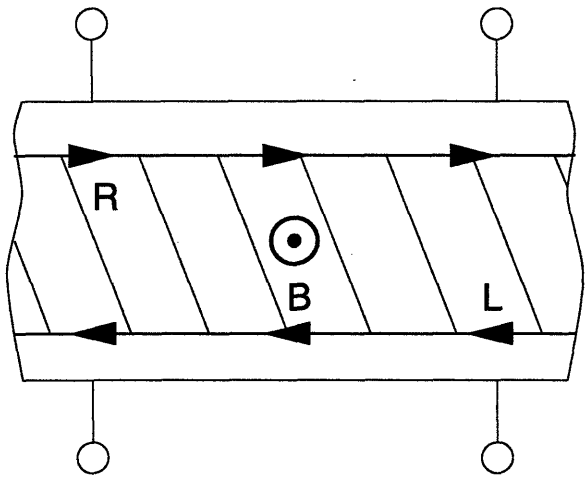

Figure 1-1: Chiral Luttinger liquids exist on the edges of quantum Hall fluids. The left and right moving excitations are separated by the quantum Hall liquid (shaded area), so that backscattering is suppressed. In a semi-classical picture, the direction for the motion of the excitations on a given edge can be determined by the $\vec{E} \times \vec{B}$ drift of the charge carriers, where the electric field results from the confining potential on the boundaries of the quantum Hall liquid.

chiral Luttinger liquid theory was shown by Wen [4, 5, 6, 7, 8]. The fact that bulk excitations of quantum Hall states have a finite energy gap is fundamental in the derivation of the low energy effective theory for the gapless edge excitations. For a thoroughly, clear and enlightening review, the reader is suggested to see Ref. [9]. We briefly review here the description of the edge excitations of fractional quantum Hall (FQH) states using bosonization.

The right and left moving excitations along the edges can be described by boson fields $\phi_{R,L}$. Right and left moving electron and quasiparticle operators on the edges of a FQH liquid can be written as $\Psi_{R,L}(t,x) \propto e^{\pm i\sqrt{g}\phi_{R,L}(t,x)}$, where g is related to the FQH bulk state. For example, for a Laughlin state with filling fraction $\nu = 1/m$ we have $g = m$ for electrons and $g = 1/m$ for quasiparticles carrying fractional charge e/m. The $\phi_{R,L}$ fields satisfy the equal-time commutation relations

$$[\phi_{R,L}(t,x) \ , \ \phi_{R,L}(t,y)] = \pm i\pi \ \mathrm{sign}(x-y) \ . \tag{1.13}$$

The dynamics of $\phi_{R,L}$ is described by

$$\mathcal{L}_{R,L} = \frac{1}{4\pi}\, \partial_x \phi_{R,L}\, (\pm\partial_t - v\partial_x)\phi_{R,L}\ , \tag{1.14}$$

where v is the velocity of edge excitations (which we will set to 1). Density operators can be defined in terms of the $\phi_{R,L}$ through $\rho_{R,L} = \frac{\sqrt{\nu}}{2\pi}\partial_x \phi_{R,L}$. Here, for convenience, we have set the unit charge in the definition of the density to be the electron charge e, so that $e = 1$ and $e^* = \nu$. One can verify that

$$[\rho_{R,L}(t,x)\ ,\ \Psi^\dagger_{R,L}(t,y)] = \sqrt{\nu g}\ \Psi^\dagger_{R,L}(t,y)\delta(x-y)\ , \tag{1.15}$$

so that indeed the cases $g = \nu^{-1}$ and $g = \nu$ correspond to electron and quasiparticle charged operators, respectively.

The description above can be generalized for hierarchical FQH states more complex than the simple Laughlin states. The generalization involves several branches of edge excitations, and is described in terms of a K-matrix as in Ref. [9].

Chiral Luttinger liquids, which do not suffer from the problem of localization, provides us with the experimentally realizable test of a theoretically well understood model of a strongly correlated system where the Fermi liquid picture breaks down. In order to probe the Luttinger liquid behavior of the edge states of FQH liquids, one must study the manifestations of the strong correlations in experiments. The Luttinger liquid behavior appears in transport measurements, such as the tunneling current between edge states. Deeper information is contained in the noise spectrum, which probes dynamical correlations. This Thesis contains such studies of transport and noise in chiral Luttinger liquids.

1.4 Thesis organization

In Chapter 2, the problem of tunneling in chiral Luttinger liquids is stated using the language of bosonization. The effective Hamiltonian describing a chiral Luttinger liquid is modified in the presence of tunneling by the introduction of the a tunneling

operator that moves charge from one edge to the other. The coupling constant of the tunneling operator (tunneling amplitude) can be varied experimentally. The tunneling current is calculated perturbatively to lowest order. Characteristic features of Luttinger liquid behavior, such as a nonlinear dependence of the current on the applied voltage and on the temperature, appear even at lowest order.

The study of noise in chiral Luttinger liquids is introduced in Chapter 3. Noise is studied first to lowest order in perturbation theory. A systematic perturbative expansion is obtained by mapping the distribution of tunneling events into a Coulomb gas in a one-dimensional contour. In order to study noise out of thermodynamical equilibrium, we must deal with a field theoretical approach that is able to incorporate non-equilibrium phenomena. One approach is the Keldysh non-equilibrium formalism, which is rederived in the context of the Coulomb gas expansion for tunneling events.

The charges in the Coulomb gas tend to reorganize as a dipole gas, which can be used to describe the tunneling statistics. The dipole-gas picture allows us to have a unified description of the low frequency shot noise and the high frequency "Josephson" noise. The correlation between the charges within a dipole (intra-dipole) contributes to the high-frequency "Josephson" noise, which has an algebraic singularity at $\omega = e^*V/\hbar$, whereas the correlations between dipoles (inter-dipole) are responsible for the low-frequency noise. We show that an independent or non-interacting dipole approximation gives a Poisson distribution for the locations of the dipole centers of mass, which gives a flat noise spectrum at low-frequencies and corresponds to uncorrelated shot noise. Including inter-dipole interactions gives an additional $1/t^2$ correlation between the tunneling events that results in a $|\omega|$ singularity in the noise spectrum. We present a diagrammatic technique to calculate the correlations in perturbation theory, and show that contributions from terms of order higher than the dipole-dipole interaction should only affect the strength of the $|\omega|$ singularity, but its form should remain $\sim |\omega|$ to all orders in perturbation theory. A counting argument also suggests that an algebraic singularity at ω_J should remain to all orders in perturbation theory in the case when the tunneling particles are electrons.

Chapter 4 presents the study of non-equilibrium noise in Chiral Luttinger Liquids using the Landauer-Buttiker Scattering approach, obtaining the current and voltage noise spectrum for a four-terminal measurement scheme. Experimental consequences of the tunneling of charges are present in the four-terminal measurement of both the low-frequency shot noise (ω near 0), and the high-frequency Josephson noise (ω near $\omega_J = e^*V/\hbar$). Within perturbation theory, an algebraic singularity is present at the Josephson frequency $\omega_J = e^*V/\hbar$, whose position depends on the charge e^* of the tunneling particles, either electrons or fractionally charged quasiparticles. In the case of electron tunneling ($e^* = e$) the singularity remains to all orders in perturbation theory, as found in Chapter 3. The electron and quasiparticle types of tunneling are related by a strong-weak coupling duality transformation. We show in a non-perturbative calculation for an exactly solvable point that the singularity at the quasiparticle frequency exists only in the limit of vanishing coupling, whereas the singularity at the electron frequency is present for all coupling strengths. The vanishing coupling limit corresponds to perfectly quantized Hall conductance in the case of quasiparticle tunneling between edge states in the fractional quantum Hall regime, and thus tunneling destroys the singularity at the quasiparticle frequency concomitantly with the quantized current.

Chapter 2

Transport Properties of Chiral Luttinger Liquids

2.1 Introduction

Tunneling and resonant tunneling in mesoscopic systems have been actively studied recently both experimentally and theoretically [10]. Many studies concentrate on interaction effects inside the tunneling junction [11, 12]. In this chapter we will study the tunneling current between the edges of a Hall bar in the fractional quantum Hall (FQH) regime. We will focus not so much on the tunneling junction, but instead on the "leads", *i.e.*, the strongly correlated chiral Luttinger liquid edges of the FQH state. The correlation effects appear on the tunneling current in the form of a non-linear dependence on the applied voltage and temperature. The tunneling current is thus a probe to observe the non-Fermi liquid behavior of the edges of FQH states.

There are two distinct geometries in which tunneling can take place between the edges of a Hall bar in the QH regime, as shown in Figure 2-1. The configurations can be accessed experimentally using metallic gates placed on top of the 2-D electron gas. Applying a negative gate voltage V_G depletes the electron concentration underneath the gate, causing the two branches of edge states to get closer, and thus enhancing the tunneling between the channels (see Fig. 2-1a). Because in this configuration both edges form the boundary of the same QH liquid, there can be either electron or

quasiparticle (carrying fractional charge) tunneling. By applying a sufficiently large V_G, one can obtain the situation in Fig. 2-1b, where the edges form the boundaries of two disconnected QH liquids, and thus only electrons can tunnel from one edge to the other. These two distinct situations can be studied in a very similar way, which we explore below.

2.2 Tunneling in 1-D Luttinger Liquids

The low energy excitations of chiral Luttinger liquids is better described in the language of bosonization, as presented in Chapter 1. As shown there, right and left moving electron and quasiparticle operators can be written as $\Psi_{R,L}(x,t) =: e^{\pm i\sqrt{g}\phi_{R,L}(x,t)} :$, where g is related to the FQH bulk state. For a Laughlin state with filling fraction $\nu = 1/m$, for example, $g = m$ for electrons and $g = 1/m$ for quasiparticles carrying fractional charge e/m. The dynamics of $\phi_{R,L}$ is described by

$$\mathcal{L}_{R,L} = \frac{1}{4\pi}\,\partial_x\phi_{R,L}\,(\pm\partial_t - v\partial_x)\phi_{R,L}\ , \tag{2.1}$$

and the bosonic $\phi_{R,L}$ fields satisfy the equal-time commutation relations

$$[\phi_{R,L}(t,x)\ ,\ \phi_{R,L}(t,y)] = \pm i\pi\ \mathrm{sgn}(x-y)\ . \tag{2.2}$$

The tunneling operators from right to left moving branches and vice-versa can be written as $\Psi_L^\dagger\Psi_R$ and $\Psi_R^\dagger\Psi_L$. Thus we can write, in terms of $\phi = \phi_R + \phi_L$, the following total Lagrangian density:

$$\mathcal{L} = \frac{1}{8\pi}[(\partial_t\phi)^2 - v^2(\partial_x\phi)^2] - \ \Gamma\delta(x)\ e^{i\sqrt{g}\phi(t,0)} + H.c.\ , \tag{2.3}$$

with ϕ satisfying $[\phi(t,x), \partial_t\phi(t,y)] = 4\pi i\delta(x-y)$. In the following we will set the edge velocity $v = 1$. The tunneling operator $e^{i\sqrt{g}\phi(t,0)}$ has an anomalous dimension which we will absorb in the definition of Γ. This redefinition can be viewed as multiplying Γ by powers of a cutoff obtained from self-interactions of the $e^{i\sqrt{g}\phi(t,0)}$.

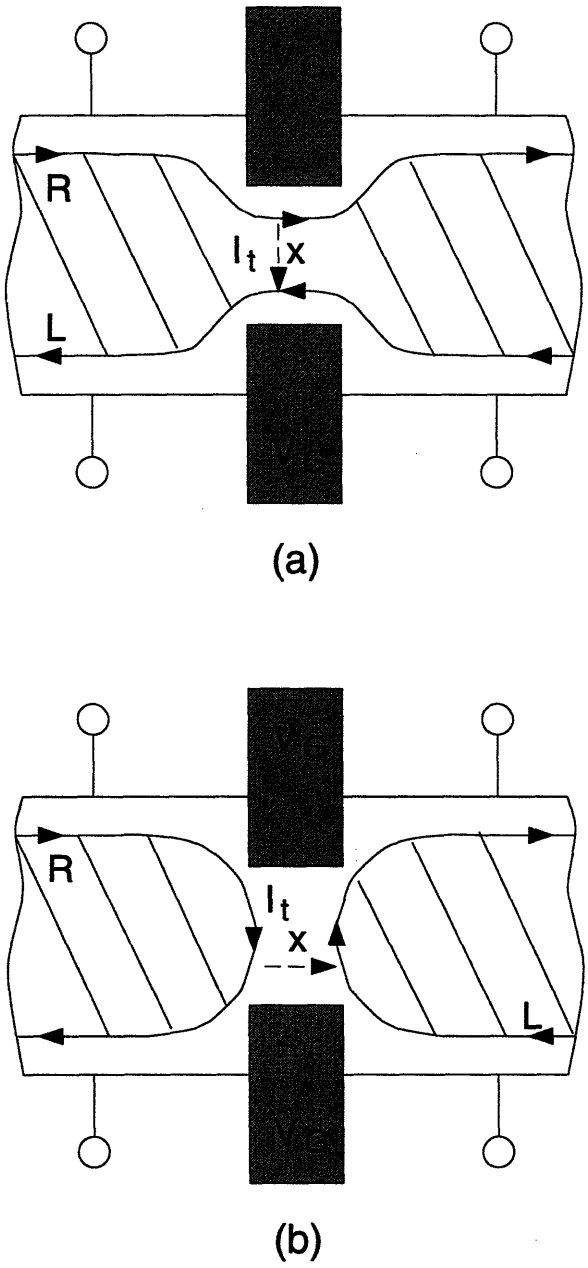

Figure 2-1: Geometries for tunneling between edge states. By adjusting the gate voltage V_G one can obtain either a simply connected QH droplet (a), or two disconnected QH droplets (b). For the geometry in (a) both electrons and quasiparticles (carrying fractional charge) can tunnel from one edge to the other, whereas for the tunneling geometry in (b) only electrons can tunnel. The Luttinger liquid behavior is characterized by the exponent $g = \nu$ in (a), and $g = \nu^{-1}$ in (b). The tunneling current I_t depends on the applied voltage between the right and left edges, and by increasing this voltage one can also cross over from the geometry (b) to the geometry (a).

A voltage difference between the two edges of the QH liquid can be easily introduced in the model by letting $\Gamma \to \Gamma e^{-i\omega_0 t}$, where $\omega_0 \equiv \omega_J \equiv e^* V/\hbar$, with $e^* = e$ for electron tunneling and $e^* = e/m$ for quasiparticle tunneling.

Notice that in order to obtain the coupling term we assume that we only have contributions from $x = 0$ for the tunneling operators. This is the case when the width of the barrier is narrow. Also, if the barrier is narrow, the time spent in the tunneling is small compared to the spacing between tunneling events. Indeed, in this case we can speak of tunneling events that occur at rather well defined time coordinates.

Using this model, the average tunneling current through a barrier in a one dimensional channel and between edge states in the FQH regime was calculated [13, 14, 15, 16]. The current has a nonlinear dependence on the applied voltage between the terminals, with the power dependence on the voltage intimately related to the exponent g in the electron propagator. For non-resonant tunneling between FQH edge states, one finds that $I_t \propto V^{2g-1}$ at zero temperature, and that the linear conductance σ scales with the temperature as $\sigma \propto T^{2(g-1)}$. The calculation of these results are presented below.

2.3 Perturbative Calculation of the Current

The first step in the calculation is to obtain the tunneling current operator $j(t)$. In the case of tunneling between edges (such as in Figs. 2-1a & 2-1b) we simply use that $j = -\frac{1}{i\hbar}[N_L, H] = \frac{1}{i\hbar}[N_R, H]$ (where $N_{R,L}$ are the total charge operators on the R, L edges) and the commutation relations to obtain the expression for j:

$$j(t) = ie^*\Gamma e^{i\sqrt{g}\phi(t,0)} + H.c. \; . \tag{2.4}$$

The next step is to calculate $\langle j \rangle$ perturbatively. Because there is a voltage difference between the R and L terminals, the system is out of thermodynamical equilibrium. We must then use field theoretical tools appropriate for such non-equilibrium problem. However, non-equilibrium effects appear only to second and higher orders

in perturbation theory. We will calculate the tunneling current to first order in the coupling Γ, so that we will delay our incursions into non-equilibrium field theory to the next chapter, when we study noise.

The expectation value for the current at time t is

$$\langle j(t)\rangle = \langle 0|S^{\dagger}(t,-\infty)\; j(t)\; S(t,-\infty)|0\rangle\;, \tag{2.5}$$

where $S(t,-\infty)$ is the time evolution operator. To lowest order in the tunneling perturbation $H_{\rm tun} = \Gamma e^{-i\omega_0 t}e^{i\sqrt{g}\phi(t)} + H.c.$ we have

$$\langle j(t)\rangle = -i\int_{-\infty}^{t} dt'\; \langle 0|[j(t), H_{\rm tun}(t')]|0\rangle\;. \tag{2.6}$$

In the calculation of

$$\begin{aligned}\langle 0|j(t)\; H_{\rm tun}(t')|0\rangle \;&=\; e^{*}\langle 0|(i\Gamma e^{-i\omega_0 t}e^{i\sqrt{g}\phi(t)} - i\Gamma^{*}e^{i\omega_0 t}e^{-i\sqrt{g}\phi(t)})\\ &\quad\times\;(\Gamma e^{-i\omega_0 t'}e^{i\sqrt{g}\phi(t')} + \Gamma^{*}e^{i\omega_0 t'}e^{-i\sqrt{g}\phi(t')})|0\rangle\end{aligned} \tag{2.7}$$

the non-vanishing terms are those that transfer zero total charge when applied to $|0\rangle$. We then have

$$\begin{aligned}&\langle 0|j(t)\; H_{\rm tun}(t')|0\rangle =\\ &= ie^{*}|\Gamma|^{2}\left(e^{-i\omega_0(t-t')}\langle 0|e^{i\sqrt{g}\phi(t)}e^{-i\sqrt{g}\phi(t')}|0\rangle - e^{i\omega_0(t-t')}\langle 0|e^{-i\sqrt{g}\phi(t)}e^{i\sqrt{g}\phi(t')}|0\rangle\right)\\ &= ie^{*}|\Gamma|^{2}\;(e^{-i\omega_0(t-t')} - e^{i\omega_0(t-t')})\;e^{g\langle 0|\phi(t)\phi(t')|0\rangle}\;.\end{aligned} \tag{2.8}$$

The ϕ field correlation is $\langle 0|\phi(t)\phi(0)|0\rangle = -2\ln(\delta + it)$, where δ is an ultraviolet cut-off scale. Using the expressions above, we can write

$$\begin{aligned}-i\langle[j(t), H_{\rm tun}(t')]\rangle \;&=\; e^{*}|\Gamma|^{2}\;\left(e^{-i\omega_0(t-t')} - e^{i\omega_0(t-t')}\right)\\ &\quad\times\;\left(\frac{1}{[\delta + i(t-t')]^{2g}} - \frac{1}{[\delta + i(t'-t)]^{2g}}\right)\;.\end{aligned} \tag{2.9}$$

Inserting the above expression into Eq.(2.6) and performing the t' integration, we

obtain the current expectation value:

$$\langle j(t)\rangle \;=\; e^*|\Gamma|^2[c_+(\omega_0)-c_-(\omega_0)]\;, \tag{2.10}$$

where

$$c_\pm(\omega)=\int_{-\infty}^{\infty}dp\frac{e^{-i\omega p}}{(\delta\mp ip)^{2g}}=\frac{2\pi}{\Gamma(2g)}|\omega|^{2g-1}e^{-|\omega|\delta}\;\theta(\pm\omega)\;. \tag{2.11}$$

The $c_\pm(\omega)$ will appear frequently in this work.

We can obtain the finite temperature results for $c_\pm$ by a conformal transformation [17]:

$$\int_{-\infty}^{\infty}dp\frac{e^{-i\omega_0 p}}{(\delta-ip)^{2g}}\rightarrow\int_{-\infty}^{\infty}dp\;e^{i\pi g\;\mathrm{sgn}(p)}\frac{e^{-i\omega_0 p}}{|\frac{\sinh(\pi T p)}{\pi T}|^{2g}}\;, \tag{2.12}$$

which gives

$$\begin{aligned} c_+(\omega_0) &= c_-(-\omega_0) \\ &= 2(\pi T)^{2g-1}B(g+\frac{i\omega_0}{2\pi T},g-\frac{i\omega_0}{2\pi T})\;\cosh(\frac{\omega_0}{2T})\;[1+\tanh(\frac{\omega_0}{2T})]\;, \end{aligned} \tag{2.13}$$

where B is the Beta function. Using these expressions for $c_\pm$ we obtain

$$I_t=4e^*|\Gamma|^2(\pi T)^{2g-1}B(g+\frac{i\omega_0}{2\pi T},g-\frac{i\omega_0}{2\pi T})\;\sinh(\frac{\omega_0}{2T})\;, \tag{2.14}$$

which is the same expression found by first order perturbation theory in Ref. [13]. For $T=0$, in particular, we find that $I_t\sim e^*|\Gamma|^2V^{2g-1}$. For $\omega_0\ll T$, we have $I_t\sim e^*|\Gamma|^2T^{2(g-1)}V$, so that the tunneling conductance depends nonlinearly on temperature: $\sigma\propto T^{2(g-1)}$.

The nonlinear dependence of the tunneling conductance between the edge states is a characteristic property of (chiral) Luttinger liquids, and can be traced back to the correlation functions of charged operators in the system. By experimentally studying the tunneling between edge states in the FQH regime using a point contact geometry, Milliken, Umbach, and Webb [18] found this type of power law dependence of the tunneling conductance on the temperature. Their finding is consistent with the theoretical prediction $\sigma\propto T^4$ for the $\nu=1/3$ FQH state [13, 19].

The experimental confirmation of the Luttinger liquid behavior in tunneling between edge states has boosted theoretical interest in further studies of properties of the conductance [20, 21, 22]. An exact solution for the conductance has been obtained for the interesting and relevant case of $g = 1/3$ (which correspond to a $\nu = 1/3$ FQH state) using the thermodynamic Bethe Ansatz, and an exact duality between the g and $1/g$ cases has been shown [23, 24] in the context of the tunneling current, as suggested in Ref. [25].

Signatures of Luttinger liquid behavior appear not only in transport properties, but also in the noise spectrum, which carries a lot of information on the dynamics of the underlying strongly correlated system. The noise spectrum can be used as a powerful probe to study the physical properties of correlated systems, and we explore this tool in the following chapters.

Chapter 3

Quantum Noise in Chiral Luttinger Liquids

3.1 Introduction

The noise spectrum in a two-terminal conductor in the absence of an applied voltage is proportional to the conductance and to the temperature. This result was found experimentally by Johnson in 1927 [26] and explained theoretically by Nyquist in 1928 [27]. Such relation between equilibrium noise and conductance can be seen as a consequence of the fluctuation-dissipation theorem. The noise in the presence of transport (non-equilibrium noise) can also be related to transport coefficients for non-interacting systems [28, 29], but now these transport coefficients, in the most general case, cannot be determined from conductance measurements alone. For interacting systems one should expect an even richer behavior, as new features in the noise should appear as a consequence of correlations due to interactions. In general the shape of the noise spectrum is determined by the dynamical properties of the system, which contain information about the excited states. Thus the noise spectrum is a powerful probe which allows us to study dynamics of strongly correlated systems. In this chapter we will study the noise spectrum in the tunneling current between (chiral) Luttinger liquids. The noise spectrum carries rich information about dynamical properties of (chiral) Luttinger liquids, which will help us identify such strongly correlated

states in experiments.

Recent studies of noise in non-interacting systems reveal that the noise spectrum contain features that come from the statistics of the tunneling particles [30]. These statistics-dependent features are not contained in the DC conductance. For Luttinger liquids, the tunneling particles sometimes carry fractional statistics and fractional charges. It is then very interesting to study the noise spectrum for tunneling between (chiral) Luttinger liquids, especially those features that come from the strongly correlated properties of (chiral) Luttinger liquids (such as fractional statistics and fractional charges).

Two kinds of noise may appear in tunneling at a finite voltage V, the shot noise and the "Josephson" noise. The shot noise can be understood from a classical picture in which the average tunneling current is viewed as a result of many tunneling events. A tunneling event represents a single particle (which can be an electron or a charged quasiparticle) that tunnels through the junction. The spectrum of the shot noise is determined by the correlations between tunneling events. In this chapter we always assume that the tunneling time is much shorter than the average spacing between two tunneling events. Under this approximation, we will ignore the retardation and model the tunneling by an instantaneous tunneling operator $\Gamma\psi_L^\dagger\psi_R + H.c.$, which transfers particles between two reservoirs. The "Josephson" noise is related to the fact that the two systems connected by the junction have different chemical potentials. The quantum interference between wave functions on the two sides of the junction may cause a singularity at frequency $\omega = e^*V/\hbar$ in noise spectrum (here e^* is the charge of the tunneling particle). Such features near the "Josephson" frequency $\omega_J \equiv e^*V/\hbar$ are called "Josephson" noise. In this chapter we will develop a language for non-equilibrium noise in 1-D Luttinger liquids which covers both the shot noise and the "Josephson" noise.

We start with the Keldysh formalism, in which the tunneling events are described by a Coulomb gas of charges on a Keldysh contour. Under certain conditions the charges at different branches of the contour pair into dipoles (in this case the Coulomb gas is said to be in the dipole phase). The dipoles correspond to the tunneling

events in the shot-noise picture. The non-interacting dipole approximation leads to a Poisson distribution for the separation of dipoles, which results in a white noise (*i.e.* a frequency independent noise) at low frequencies. However, for a finite voltage across the junction, we find that the dipoles have a non-zero dipole moment which leads to a long range $1/t^2$ interaction between dipoles. The dipole-dipole interaction gives rise to a non-trivial distribution of the tunneling events which induces a $|\omega|$ singularity in the low frequency noise spectrum. The dipoles have finite size and the intra-dipole structures are found to be responsible for the high frequency "Josephson" noise, which appear as an algebraic singularity of the form $|\omega - \omega_J|^{2g-1}$ in the noise spectrum within perturbation theory.

The full expression for the singularity at zero frequency in the noise spectrum due to the dipole-dipole interaction is found to be

$$S_{sing.}(\omega) = 4\pi g(2g-1)^2(\frac{I_t}{\omega_J})^2 \ |\omega| \ , \tag{3.1}$$

where I_t is the average tunneling current and g contains information on the interactions in the Luttinger liquid (or filling fraction of the FQH states, in the case of chiral Luttinger liquids). Because of the nonlinear dependence of I_t on ω_J [13, 14, 15, 16], the strength of the singularity in the noise spectrum at zero frequency will also have a non-linear dependence on ω_J ($(\frac{I_t}{\omega_J})^2 \propto \omega_J^{4(g-1)}$). The particular case of non-interacting electrons can be obtained with $g = 1$, where one recovers the $|\omega|$ singularity that appears to order D^2 in the transmission coefficient D [31]. The correlations in the case of non-interacting electrons come from the Pauli principle, which enters very simply in the formulation used in this chapter through the language of bosonization.

The chapter is organized as the following. In section 3.2 we calculate the noise perturbatively. In section 3.3 we use the non-equilibrium (Keldysh) scattering operator as a means to obtain a joint probability distribution for tunneling events. The tunneling events can be mapped into charges of a Coulomb gas, which tend to reorganize as a dipole gas. A non-interacting dipole approximation leads to uncorrelated noise. Dipole-dipole interactions and correlations will be discussed in section 3.4,

which lead to an $|\omega|$ singularity in the low frequency noise spectrum. In section 3.5 a diagrammatic technique is presented that accounts for the correlations in a systematic way. We show the existence of the $|\omega|$ singularity at zero frequency to all orders in perturbation theory. A counting argument also suggests that the leading singularity at ω_J should remain of the form $|\omega - \omega_J|^{2g-1}$ to all orders in perturbation theory for $g > 1$.

3.2 Perturbative Calculation

We have shown in Chapter 2 that the tunneling current operator is given by $j(t) = ie^*\Gamma e^{i\sqrt{g}\phi(t,0)} + H.c.$. The noise spectrum can be obtained by calculating two-point correlations involving the operator $j(t)$. The dynamics of the ϕ field is governed by the total Lagrangian density

$$\mathcal{L} = \frac{1}{8\pi}[(\partial_t\phi)^2 - (\partial_x\phi)^2] - \Gamma\delta(x)\, e^{i\sqrt{g}\phi(t,0)} + H.c. \ , \tag{3.2}$$

with ϕ satisfying $[\phi(t,x), \partial_t\phi(t,y)] = 4\pi i\delta(x-y)$ (see Chapter 2).

Notice that, as the problem under consideration is intrinsically non-equilibrium, one should use the Keldysh (or non-equilibrium) formalism [32] in computing expectation values of operators. This is the case here, where if we treat the coupling term perturbatively and introduce an adiabatic turning on and off of the interaction, the state at $t = -\infty$ differs from the one at $t = \infty$; the charge transfer in one direction due to the applied voltage clearly makes the two states at $\pm\infty$ different, as the total charge in one edge branch (or reservoir) decreases whereas in the other the total charge increases. This problem could, in principle, be circumvented by including another term in the Hamiltonian that would close the circuit and bring the charges that tunneled through the barrier back to the reservoirs (a "battery"). Such a way of thought is relevant to clarify the distinction between the equilibrium and non-equilibrium formalism, and how they can be connected in principle. However, in practice, adding the restoring charge coupling in the Hamiltonian only would make

the problem more cumbersome and poorly defined, which makes the non-equilibrium formalism a natural choice.

For perturbative calculations of zeroth and first order, however, there is no difference between the results for expectation values obtained with either the equilibrium or the non-equilibrium formalism. This is the case in the calculation of the current-current correlation, where the lowest order contribution is the zeroth order:

$$\begin{aligned}\langle j(t)j(0)\rangle &= e^{*2}\,\langle 0|\Big(i\Gamma e^{-i\omega_0 t}e^{i\sqrt{g}\phi(t)} - i\Gamma^* e^{i\omega_0 t}e^{-i\sqrt{g}\phi(t)}\Big) \\ &\quad\times\Big(i\Gamma e^{i\sqrt{g}\phi(0)} - i\Gamma^* e^{-i\sqrt{g}\phi(0)}\Big)|0\rangle\ . \end{aligned} \tag{3.3}$$

The non-zero contributions come from the terms that, when applied to $|0\rangle$, transfer zero total charge, so we can write

$$\begin{aligned}\langle j(t)j(0)\rangle &= e^{*2}|\Gamma|^2\left(e^{-i\omega_0 t}\langle 0|e^{i\sqrt{g}\phi(t)}e^{-i\sqrt{g}\phi(0)}|0\rangle + e^{i\omega_0 t}\langle 0|e^{-i\sqrt{g}\phi(t)}e^{i\sqrt{g}\phi(0)}|0\rangle\right) \\ &= e^{*2}|\Gamma|^2\left(e^{-i\omega_0 t}+e^{i\omega_0 t}\right)e^{g\langle 0|\phi(t)\phi(0)|0\rangle}\ . \end{aligned} \tag{3.4}$$

The ϕ field correlation is $\langle 0|\phi(t)\phi(0)|0\rangle = -2\ln(\delta + it)$, where δ is an ultraviolet cut-off scale. The current-current correlation is then given by

$$\langle j(t)j(0)\rangle = e^{*2}|\Gamma|^2\,\frac{2\cos(\omega_0 t)}{(\delta+it)^{2g}}\ , \tag{3.5}$$

which displays clearly oscillations at frequency $f = \omega_0/2\pi = e^*V/h$. This implies that the noise spectrum will also display structure at this frequency. The noise spectrum is calculated from the current-current correlation:

$$\begin{aligned}S(\omega) &= \int_{-\infty}^{\infty} dt\ e^{i\omega t}\langle\{j(t),j(0)\}\rangle \\ &= e^{*2}|\Gamma|^2[c_+(\omega_0+\omega)+c_-(\omega_0+\omega)+c_+(\omega_0-\omega)+c_-(\omega_0-\omega)]\ , \end{aligned} \tag{3.6}$$

where

$$c_\pm(\omega) = \int_{-\infty}^{\infty} dp\frac{e^{-i\omega p}}{(\delta\mp ip)^{2g}} = \frac{2\pi}{\Gamma(2g)}|\omega|^{2g-1}e^{-|\omega|\delta}\ \theta(\pm\omega) \tag{3.7}$$

as in Chapter 2. The noise spectrum to order $|\Gamma|^2$ is then given by

$$\begin{aligned} S(\omega) &= \frac{2\pi}{\Gamma(2g)} e^{*2}|\Gamma|^2 \left[|\omega-\omega_0|^{2g-1} + |\omega+\omega_0|^{2g-1} \right] \\ &= e^* I_t \left[|1-\omega/\omega_0|^{2g-1} + |1+\omega/\omega_0|^{2g-1} \right], \end{aligned} \tag{3.8}$$

where we used the perturbative result to order $|\Gamma|^2$ for the tunneling current $I_t = \frac{2\pi}{\Gamma(2g)} e^*|\Gamma|^2\omega_0^{2g-1}$ [13].

From the expression for $S(\omega)$ above we can deduce some features of the noise to order $|\Gamma|^2$. First notice that for $\omega \ll \omega_0$ we obtain $S(\omega) \approx 2e^*I_t$, the classical shot noise result, independent of g. Notice also the singularities at $\omega = \pm\omega_0$. In the particular case of non-interacting electrons ($g = 1$) we have $S(\omega) = 2e^*I_t$ for $|\omega| < \omega_0$, and $S(\omega) = 2e^*I_t|\omega|/\omega_0$ for $|\omega| > \omega_0$, which agrees, to lowest order in the transmission coefficient D (lowest order in $|\Gamma|^2$), with previous results for the noise spectrum of non-interacting electrons [31]. To get the term in D^2 we need to go beyond this zeroth order perturbation theory, as we will do later in the chapter. The sharp edge of the noise spectrum at $\omega = e^*V/\hbar$ for $g = 1$ finds its origin in the Pauli principle, which is the sole factor responsible for correlations in the non-interacting case [30]. In our model, particle statistics enter automatically in the way we construct the electron/quasiparticle operator from the boson fields and their commutation relations.

In the following sections we shall see how the low-frequency noise spectrum is modified once we go beyond this perturbative calculation.

3.3 The Joint Probability Distribution

As we have previously mentioned, when the tunneling barrier is narrow so that the time the charge spends in the tunneling process is small compared to the times between two consecutive tunnelings, one can speak of well defined tunneling events at certain specific times. In this section we will find a joint probability distribution for the times for these tunneling events.

The term $e^{i\gamma\phi}$ in the Hamiltonian (where we use $\gamma = \sqrt{g}$) transfers charge from one edge branch to the other (say, in the case of the geometry of Fig. 2-1a & 2-1b, from the R to the L edge branch). The term $e^{-i\gamma\phi}$ does the converse (from L to R). We will map the problem to a Coulomb gas in a 1-D space, associating a charge $+$ to the term $e^{i\gamma\phi}$ and a charge $-$ to $e^{-i\gamma\phi}$. Let $Z = \langle 0|S_c(-\infty,-\infty)|0\rangle$, where $S_c(-\infty,-\infty)$ is the scattering operator in the contour from $t = -\infty$ to $t = \infty$, and back to $t = -\infty$ (the Keldysh formalism contour). In terms of the usual scattering operator S, we can write:

$$\begin{aligned} Z &= \langle 0|S(-\infty,\infty)\ S(\infty,-\infty)|0\rangle \\ &= \langle 0|S^\dagger(\infty,-\infty)\ S(\infty,-\infty)|0\rangle\ . \end{aligned} \tag{3.9}$$

In this form the contributions from the forward ($t = -\infty \to \infty$) and return ($t = \infty \to -\infty$) branches are easily identified in terms of the more commonly used (equilibrium) scattering operators. Clearly, since S is unitary, $Z = 1$. Now let's expand Z perturbatively in Γ. We will use the scripts t and b to denote the top (or forward) and bottom (or return) branches, and $+$ and $-$ to denote whether the inserted operator is $e^{i\gamma\phi}$ $(+)$ or $e^{-i\gamma\phi}$ $(-)$. $Q^{t,b}_{+,-}$ will denote the number of times that $e^{i\gamma\phi}$ or $e^{-i\gamma\phi}$ appear in the top and bottom contours (see Fig. 3-1). With this notation, we can expand the scattering operator as:

$$\begin{aligned} S(\infty,-\infty) \ =\ & \\ \sum_{Q^t_+,Q^t_-} & \left\{ \frac{(-i\Gamma)^{Q^t_+}\ (-i\Gamma^*)^{Q^t_-}}{Q^t_+!\ Q^t_-!} \right. \\ & \left. \times \int \prod_{i=1}^{Q^t_+} dt_i^{t+} \prod_{j=1}^{Q^t_-} dt_j^{t-}\ T\left(\prod_{i=1}^{Q^t_+} e^{-i\omega_0 t_i^{t+}} e^{i\gamma\phi(t_i^{t+})} \prod_{j=1}^{Q^t_-} e^{i\omega_0 t_j^{t-}} e^{-i\gamma\phi(t_j^{t-})} \right) \right\} \end{aligned} \tag{3.10}$$

and

$$S(-\infty,\infty) \ =\ S^\dagger(\infty,-\infty) \ =$$

$$\sum_{Q_+^b,Q_-^b} \left\{ \frac{(i\Gamma)^{Q_+^b}\ (i\Gamma^*)^{Q_-^b}}{Q_+^b!\ Q_-^b!} \right.$$
$$\left. \times \int \prod_{k=1}^{Q_+^b} dt_k^{b+} \prod_{l=1}^{Q_-^b} dt_l^{b-}\ \tilde{T}\left(\prod_{k=1}^{Q_+^b} e^{-i\omega_0 t_k^{b+}} e^{i\gamma\phi(t_k^{b+})} \prod_{l=1}^{Q_-^b} e^{i\omega_0 t_l^{b-}} e^{-i\gamma\phi(t_j^{b-})} \right) \right\}$$

where $\tilde{T}$ stands for reverse time ordering. Notice that in the operator $S_c(-\infty,-\infty) = S(-\infty,\infty)\ S(\infty,-\infty)$ the $\tilde{T}$ ordering occurs to the left of the T ordering, so that we replace both by a T_c ordering operator such that times in the top branch are ordered increasingly, times in the bottom branch are ordered decreasingly, and times in the bottom branch are always ordered after the ones in the top branch (see Fig. 3-1). Using T_c we can write $S_c(-\infty,-\infty)$ as

$$\sum_{Q_+^t,Q_-^t,Q_+^b,Q_-^b} \left\{ \frac{(-i\Gamma)^{Q_+^t}\ (-i\Gamma^*)^{Q_-^t}\ (i\Gamma)^{Q_+^b}\ (i\Gamma^*)^{Q_-^b}}{Q_+^t!\ Q_-^t!\ Q_+^b!\ Q_-^b!} \right. \tag{3.11}$$
$$\times \int \prod_{i=1}^{Q_+^t} dt_i^{t+} \prod_{j=1}^{Q_-^t} dt_j^{t-} \prod_{k=1}^{Q_+^b} dt_k^{b+} \prod_{l=1}^{Q_-^b} dt_l^{b-}\ T_c \left(\prod_{i=1}^{Q_+^t} e^{-i\omega_0 t_i^{t+}} e^{i\gamma\phi(t_i^{t+})} \right.$$
$$\left. \left. \prod_{j=1}^{Q_-^t} e^{i\omega_0 t_j^{t-}} e^{-i\gamma\phi(t_j^{t-})} \prod_{k=1}^{Q_+^b} e^{-i\omega_0 t_k^{b+}} e^{i\gamma\phi(t_k^{b+})} \prod_{l=1}^{Q_-^b} e^{i\omega_0 t_l^{b-}} e^{-i\gamma\phi(t_l^{b-})} \right) \right\}.$$

In order to calculate the bracket

$$\langle 0|T_c(e^{i\gamma[\ \sum_{i=1}^{Q_+^t}\phi(t_i^{t+}) - \sum_{j=1}^{Q_-^t}\phi(t_j^{t-}) + \sum_{k=1}^{Q_+^b}\phi(t_k^{b+}) - \sum_{l=1}^{Q_-^b}\phi(t_l^{b-})\ ]})|0\rangle \tag{3.12}$$

we use

$$\langle 0|T_c(e^{iq\phi(t)}\ e^{iq'\phi(t')})|0\rangle = e^{-qq'\langle 0|T_c(\phi(t)\phi(t'))|0\rangle} \tag{3.13}$$

and the contour-ordered two-point correlation

$$\langle 0|T_c(\phi(t_1)\phi(t_2))|0\rangle = \begin{cases} -2\ln(\delta + i|t_1 - t_2|) & , t_1 \text{ and } t_2 \text{ in the top branch} \\ -2\ln(\delta - i|t_1 - t_2|) & , t_1 \text{ and } t_2 \text{ in the bottom branch} \\ -2\ln(\delta - i(t_1 - t_2)) & , t_1 \text{ in the top, } t_2 \text{ in the bottom} \\ -2\ln(\delta + i(t_1 - t_2)) & , t_1 \text{ in the bottom, } t_2 \text{ in the top} \end{cases}$$

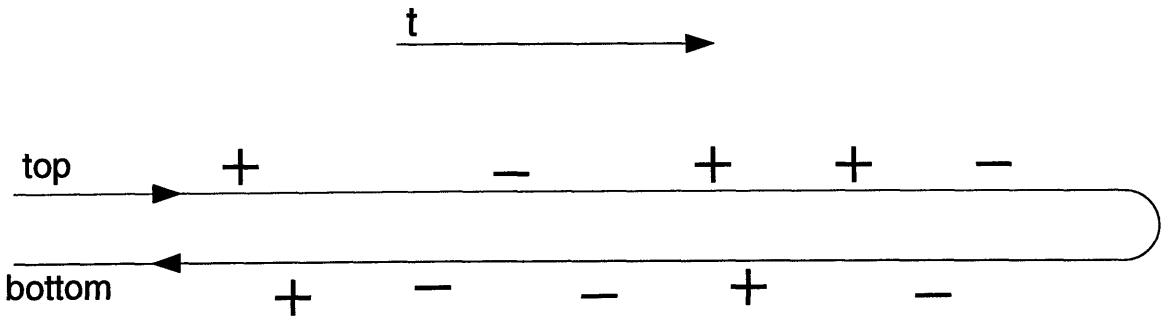

Figure 3-1: An insertion of an operator $e^{+i\gamma\phi(t)}$ correspond to the insertion of a charge $+$ on the contour at time t. Similarly, an insertion of an operator $e^{-i\gamma\phi(t)}$ correspond to an insertion of a charge $-$ at time t. The time t is ordered along the contour shown, and there is a distinction between charges placed on the top and bottom branches. For illustration, in the example shown we have for the number of $+$ and $-$ charges in the t and b branches $Q^t_+ = 3$, $Q^t_- = 2$, $Q^b_+ = 2$ and $Q^b_- = 3$. Only terms that have zero total charge $Q = Q^t_+ + Q^b_+ - Q^t_- - Q^b_-$ can give a non-zero contribution to Z.

The bracket in Eq. (3.12) contains the contributions from all pairs of charges, which interact via a two body potential that is determined by the T_c ordered two-point correlation. The phase terms due to ω_0 ($e^{-i\omega_0 t}$ for a $+$ charge, and $e^{i\omega_0 t}$ for a $-$ charge) correspond to an underlying background, which tends to polarize the gas, leaving (in the case of positive ω_0, for example) more $+$ charges than $-$ ones in the top branch, and more $-$ charges than $+$ ones in the bottom branch. An illustrative picture of the imbalance created by the applied voltage V (non-equilibrium) is shown in Fig. 3-2. One can think of V as an "electric field" that polarizes the Coulomb gas, leaving an imbalance of $+$ and $-$ charges in the t and b contours, which gives rise to a net current in one direction or the other (excess of $+(-)$ charges, or $R \to L$ ($L \to R$) tunneling), depending on the sign of V.

The expression for Z obtained as an expansion in Γ is exact so far. Also, the map into a Coulomb gas model is now complete. An expansion similar to the one we present here appears in the study of dissipative quantum mechanics models in a periodic potential [33, 34]. There the charges are grouped in terms of the so called "soujourns" and "blips". We find the idea of keeping the $+$ and $-$ charges more

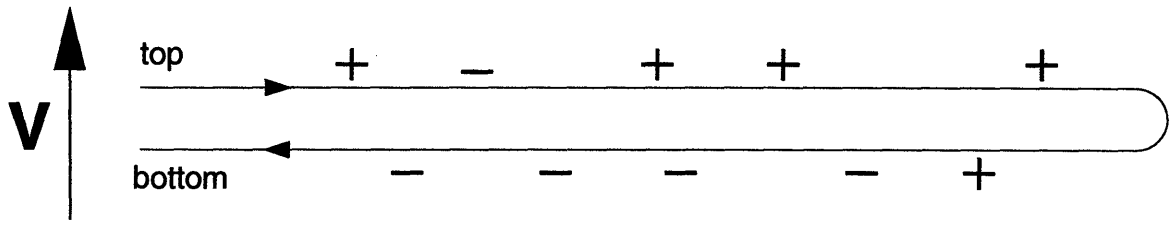

Figure 3-2: The applied voltage V between the terminals or edges creates an imbalance of charge between the top and bottom branches. Since $+$ and $-$ charges correspond respectively to tunneling from $R \to L$ and $L \to R$, an excess of charge in the top branch correspond to net tunneling in one direction.

intuitive, as is the idea of having the non-equilibrium voltage be thought of as a "field" that polarizes the gas and changes the densities within the t and b contours. This language, as we will show, makes it easier for us to go beyond the independent blip approximation, and study correlations.

We will now focus in showing how the expression for Z can be used to define a joint probability of tunneling events. In the limit of a narrow barrier, as we pointed out previously, one can speak of rather well defined tunneling times or tunneling events. In this limit we can interpret the times that enter in the perturbative expansion of Z as the times for real tunneling events, and the sums and integrations as the means of including all tunneling histories in a partition function. Notice that it is very important that we understand that this interpretation has a meaning only when the tunneling barrier is narrow.

Also notice that only the tunneling times in the forward or top branch can have a physical interpretation as a tunneling of a real charge (we only observe increasing times, with the return branch being just a mathematical tool). The correct joint probability distribution of tunneling events should be obtained by integrating out all $t^{b\pm}$'s. This is a difficult task, and we shall appeal to a more intuitive picture that will allow us to sort out the most important contributions. This more intuitive picture can be extracted from the Coulomb gas model depicted in Figure 3-3.

The first step we take is to recast the sum in terms of dipole configurations, as opposed to a sum of charge configurations. The dipole is determined by a center of

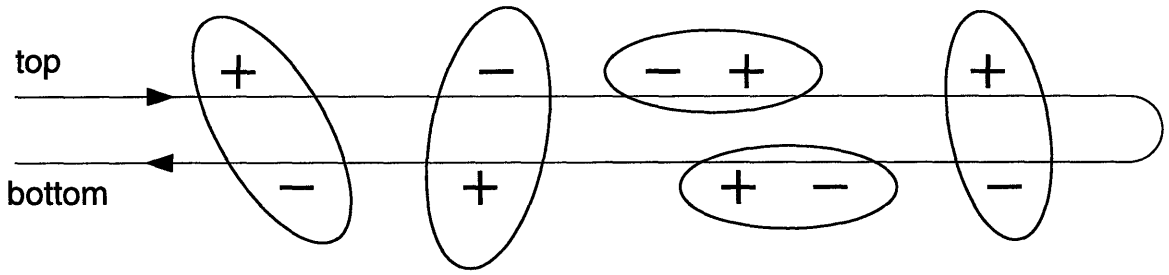

Figure 3-3: The charges that form the Coulomb gas can form a dipole phase. In this phase, the expression for Z can be recast as a sum over dipole strengths and positions, instead of summing over the locations of the + and − charges.

mass coordinate t_{cm} and a dipole strength p. There are four types of dipoles, as shown in Fig. 3-4. The type of dipole depends on which branches the + and − charges are located at. We call a t dipole one in which both charges are in the top branch. A b dipole is one where the charges are in the bottom branch. In a c_+ the + charge is on the top and the − on the bottom. In a c_- the converse is true, the − is on the top and the + on the bottom. This distinction is important, as we will see it later.

For a given charge configuration labeled by $\{Q_+^t, Q_-^t, Q_+^b, Q_-^b\}$ we associate a dipole configuration $\{n_t, n_b, n_+, n_-\}$, where the n's are, respectively, the number of t, b, c_+, and c_- dipoles. The n's and Q's are related by:

$$Q_+^t = n_t + n_+ \qquad Q_-^t = n_t + n_-$$
$$Q_+^b = n_b + n_- \qquad Q_-^b = n_b + n_+ \ .$$

Rewriting Z in terms of the n's instead of the Q's becomes a simple combinatoric task, which gives:

$$Z = \sum_{n_t,n_b,n_+,n_-} \frac{(-i)^{Q_+^t+Q_-^t}\ (i)^{Q_+^b+Q_-^b}}{Q_+^t!Q_-^t!\ Q_+^b!\ Q_-^b!}\ |\Gamma|^{Q_+^t+Q_-^t+Q_+^b+Q_-^b}$$
$$\times \binom{Q_+^t}{n_t} \binom{Q_-^t}{n_t} \binom{Q_+^b}{n_b} \binom{Q_-^b}{n_b} n_t!n_b!n_+!n_-! \times \text{ INTEGRAL}$$

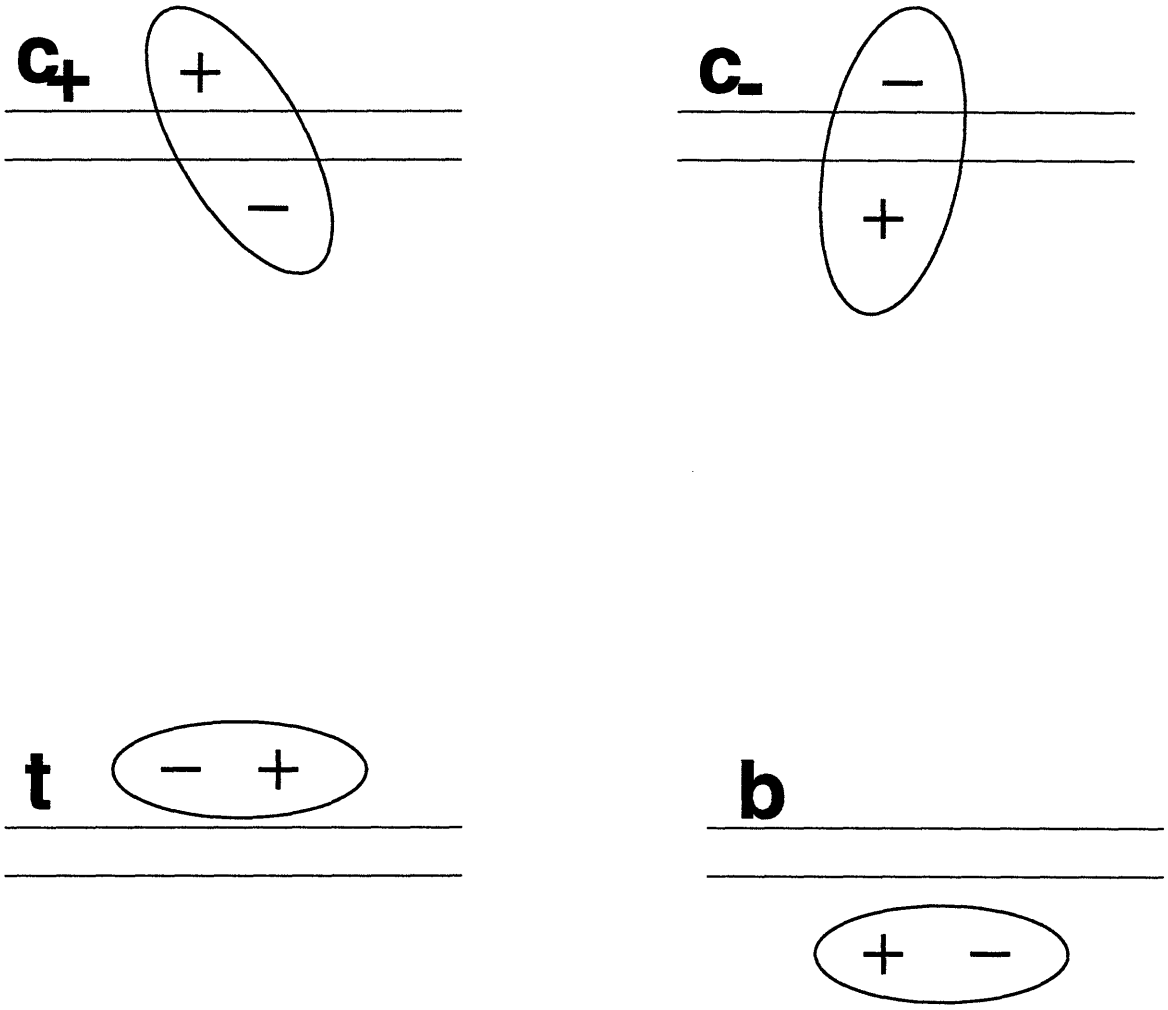

Figure 3-4: The four types of dipole, classified according to the position of the + and − charges comprising it. In the c_+ dipole the + charge is on the top branch and the − charge is on the bottom. In the c_- the − charge is on the top and the + is on the bottom. In the t dipole both charges are on the top branch, and in the b dipole both charges are on the bottom branch. Notice that only the $c_\pm$ dipoles contribute to a net current, as they create an imbalance of charge between the top and bottom branches. The t and b dipoles contribute to the noise, but not to the current.

$$= \sum_{n_t,n_b,n_+,n_-} \frac{(-1)^{n_t+n_b}\ |\Gamma|^{2(n_t+n_b+n_++n_-)}}{n_t!\ n_b!\ n_+!\ n_-!} \times \text{INTEGRAL} \tag{3.14}$$

where the INTEGRAL term contains the interactions between the charges integrated over all positions. The first approximation we will make is what we will call the "independent dipole" approximation. The attraction between opposite charges tends to bind them together, and, if the fugacity of the gas (measured by $|\Gamma|^2$) is small, we can to lowest order neglect the interaction between dipoles. The only interactions entering in the calculation of Z are the intra-dipole interactions. The INTEGRAL term in the dipole approximation can be factored as a product of the contributions of individual dipoles.

$$\text{INTEGRAL} = t^{n_t}\ b^{n_b}\ c_+^{n_+}\ c_-^{n_-} \tag{3.15}$$

where

$$t = \int_{-\infty}^{\infty} dp \frac{e^{-i\omega_0 p}}{(\delta + i|p|)^{2g}}\ ,\ b = \int_{-\infty}^{\infty} dp \frac{e^{-i\omega_0 p}}{(\delta - i|p|)^{2g}}\ ,\ c_\pm = \int_{-\infty}^{\infty} dp \frac{e^{-i\omega_0 p}}{(\delta \mp ip)^{2g}}\ . \tag{3.16}$$

One can check that $t + b = c_+ + c_-$, so that summing over all n_t and n_b in Eq. (3.14) can be shown to yield:

$$Z = e^{-|\Gamma|^2(c_+ + c_-)} \sum_{n_+,n_-} \frac{(|\Gamma|^2 c_+)^{n_+}}{n_+!} \frac{(|\Gamma|^2 c_-)^{n_-}}{n_-!}\ . \tag{3.17}$$

Let us now interpret this expression. As we mentioned above, only events occurring in the forward or top branches can be observed. Therefore, the occurrence of a dipole of the c_+ type implies a tunneling event in one direction occurring at the vicinity of the center of mass coordinate of the dipole. Conversely, a dipole c_- implies a tunneling event in the opposite direction. The statistical distribution of these center of mass coordinates of dipoles appears in the noise. The uncertainty of the location of the charges comprising the dipole with respect to the dipole center of mass also contributes to the noise; this intra-dipole contribution, however, is already partly taken care of in the first order perturbative calculation of noise, which can be seen to be nothing but the correlation between the position of the two charge components of a dipole.

The intra-dipole noise is in the high-frequency range, centered at $\omega = \omega_0 = e^*V/\hbar$. The contribution to the noise that we obtain with the Z in Eq.(3.17) is in the low-frequency range ($\omega \ll \omega_0$), where the positions of the charges and dipole centers are not distinguished. The reason why we summed over the dipoles of type t and b is that they do not contribute to the noise beyond the intra-dipole order. These types of dipole correspond to tunneling in one direction shortly followed by tunneling in the opposite direction, which contribute to noise in the time scale of the dipole size, included in the intra-dipole contribution.

With the interpretation above in hand, we can use Eq. (3.17) to argue that, in the dipole approximation, the tunneling events in either direction are independent, with a distribution that is Poisson-like with two parameters: $|\Gamma|^2 c_+$ and $|\Gamma|^2 c_-$. The probability of tunneling in one direction in an infinitesimal time Δt is $P_+ = |\Gamma|^2 c_+ \, \Delta t$, the probability of tunneling in the opposite direction is $P_- = |\Gamma|^2 c_- \, \Delta t$, and the probability of no tunneling event in this time is $1 - (P_+ + P_-)$.

This two-parameter Poisson distribution can be used to reproduce the results obtained for the tunneling current to first order in perturbation theory. The tunneling current is simply given by $I_t = e^*|\Gamma|^2(c_+ - c_-)$, *i.e.*, the net rate of tunneling in one direction. To obtain an expression for I_t in terms of V we need to evaluate c_+ and c_-:

$$c_+(\omega_0) = c_-(-\omega_0) = \int_{-\infty}^{\infty} dp \frac{e^{-i\omega_0 p}}{(\delta - ip)^{2g}} = 2\pi \frac{|\omega_0|^{2g-1}}{\Gamma(2g)} \, \theta(\omega_0) \; . \tag{3.18}$$

We can obtain the finite temperature results for $c_\pm$ by a conformal transformation [17]:

$$\int_{-\infty}^{\infty} dp \frac{e^{-i\omega_0 p}}{(\delta - ip)^{2g}} \rightarrow e^{i\pi g} \int_{-\infty}^{\infty} dp \frac{e^{-i\omega_0 p}}{|\frac{\sinh(\pi T p)}{\pi T}|^{2g}} \; , \tag{3.19}$$

which gives

$$\begin{aligned} c_+(\omega_0) &= c_-(-\omega_0) \qquad (3.20) \\ &= 2(\pi T)^{2g-1} B(g + \frac{i\omega_0}{2\pi T}, g - \frac{i\omega_0}{2\pi T}) \, \cosh(\frac{\omega_0}{2T}) \, (1 + \tanh(\frac{\omega_0}{2T})) \; , \end{aligned}$$

where B is the Beta function. Using these expressions for $c_\pm$ we obtain

$$I_t = 4e^*|\Gamma|^2(\pi T)^{2g-1}B(g+\frac{i\omega_0}{2\pi T}, g-\frac{i\omega_0}{2\pi T})\ \sinh(\frac{\omega_0}{2T})\ , \tag{3.21}$$

which is the same expression found by first order perturbation theory in Ref. [13]. For $T=0$, in particular, we find that $I_t \sim e^*|\Gamma|^2 V^{2g-1}$.

We now turn to the noise properties derived from this dipole approximation. Because the distribution in this approximation is Poisson like (and therefore uncorrelated), we should expect the noise to have a flat frequency dependence, *i.e.*, white noise. We are left with the problem of determining the amplitude of the noise. For this purpose, we will follow a calculation similar to one presented by Landauer [35]. Let $\langle j^2\rangle_{\Delta f}$ be the component of the noise power spectrum that falls in the frequency interval Δf. Let also $S(f) = \int_0^\Theta dt\ j(t)\ e^{-i\omega_0 t}$, where Θ is a time interval. These quantities are related by:

$$\langle j^2\rangle_{\Delta f} = \lim_{\Theta\to\infty}\frac{2|S(f)|^2}{\Theta}\ \Delta f\ . \tag{3.22}$$

The charge transferred in a small interval of time τ is $\pm e^*$ (with probabilities $|\Gamma|^2 c_\pm \tau$), or 0. We can write $j(t) = \sum_n j_0(t-n\tau)\ q_n$, with $q_n = \pm 1, 0$. Here j_0 is a narrow current pulse that fits a slot of time τ (the width of the pulse should determine a cut-off frequency above which the spectrum is no longer flat). We can then write

$$S(f) = \int_0^\Theta dt e^{-i\omega t}\sum_n j_0(t-n\tau) = \sum_n e^{-i\omega n\tau}q_n\int_{-n\tau}^{\Theta-n\tau} du\ e^{-i\omega u}j_0(u)\ . \tag{3.23}$$

The last integral can be approximated by the total charge that tunnels (e^*), since the pulse is narrow compared to τ. We then have $S(f) = e^*\sum_n e^{-i\omega n\tau}q_n$, and thus

$$|S(f)|^2 = e^{*2}\sum_{n,n'} e^{-i\omega n\tau}e^{i\omega n'\tau}q_n q_{n'}\ . \tag{3.24}$$

The uncorrelated tunneling implies that $\langle q_n q_{n'}\rangle = \langle q\rangle^2 + (\langle q^2\rangle - \langle q\rangle^2)\delta_{n,n'}$. After summing over n and n' we obtain that $|S(f)|^2 = e^{*2}N(\langle q^2\rangle - \langle q\rangle^2)$, where $N = \Theta/\tau$

is the number of time slots. Now $\langle q \rangle = |\Gamma|^2(c_+ - c_-)\ \tau$ and $\langle q^2 \rangle = |\Gamma|^2(c_+ + c_-)\ \tau$, and for small tunneling times compared to the time between tunneling $\langle q \rangle \ll 1$, so that we can neglect $\langle q \rangle^2$ and obtain

$$\langle j^2 \rangle_{\Delta f} = 2e^{*2}|\Gamma|^2(c_+ + c_-)\Delta f\ . \tag{3.25}$$

We can connect the white noise amplitude to the tunneling current using Eqs. (3.20) and (3.21), and obtain

$$\langle j^2 \rangle_{\Delta f} = 2e^* I_t\ \coth(\frac{\omega_0}{2T})\Delta f\ . \tag{3.26}$$

If we write $I_t = GV = G\omega_0/e^*$ and take the $\omega_0 \to 0$ limit, we obtain $\langle j^2 \rangle_{\Delta f}^{eq.} = 4TG\Delta f$, which is nothing but the Johnson-Nyquist equilibrium ($V = 0$) result. The non-equilibrium white noise can then be cast in a simple relation to the equilibrium Johnson-Nyquist noise, which is

$$\langle j^2 \rangle_{\Delta f} = (\frac{e^*V}{2T})\coth(\frac{e^*V}{2T})\ \langle j^2 \rangle_{\Delta f}^{eq.}\ . \tag{3.27}$$

The expression above for $T \to 0$ gives $\langle j^2 \rangle_{\Delta f} = 2e^* I_t\ \Delta f$, which is the classical expression for shot noise. Quantum corrections to the shot noise only come to order $|\Gamma|^4$ and higher, and thus do not appear in the independent dipole approximation (order $|\Gamma|^2$). Also notice that the expression connecting equilibrium and non-equilibrium noise $\frac{e^*V}{2T}\coth(\frac{e^*V}{2T})$ is universal independent of g and thus independent of interactions. This is consistent with the fact that the independent dipole approximation is a lowest order perturbative result, so that the assumptions necessary for the fluctuation-dissipation theorem are satisfied.

The dipole approximation therefore captures the uncorrelated part of the noise. In the next section we shall see how correlations come about.

3.4 Beyond the Independent Dipole Approximation

In this section we shall improve the dipole approximation. We have seen that the location of the centers of mass of two dipoles is uncorrelated in the approximation of the preceding section. In order to observe correlations one must include in the model the interactions between distinct dipoles. This is the next order correction to the INTEGRAL term in Eq. (3.14).

Consider two dipoles as show in Fig. 3-5. We take them, for the sake of illustration, to be both of the c_+ type. The INTEGRAL term can be written for this case as:

$$\int dt_1 dt_2 dp_1 dp_2 \frac{e^{-i\omega_0 p_1}}{(\delta - ip_1)^{2g}} \frac{e^{-i\omega_0 p_2}}{(\delta - ip_2)^{2g}} \tag{3.28}$$

$$\times \frac{[\delta + i(t_2 + p_2/2 - t_1 - p_1/2)]^{2g}}{[\delta + i(t_2 - p_2/2 - t_1 - p_1/2)]^{2g}} \frac{[\delta - i(t_2 - p_2/2 - t_1 + p_1/2)]^{2g}}{[\delta - i(t_2 + p_2/2 - t_1 + p_1/2)]^{2g}} .$$

For dipole separations that are large compared to dipole sizes ($|t_2 - t_1| \gg |p_1|, |p_2|$), we can expand the expression in the integrand to obtain

$$\int dt_1 dt_2 dp_1 dp_2 \frac{e^{-i\omega_0 p_1}}{(\delta - ip_1)^{2g}} \frac{e^{-i\omega_0 p_2}}{(\delta - ip_2)^{2g}} \left[1 + 2g \frac{p_1 p_2}{(t_2 - t_1)^2}\right] , \tag{3.29}$$

which after the p_1 and p_2 integration yields

$$\int dt_1 dt_2 \left(c_+ c_+ - 2g \frac{c'_+ c'_+}{(t_2 - t_1)^2}\right) \approx c_+ c_+ \int dt_1 dt_2 \, e^{-2g \frac{(c'_+/c_+)(c'_+/c_+)}{(t_2 - t_1)^2}} . \tag{3.30}$$

This can be generalized to any two types of dipole to

$$d_1 d_2 \int dt_1 dt_2 \, e^{-2g \frac{(d'_1/d_1)(d'_2/d_2)}{(t_2 - t_1)^2}} , \tag{3.31}$$

where $d_{1,2}$ can be any of t, b, c_+ or c_-, and $d'_{1,2}$ stands for the derivative of $d_{1,2}$ with respect to ω_0. Using a similar argument to the one we used to obtain the finite temperature expression for $c_\pm(\omega_0)$, we can obtain the finite temperature version of

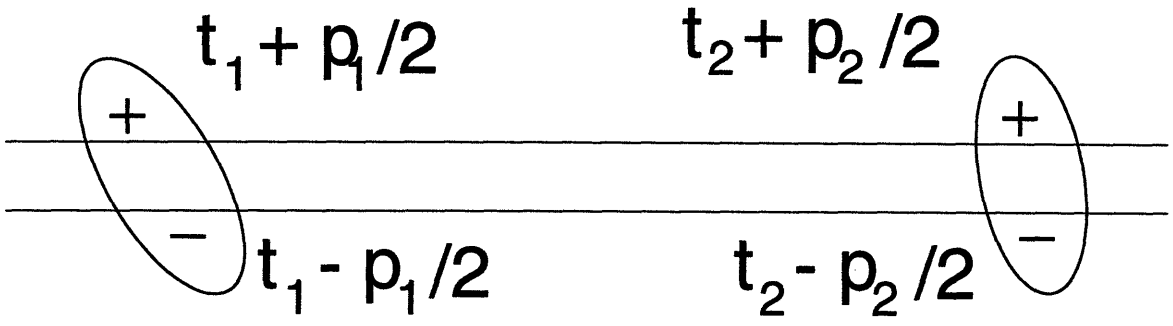

Figure 3-5: Two dipoles will interact because of the relative position between the charges that comprise them. The figure shows two dipoles with center of mass positions t_1 and t_2 and strengths p_1 and p_2.

the dipole-dipole interaction by simply substituting $t_2 - t_1$ by $\sinh[\pi T(t_2 - t_1)]/(\pi T)$ and using the $T \neq 0$ results for $c_\pm(\omega_0)$. Nevertheless, we will just concentrate for the rest of the chapter on the $T = 0$ problem.

From Eq. (3.31) we read that the dipoles interact through a $1/t^2$ potential. This dipole-dipole interaction gives rise to a non-trivial distribution of tunneling events, which show up in the noise spectrum as a cusp at zero frequency. Before proceeding to obtain the explicit form, including the strength of the singularity, we must understand when this picture that the charges can be assembled in pairs starts to break down, and correlations not contained in this dipole picture become important.

The assumption we made in order to obtain correlations as in Eq. (3.31) was simply that the dipole sizes were small compared to the separation between dipoles. The mean dipole separation is related to the average current I_t, and is given by e^*/I_t. The dipole size can be taken to be the d'/d in Eq. (3.31), since it is this term that enters in the interaction between the dipoles, and thus measures the distance between the $+$ and $-$ charges that form the dipole (Notice that, because the charges in the Coulomb gas are ± 1, the distance between the $+$ and $-$ charges equals the dipole strength). The expressions for t and b depend on the cut-off scale δ, whereas $c_\pm$ are finite as we take $\delta \to 0$ (we can show that $c_+ + c_- = t + b$, and that the divergences in t and b, which are purely imaginary, cancel each other). We then have that t'/t and b'/b must both scale as δ, and $c'_\pm/c_\pm = (2g-1)\omega_0^{-1}$ (using Eq. (3.20) and setting

$T \to 0$). Therefore the dipole approximation is good as long as $\omega_0^{-1} \ll e^*/I_t$, or $I_t \ll (e^{*2}/h)V$.

In the case of tunneling between edge states, this is the limit of a small tunneling current as compared to the Hall current. In the case of the 1-D channel, this limit corresponds to a small tunneling current as compared to the current for the non-interacting case. Because of the non-linear $I - V$ characteristic of the tunneling current in 1-D Luttinger liquids ($I_t \propto V^{2g-1}$), the cases $g > 1$ and $g < 1$ are quite distinct. For $g > 1$ the dipole phase exists for small applied voltages V, whereas for $g < 1$ the dipole phase exists for large V. Now, one can still use the results of the dipole phase to study the noise in the case of $g > 1$ and large V, and the case of $g < 1$ and small V, by resorting to the duality $g \leftrightarrow 1/g$ that connects the two configurations shown in Figs. 2-1a & 2-1b. The idea is that as one increases the applied voltage between the R and L edges in the configuration shown in Fig. 2-1b, the tunneling current I_t increases asymptotically, tending to the Hall current. Deviations from the Hall current correspond to "defects", or tunneling in the direction perpendicular to the Hall current, which is exactly the direction of tunneling shown in Fig. 2-1a. Similarly, one can go from the situation in Fig. 2-1a to the one in Fig. 2-1b by decreasing the applied voltage between the R and L edges. The bottom line is that, by wisely choosing which current direction to focus on, one can most often place the problem in the dipole limit for either one configuration or its dual with $g \leftrightarrow 1/g$. The regime in which the dipole picture fails is then at the crossover between the two configurations, where the gas will be in a plasma phase.

Now that we understand when the approximation is valid, let us look at its consequence in the noise spectrum. At zero temperature we only have either one of c_+ or c_- dipole types, depending on the sign of ω_0 (see Eq. (3.18)). For concreteness, let us take $\omega_0 > 0$, so that c_+ dipoles survive. Since $t'/t, b'/b \sim \delta$, the main correlations come from the interactions between c_+ dipoles (for voltages small compared to $1/\delta$), so that for large times the density-density correlation for c_+ dipoles (which equals the

current-current correlation) is given by

$$\langle \rho_+(t)\ \rho_+(0)\rangle_c \sim \langle \rho_+\rangle^2 \frac{-2g(2g-1)^2}{\omega_0^2 t^2}, \tag{3.32}$$

which gives a noise spectrum $S(\omega) = 4\pi g(2g-1)^2 \left(\frac{I_t}{\omega_0}\right)^2 e^{-|\omega|\lambda_c}/\lambda_c$, where λ_c is a short time scale cut-off (of order ω_0^{-1}) for the $1/t^2$ correlation. The leading singularity at low-frequency is then

$$S_{sing.}(\omega) = 4\pi g(2g-1)^2 (\frac{I_t}{\omega_0})^2\ |\omega|\ . \tag{3.33}$$

Since $I_t \propto V^{2g-1}$, the strength of the singularity has a non-linear dependence $V^{4(g-1)}$ on the applied voltage.

For the particular case of non-interacting electrons ($g = 1$) one can write $\frac{I_t}{\omega_0} = \frac{e^* D}{2\pi}$, where D is the transmission coefficient. The noise spectrum singularity is then $S_{sing.}(\omega) = \frac{e^{*2} D^2}{\pi}|\omega|$, which recovers the result of Ref. [31]. The effects of correlation due to the Pauli principle enter automatically in our formulation of the problem through the bosonization.

To finish this section, let us consider the case of equilibrium noise within the interacting dipole approximation. For $g > 1$ the tunneling current vanishes for $V = 0$. In the case of $g < 1$, however, we have to invoke the dual picture ($g \to 1/g$) in order to use the dipole language. In any case the $|\omega|$ singularity due to the dipole-dipole interaction vanishes for $V = 0$. The reason can be viewed very simply: the non-equilibrium voltage was responsible for the polarization of the dipole gas, and the dipole-dipole interaction gave the $1/t^2$ correlation. At equilibrium, the average dipole strength vanishes, and the interactions in this case must come from induced dipole, or "Van der Waal's" attraction, which for our log potentials goes as $1/t^4$. We can show that the low-frequency behavior of the noise no longer has the $|\omega|$ singularity, but has leading contributions from ω^2 and $|\omega|^3$. The leading singularity is then $\propto |\omega|^3$. The contributions calculated above are only the inter-dipole correlations. We should also account for the intra-dipole correlations, because for $V = 0$ the singularity at

the "Josephson" frequency falls to $\omega = 0$. We already calculated the intra-dipole contribution to the noise spectrum perturbatively in section 3.2, which for zero applied voltage is $S(\omega) \propto |\omega|^{2g-1}$. At low frequencies, the intra-dipole noise will be dominant for $g < 2$, while the inter-dipole noise will be dominant for $g > 2$. Notice that, in the equilibrium case, an expansion for Z like the one in Eq. (3.11) could be carried out with only one branch, since in equilibrium there is no need for the two branches of the Keldysh contour.

3.5 Diagrammatic Technique

The dipole gas picture we used to expand Z can be justified in more formal manner. In this section we shall present a systematic way to expand Z diagrammatically, which is used in one-dimensional dissipative quantum mechanics models [36]. In this expansion we can identify the terms we included in the dipole picture. The expansion is the formal support for the more intuitive and physical picture of the dipole gas. We will first present an introduction to the diagrammatic expansion, followed by the calculation for the equilibrium case and implications for the non-equilibrium case.

3.5.1 Introduction to the Diagrammatic Expansion

We start by returning to the expansion of $S(-\infty, -\infty)$ in terms of the bare charges in Eq. (3.11). We will focus on the expectation value of the T_c ordered product. Let us use a slightly different notation, using t's to denote the positions of $+$ charges and s's to denote the positions of $-$ charges. Let us take some configuration of charges labeled by t_i and s_j, with some of them on the top and some on the bottom branch (this way we do not have to worry about the superscripts for top and bottom branches, since we can keep track of where each charge is by its index). Using this notation, we can write for the T_c bracket:

$$P = \left(\frac{\prod_{i<j\leq Q}[\delta + i(t_i - t_j)\alpha_c(t_i, t_j)] \prod_{i<j\leq Q}[\delta + i(s_i - s_j)\alpha_c(s_i, s_j)]}{\prod_{i,j}[\delta + i(t_i - s_j)\alpha_c(t_i, s_j)]} \right)^{2g} , \qquad (3.34)$$

where $Q = Q^t_+ + Q^b_+ = Q^t_- + Q^b_-$, and $\alpha_c(t,t') = \pm 1$ depending on the ordering of t and t' along the Keldysh contour.

Consider now integer g's, such that $2g$ is even and the expression above does not change if we take $[\delta + i(t-t')\alpha_c(t,t')] \to [\delta\alpha_c(t,t') + i(t-t')]$. The expression for the T_c bracket can be simplified with the aid of the following identity which can be proved using partial fractions or properties of determinants [37]:

$$\frac{\prod_{i<j}(z_i - z_j)\prod_{i<j}(w_i - w_j)}{\prod_{i,j}(z_i - w_j)} = \det M(z,w) \ , \tag{3.35}$$

where M is a matrix defined by

$$M_{ij} = \frac{1}{z_i - w_j} \ . \tag{3.36}$$

The presence of the regulators δ in the expression for the T_c bracket slightly complicates how we apply the identity to the problem. By naively defining

$$M_{ij} = \frac{1}{\delta\alpha_c(t_i, s_j) + i(t_i - s_j)} \tag{3.37}$$

we would obtain terms in the numerator to order δ and higher that would not match the numerator of the expression for the T_c bracket. This corresponds to a different choice of regularization, and we shall return to this point later. The leading term (order δ^0), however, is exactly the same, and we proceed with the program, writing $(\det M)^{2g}$ for the T_c bracket.

Now notice that the terms M_{ij} correspond to the interaction between $+$ and $-$ charges, and that the expansion of the determinant will be comprised of all ways of combining $+$ to $-$ charges in pairs such that each charge only appears once in the expansion. Let us then associate a graph for any such dipole combination, as show in Fig. 3-6. When we raise the determinant to the power $2g$, the effect is to obtain all different ways to connect the $+$ and $-$ charges with lines, such that each charge is connected by exactly $2g$ lines (see Fig. 3-6, where we illustrate the case of $g = 1$).

The graphs so obtained give us a systematic way to account for the contributions

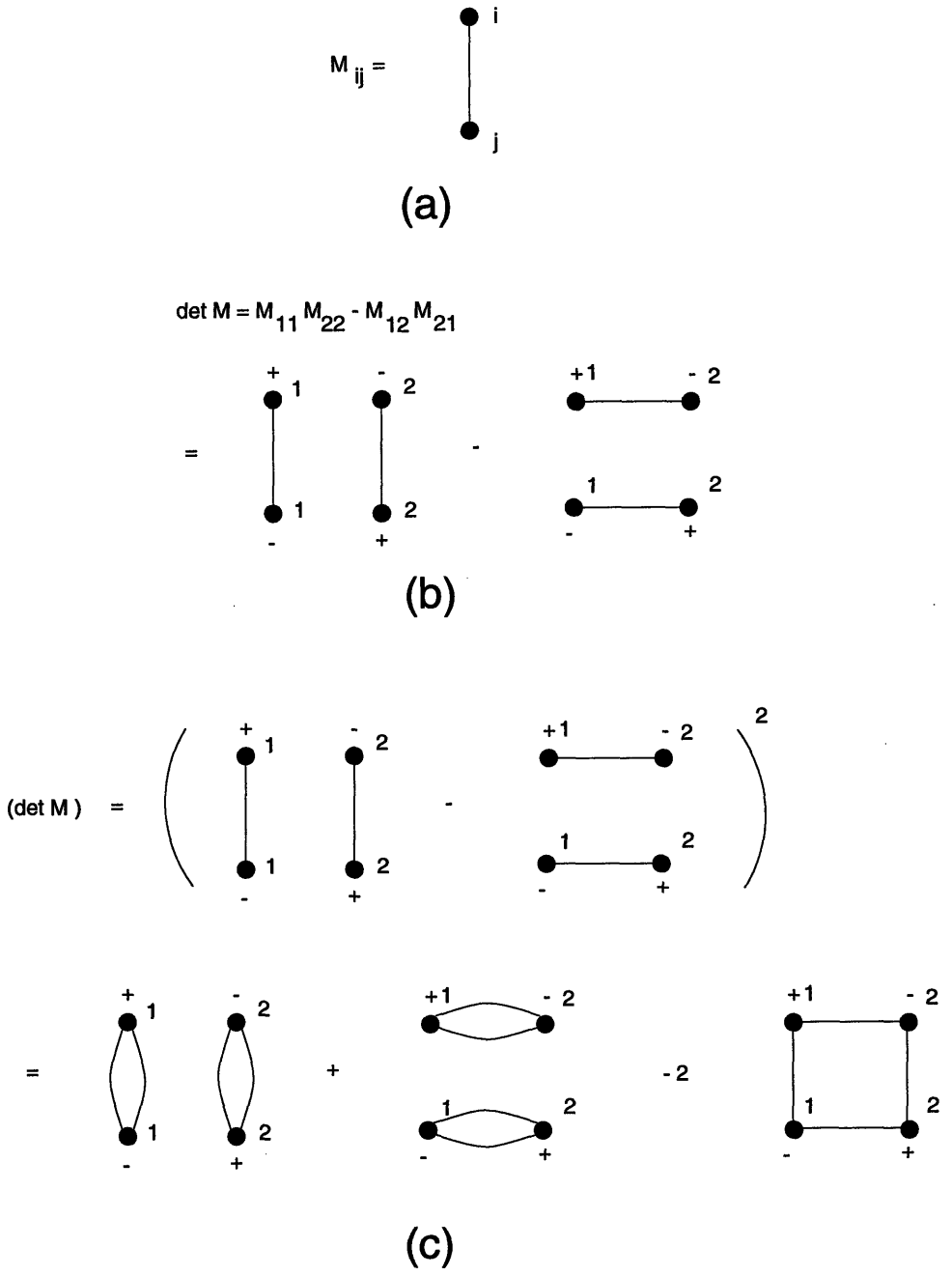

Figure 3-6: The expression for the correlation between many charges can be expressed as a power of the determinant of a matrix M. The matrix element M_{ij} can be represented diagrammatically as a line connecting a + charge at position t_i to a − charge at position s_j, as shown in (a). The determinant contains different ways of pairing the charges (b). Finally, when raising the determinant to the power $2g$ (done in this figure for $g = 1$), we generate different ways of connecting the charges such that exactly $2g$ lines leave each + charge and exactly $2g$ lines arrive at each − charge, as shown in (c).

to Z. The terms in the expansion where all charges are connected to one and only one other charge, as in Fig. 3-7a, are the independent dipole terms. Notice that each line in the graph that connects two distant charges roughly corresponds to $1/t$. When there are 4 charges, the lowest order in $1/t$ that can be obtained from the expansion comes from taking two dipoles and using one line from each to connect it to the other, so that there are 2 lines connecting the dipoles (Fig. 3-7b). In this way we obtain a $1/t^2$ term which corresponds to the leading dipole-dipole interaction. This systematic way to expand Z can be used as the formal support for the dipole picture developed in the previous section.

3.5.2 Equilibrium Case

To illustrate the power of the formalism described in the previous subsection, we will consider the equilibrium case at zero temperature. According to the dipole approximation, we expect that the current-current correlation should go as $1/t^4$ for $g \geq 2$. In this section we will show this is the case for any integer $g \geq 2$.

In equilibrium, we no longer need to use the Keldysh contour. Instead, to simplify the calculations we will work in Euclidean space, and we will take the ϕ field correlator to be $\langle 0|\phi(t)\phi(0)|0\rangle = -\ln(t^2+\delta^2)$. This differs from the original choice of correlation function only in that we have used a different cut-off. The choice given here corresponds to left and right movers scattering off each other instead of left movers with left movers, as in the original choice. However, for a single impurity, left movers and right movers should really be equivalent, so this choice should not make any important difference in the results. More importantly, in both cases we choose to regulate the correlator $\langle 0|\phi(t)\phi(0)|0\rangle$ consistently, no matter where it appears in the expression for P in Eq. (3.34). It may appear that whenever two tunneling events with the same charge interact, we could just ignore the cut-off in the numerator of P, since $\langle e^{i\gamma\phi(t)}e^{i\gamma\phi(0)}\rangle = (t^2+\delta^2)^g$ is not singular as δ goes to zero; recall that $\gamma = \sqrt{g}$. However, the δ's in this correlator will be multiplied by other correlators that are singular as δ goes to zero, so it turns out that the answer depends on how we regulate the numerator. Because we are using the Coulomb gas picture, for now we will choose

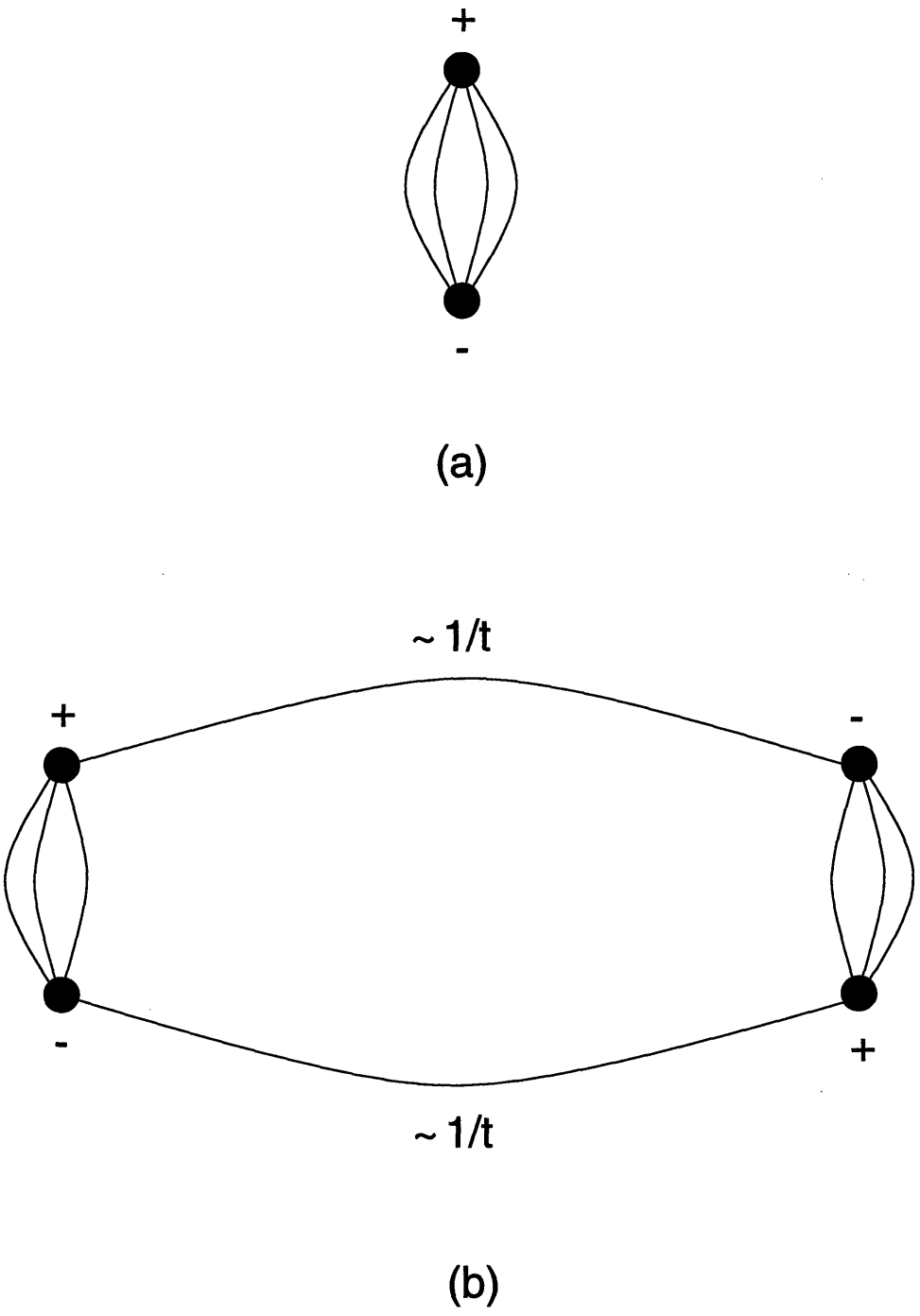

Figure 3-7: The graph corresponding to independent dipoles is shown in (a), with all lines leaving the + charge arriving at the − charge (here we use $g = 2$ for illustration). One of the graphs contributing to the dipole-dipole correlation is shown in (b). Each leg connecting the two dipoles contributes to order $1/t$, so that the dipole-dipole correlation is of order $1/t^2$.

to keep the δ's in the numerator.

With our choice of regulator, the expression P for the bracket needed to evaluate $S(-\infty,-\infty)$ becomes

$$P=\left(\frac{\prod_{i<j\leq Q}((t_i-t_j)^2+\delta^2)\prod_{i<j\leq Q}((s_i-s_j)^2+\delta^2)}{\prod_{i,j}((t_i-s_j)^2+\delta^2)}\right)^g. \tag{3.38}$$

In this equation, the positive charges are at the t_i and the negative charges are at the s_i. Because we are in Euclidean space, we no longer have to use time-ordering when we evaluate the integrals over the t_i and s_i.

To simplify the expression for P for any integer g, we will use the same procedure as in Ref. [36]. We will write $P=AB$, where A equals P with the δ's in the numerator set to zero, and B is the correction due to the δ's in the numerator of P. Then

$$A=\left(\frac{\prod_{i<j\leq Q}(t_i-t_j)^2\prod_{i<j\leq Q}(s_i-s_j)^2}{\prod_{i,j}((t_i-s_j)^2+\delta^2)}\right)^g, \tag{3.39}$$

and B is equal to sums over products of $\delta^2/(t_i-t_j)^2$ and $\delta^2/(s_i-s_j)^2$, where any one of these expressions can occur at most g times in a product. B comes from writing each correlator in the numerator as $(t_i-t_j)^2\left[1+\delta^2/(t_i-t_j)^2\right]$ and factoring out the $(t_i-t_j)^2$ part.

We can again use the identity in Eq. (3.35) to simplify the expression for A. If we define the matrix $M(\delta)$ as

$$M_{ij}(\delta)=\frac{1}{t_i-s_j+i\delta}, \tag{3.40}$$

then A is given by

$$A=\left[\det M_{ij}(\delta)\det M_{ij}(-\delta)\right]^g. \tag{3.41}$$

As explained in the previous subsection, if we represent each charge by a point and each factor of $\frac{1}{t_i-s_j\pm i\delta}$ by a directed line, then we obtain all the different ways to connect the positive charges to the negative charges so that each charge is connected by exactly $2g$ lines, (half of which are pointing toward the line, and half away from

the line).

We can also give a graphical interpretation of B. Once we have a graph from A, to take into account the fact that the numerator is also regulated, we obtain our graphs for P by joining any number of pairs of similar charges with the pair of edges $1/(t_i - t_j)^2$ or $1/(s_i - s_j)^2$. Each of these edges is accompanied by a factor of δ, and any pair of charges can be joined by at most g of these pairs of edges. Thus B introduces an interaction between like-charged particles.

In the graphs of A and B, it is important to keep track of the number of vertices, V, the number of edges, E, and the number of factors of δ in the numerator, $-f$. If we are calculating the charge-charge correlation function, and we insert $2N$ additional charges, then the number of vertices is $V = 2N + 2$. For any connected graph of A, we then have $E = (2N + 2)g$ and $f = 0$. Once we include the effects of B, f is no longer equal to 0, but $E + f$ is still given by

$$E + f = (2N + 2)g. \tag{3.42}$$

Also, it is important to note that any connected graph is also 1PI. This way of describing the bracket, P, works similarly in Minkowski space.

Next, we will evaluate the connected correlation function of $\langle 0|e^{i\gamma\phi(t)}e^{-i\gamma\phi(s)}|0\rangle$ for any integer $g > 1$. (The case when $g = 1$ was considered in Ref. [36].) This calculation will also work for the correlation functions $\langle 0|e^{\pm i\gamma\phi(t)}e^{\pm i\gamma\phi(s)}|0\rangle$, so that these results can be used to find the leading dependence on $t - s$ of the current-current correlation functions.

At the $(2N)^{\text{th}}$ order in perturbation theory, we have

$$\langle 0|\Gamma e^{i\gamma\phi(t)}\Gamma^* e^{-i\gamma\phi(s)}|0\rangle = \int_{-\infty}^{\infty} \frac{|\Gamma|^{2N+2}}{N!N!} \prod_{k=1}^{N} dt_k \prod_{k=1}^{N} ds_k AB, \tag{3.43}$$

where A and B depend on t, s, the t_k's and the s_k's. To obtain the connected correlation function, we just need to consider the connected graphs in the expression on the right-hand side of the above equation.

To evaluate the integrals, we will perform contour integrals where we complete the contour in the upper half plane. Thus, for each vertex, t_j, we will be evaluating residues for all the poles occurring at $t_j = s_k + i\delta$. (Here, we are using t_j and s_k to stand for any type of vertex.) We note that in B, it appears that we will have poles on the real axis. However, we know that the original expression for AB does not have any poles on the real axis. This means that if we sum over all the graphs for B, these poles cancel, which implies that as long as we integrate over the variables in each of these graphs in the same order, we can just ignore the poles on the real axis.

We can describe the process of evaluating residues diagrammatically, as explained in Ref. [36]. If the multiplicity of the pole at $t_j = s_k + i\delta$ is equal to one, then there is only one edge, e_{jk}, that joins t_j to s_k and represents this kind of pole. In this case, when we evaluate the residue, we just "collapse" the vertex t_j and the edge e_{jk}. This means we remove the vertex t_j and edge e_{jk}, and then reconnect all the other edges that were originally connected to t_j to s_k instead. If the other end-point of any of these edges was also connected to s_k, the edge becomes $1/(ic\delta)$, for some integer c. Otherwise, it remains an edge. Consequently, the total number of edges decreases by at least one, and the sum of edges and factors of δ in the numerator decreases by exactly one. Also, the graph remains connected and 1PI.

When the multiplicity, m, of a pole is greater than one, then instead of collapsing only one edge, we must collapse all the m edges that correspond to the pole. In addition, we must take $m-1$ derivatives with respect to t_j. Each of these derivatives increases the number of other legs connected to t_j by one, so we obtain $m-1$ new legs. Once we have created these $m-1$ new edges and collapsed both the vertex and the m edges corresponding to the pole, we again find that the number of edges decreases by at least one, and the sum, $E+f$, still decreases by exactly one. Again, the graph remains 1PI.

Now we can count the number of edges and factors of δ that remain after we have done all the integrations. The original graph with $2N+2$ vertices has $E+f=$

$(2N+2)g$. After we integrate over the $2N$ inserted charges, this sum becomes

$$E + f = (2N+2)g - 2N, \tag{3.44}$$

and the only two remaining vertices are t and s. Because the graph must still be 1PI, we must have at least 2 edges connecting t and s. Since the total number of edges always decreases by at least one, we also have

$$2 \leq E \leq (2N+2)g - 2N. \tag{3.45}$$

We will let $l_N = (2N+2)g - 2N$. Lastly, because the final answer must be symmetric in t and s, after we sum over all the graphs we can only have even values for E.

Putting all of this together, we find that the correlation $\langle 0|\Gamma e^{i\gamma\phi(t)}\Gamma^* e^{-i\gamma\phi(s)}|0\rangle$ must have the form

$$|\Gamma|^2 \frac{1}{(t-s)^{2g}} + \sum_{N=1}^{\infty} |\Gamma|^{2(N+1)} \left(a_{N2} \frac{1}{\delta^{l_N-2}(t-s)^2} + a_{N4} \frac{1}{\delta^{l_N-4}(t-s)^4} + \ldots + a_{l_N} \frac{1}{(t-s)^{l_N}} \right), \tag{3.46}$$

where the a_{Nj}'s are constants that are determined from integrating the explicit graphs. In order to interpret these results, for the equilibrium case it is helpful to renormalize the coupling. We will replace each Γ and Γ^* with $\Gamma\delta^{g-1}$ and $\Gamma^*\delta^{g-1}$. This just takes into account the self-interaction of the charges and a rescaling of the time variables.

The correlation function is then

$$|\Gamma|^2 \frac{\delta^{2g-2}}{(t-s)^{2g}} + \sum_{N=1}^{\infty} |\Gamma|^{2(N+1)} \left(a_{N2} \frac{1}{(t-s)^2} + a_{N4} \frac{\delta^2}{(t-s)^4} + \ldots + a_{l_N} \frac{\delta^{l_N-2}}{(t-s)^{l_N}} \right). \tag{3.47}$$

This general form is true to all orders in Γ. Also, note that the derivation of this result did not depend on the sign of the charges at t and s, so we will obtain a similar expression for two positive charges or two negative charges at t and s. For large times,

(or small cut-off δ) the leading behavior is

$$\frac{1}{(t-s)^2}\sum_{N=1}^{\infty}|\Gamma|^{2(N+1)}a_{N2}+\frac{\delta^2}{(t-s)^4}\sum_{N=1}^{\infty}|\Gamma|^{2(N+1)}a_{N4}. \tag{3.48}$$

This expression appears to go as $1/(t-s)^2$ instead of as the $1/(t-s)^4$ predicted by the dipole picture. However, as we shall show shortly, if both the denominator and numerator are regulated in the same way, as in Eq.(3.38), then $a_{2N}=0$ for all N, so the leading behavior does go as $\delta^2/(t-s)^4$ to all orders in perturbation theory.

Before showing that $a_{N2}=0$ for all N, we will first use the previous calculation to describe a systematic way to determine the leading behavior of each graph. First, we note that a final answer of $1/(t-s)^n$ corresponds to a graph with n legs joining the vertex t to the vertex s. If we remove these n legs, the graph breaks into 2 disconnected components, one containing t, and the other containing s. Because the integrations consist only of collapsing vertices and edges and also making extra copies of edges, these n legs must have come from l legs in the original graph, where $l\leq n$. In addition, because the process of integration does not change the connectedness of the graph, when the l legs in the original graph are removed, it will break into two disjoint, connected graphs, one containing t and the other containing s. An example of this is given in Fig. 3-8. We also note that since each graph is 1PI, to break it into two we must remove at least 2 edges.

This all implies that the only graphs that can have a leading term of $1/(t-s)^2$ are those that are broken into 2 when 2 legs are removed; the only graphs that can have a contribution of $1/(t-s)^4$ are those that are broken into 2 when 2, 3 or 4 legs are removed, and, in general, only the graphs that can be broken into two connected pieces when 2, 3, ..., or n legs are removed can contribute a term of order $1/(t-s)^n$. A simple counting argument shows that when l legs are removed, the maximum net charge either of the 2 resulting graphs can have is $l/2g$. Because the net charge is always an integer, when l is equal to 2 (and g is greater than 1) this means that the net charge must be zero.

Thus we can classify the graphs according to what their leading behavior is, and

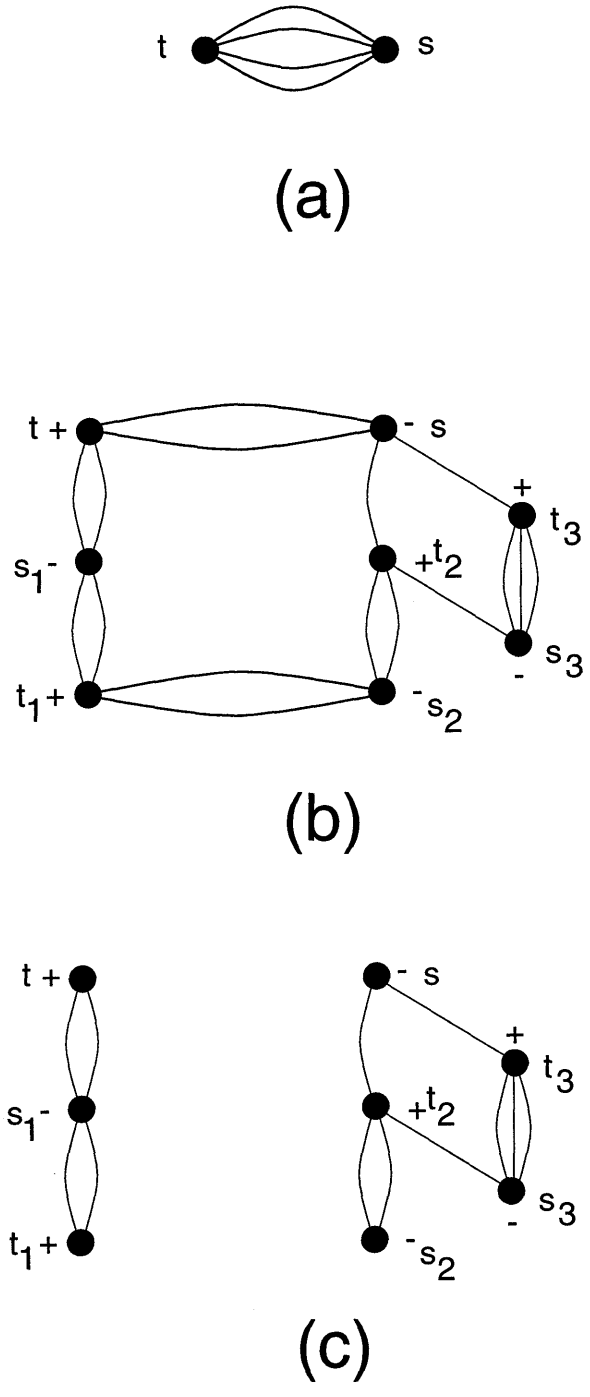

Figure 3-8: A sample graph with $g = 2$ that gives a contribution of $1/(t-s)^4$ after it is integrated. The final graph with 4 legs is shown in (a). It is obtained by integrating over the vertices t_1, t_2, t_3, s_1, s_2 and s_3 in the graph shown in (b). The 4 final legs in the final graph come from the 4 bold-faced legs. In (c), the two disjoint graphs (or multipoles) resulting from removing the 4 bold-faced legs are shown.

we can determine which graphs will contribute to any particular term in the expansion in Eq.(3.47). To make contact with the previous subsection, we remark that for the insertion of two charges, the only configuration that breaks into two graphs when two lines are removed is precisely the one shown in Fig. 3-7b.

To arrive at a useful way of estimating graphs (which should also apply in the non-equilibrium Minkowski space formalism), we observe that every time we evaluate a residue of a pole at $t_k = s_j + i\delta$, we are taking t_k to be very close to s_j. If we then evaluate an $s_j = t_l + i\delta$ residue, we evaluate s_j close to t_l, so in turn that means t_j is also close to t_l. Following through on this observation, we see that for the final result, all the points are either evaluated close to t or close to s, and whether it is t or s depends on whether, when we remove the n legs, the point is in the graph connected to t or to s. Thus it appears that the only contributions to the integral come from all the ways to take some of the vertices close to t and the remaining vertices close to s. The exponent of the leading contribution will then be determined by the net charge of each of the two resulting subgraphs. This is exactly what was done in Section 3.4 for the case of two dipoles.

We now return to calculating the coefficient, a_{N2}, of the $1/(t-s)^2$ part of the charge-charge correlator. From the previous discussion, we know that this should come from all ways of forming a neutral multipole around t and a neutral multipole around s. As long as $t - s >> \delta$, we can assume that all the charges in each multipole are much closer to each other than t and s are to each other. We will let $t_0 \ldots t_{m-1}$ and $s_0 \ldots s_m$ be the charges close to t and $t_{m+1} \ldots t_N$ and $s_{m+2} \ldots s_N$ be the charges close to s. To simplify the notation, in most of what follows we will let t_m equal t and s_{m+1} equal s. Next, we will change variables so that $t_i = p_i + t$, $s_i = q_i + t$ for the charges close to t and $t_j = p_j + s$, $s_j = q_j + s$ for the charges close to s. Then the expression for P becomes

$$P = P_1 P_2 I^g, \tag{3.49}$$

where

$$P_1 = \frac{\prod_{i,j=0;i<j}^{m} \left((p_i - p_j)^2 + \delta^2\right)^g \left((q_i - q_j)^2 + \delta^2\right)^g}{\prod_{i,j=0}^{m} \left((p_i - q_j)^2 + \delta^2\right)^g}, \tag{3.50}$$

$$P_2 = \frac{\prod_{i,j=m+1;i<j}^{N} \left((p_i - p_j)^2 + \delta^2\right)^g \left((q_i - q_j)^2 + \delta^2\right)^g}{\prod_{i,j=m+1}^{N} \left((p_i - q_j)^2 + \delta^2\right)^g}, \tag{3.51}$$

and

$$I = \frac{\prod_{i=0}^{m} \prod_{j=m+1}^{N} \left((t-s+p_i-p_j)^2 + \delta^2\right) \left((t-s+q_i-q_j)^2 + \delta^2\right)}{\prod_{i=0}^{m} \prod_{j=m+1}^{N} \left((t-s+p_i-q_j)^2 + \delta^2\right) \left((t-s+q_i-p_j)^2 + \delta^2\right)}. \tag{3.52}$$

P_1 and P_2 just look like the original integral, but for a smaller number of charges, so they contain the intra-multipole interactions. The expression for I contains all the interactions between the two different multipoles. In the numerator, the positive and negative charges of the first multipole interact with charges of the same sign in the second multipole, and in the denominator the charges of the first multipole interact with the charges of opposite sign in the second multipole. Because the multipoles are both neutral, and because every factor in Eqn. (3.52) depends on $t - s$, both the numerator and denominator have the same number of factors of $t - s$. Once we divide through by $t - s$, similar counting tells us that the number of times $p_i/(t-s)$, $q_i/(t-s)$ and $\delta^2/(t-s)^2$ each appear in the numerator equals the number of times each of these appear in the denominator. If we expand I out for large $t-s$ and count all the terms that contribute to order $1/(t-s)^2$, we find

$$I = 1 + \frac{1}{(t-s)^2} 2 \sum_{i,j} (p_i p_j + q_i q_j - p_i q_j - p_j q_i), \tag{3.53}$$

where p_i and q_i run over all the charges in the first multipole and p_j and q_j run over all the charges in the second multipole. Then

$$I^g = 1 + \frac{2g}{(t-s)^2} \sum_{i,j} (p_i p_j + q_i q_j - p_i q_j - p_j q_i). \tag{3.54}$$

The important feature of the $1/(t-s)^2$ part is that it is odd under changing the signs of the coordinates of all the charges in only one multipole. Meanwhile, $P_1 P_2$ is even under such a sign change, so once we integrate over all the coordinates, the $1/(t-s)^2$ part vanishes and we are left only with the $1/(t-s)^3$ (which should vanish once we sum over all configurations of the charges) and the $1/(t-s)^4$ parts. Thus, the

coefficients, a_{2N} should vanish to all orders in perturbation theory and the charge-charge correlation functions, $\langle 0|\Gamma e^{i\gamma\phi(t)}\Gamma^* e^{-i\gamma\phi(s)}|0\rangle$, should go as $a_4\delta^2/(t-s)^4$, for some constant a_4. It is considerably more difficult to evaluate this constant.

One final remark is that if we had regulated only the denominator, then the previous argument would not have gone through: the $\delta^2/(t-s)^2$'s from the denominator would no longer be canceled by the $\delta^2/(t-s)^2$'s from the numerator, so that a_{2N} would be non-zero. In this case, the correlation functions instead would go as $1/(t-s)^2$.

3.5.3 Implications for the Non-equilibrium Case

Even for the non-equilibrium case, we can use our analysis of the graphs in the preceding subsection to guide us in determining which graphs should give the leading contributions to the current-current correlation functions. To calculate the singularity at $\omega = 0$, we can use the same neutral multipole expansion as in the end of the previous section. The only changes to Eqs. (3.50, 3.51, and 3.52) for the intra-multipole and inter-multipole interactions are that we must now use the non-equilibrium regulators which depend on the $\alpha_c(t_i, s_j)$'s. Also, Eq. (3.50) for the multipole P_1 will now be multiplied by $\prod_{i=0}^{m} e^{i\omega_0 p_i} \prod_{j=0}^{m} e^{-i\omega_0 q_i}$ and Eq. (3.51) for P_2 will be multiplied by $\prod_{i=m+1}^{N} e^{i\omega_0 p_i} \prod_{j=m+1}^{N} e^{-i\omega_0 q_i}$. Consequently, $P_1 P_2$ no longer remains unchanged when all the signs of the vertices in one multipole are reversed. Therefore, according to Eq. (3.54) the contribution to the current-current correlation function when one multipole is close to vertex t and the other is close to vertex s goes as

$$1 + \int \prod_{\substack{k=0 \\ k\neq m}}^{N} dp_k \prod_{\substack{l=0 \\ l\neq m+1}}^{N} dq_l \, P_1 P_2 \sum_{i,j} (p_i p_j + q_i q_j - p_i q_j - p_j q_i) \frac{2g}{(t-s)^2}, \tag{3.55}$$

where p_i and q_i are in the first multipole and p_j and q_j are in the second multipole. Also, we only take the connected graphs in the multipoles P_1 and P_2. Thus, to all orders in Γ, the correlator goes as $1/(t-s)^2 + O\left(1/|t-s|^3\right)$. This means that, at low frequency, the noise spectrum should have a singularity that goes as $|\omega|$ at every order in Γ. Here we are assuming that for $g > 1$ the neutral multipoles are all bound,

just as they are in the equilibrium case.

In the non-equilibrium case, we also expect singularities at $\omega = \pm\omega_0$ and possibly also at $\omega = n\omega_0$ for other integer values of n. To find the leading behavior at these singularities we use the fact that the expression for P in Eq. (3.34) can be expressed as a product AB. As in the preceding subsection, A is a determinant, and B contains the corrections that naively go as $(1 + O(\delta))$. For the non-equilibrium case, A was defined at the beginning of this section as $\det M_{ij}$ where

$$M_{ij} = \frac{1}{\delta\alpha_c(t_i, s_j) + i(t_i - s_j)}. \tag{3.56}$$

The graphs for the A defined here are identical to those in the previous subsection, except for the choice of regulator. This means that all of our previous counting arguments should apply. However, the form of B is now much more complicated than before, so it is not clear whether it modifies the counting in the same simple way as before. Because the expression for P in Eq. (3.34) and the expression for A both contain the information about which branch each charge is on, and since the only difference between the two expressions is the choice of regulator, for convenience we will choose to work with $A = \det M_{ij}$ instead of with P. (In the equilibrium case, we have seen that picking a different regulator does not change the types of terms that can appear in the final answer; it just changes the value of the coefficient in front of each term, possibly setting some to zero. In case of a discrepancy, the choice of regulator should reflect the physics at hand, so it is useful to keep in mind that in P the interactions in the Coulomb gas are regulated and in A the fermion-like propagators in the matrix M are regulated.)

For $\det M_{ij}$, our counting and classification of graphs proceeds as before. This implies that if we can break the graph into two connected multipoles with charge Q and $-Q$, respectively, then the graph will give a leading contribution of

$$a_Q \frac{e^{iQ\omega_0 t} e^{-iQ\omega_0 s}}{(t-s)^{2Qg}}, \tag{3.57}$$

as long as all charges within a multipole are close to one another. This will give the

singularity $|\omega \pm Q\omega_0|^{2Qg-1}$. For example, the graph in Fig. 3-8b will give a contribution as in Eq. (3.57) with $Q = 1$ and $g = 2$. Without performing the integral, we cannot determine whether a_Q (which can depend on δ and ω_0) is non-zero. However, from this line of reasoning, we can conclude that the $|\Gamma|^2|\omega \pm \omega_0|^{2g-1}$ singularity should only receive corrections that go at least as $|\omega \pm \omega_0|^{2g-1}$ at all higher orders in $|\Gamma|^2$. Similarly, at higher multiples of ω_0 we expect the singularities to be even smoother because they go at least as $|\omega \pm Q\omega_0|^{2Qg-1}$.

As a check on these calculations, we note that we can apply the same analysis of the graphs and similar counting arguments even at $g = 1$. In this case, every connected graph is just a simple polygon with alternating charges at the vertices. It is straightforward to see that when any such graph is divided into two disjoint, connected parts, each part can only have a total charge of 0 or ± 1, and exactly two lines must be cut. Therefore, the only singularities we can obtain are $|\omega|$ and $|\omega \pm \omega_0|$, with no higher order corrections. These results agree with those in Ref. [31] and give strong evidence that our method of analyzing the graphs works even for the non-equilibrium case.

3.6 Conclusion

In this chapter we defined a framework for the study of both equilibrium and non-equilibrium noise in 1-D Luttinger liquids. The interactions give rise to correlations that are manifest in the noise spectrum. The correlations are responsible both for algebraic singularities in the noise power spectrum and for the nonlinear dependence of the strength of such singularities on either the applied voltage between the terminals of the 1-D system or the temperature. The information carried by both the form of the singularities and their strength can help us identify Luttinger liquid states in experiments.

The picture of the tunneling in terms of the Coulomb gas (and its dipole gas interpretation) is attractive because it gives us an intuitive way to think about the tunneling in the Keldysh formalism. This picture provides a unified description of the

low and high frequency noise: correlations between different dipoles define the structure of the noise near zero frequency, whereas correlations between the two charges within the dipole should contribute to the noise near the "Josephson" frequency $\omega_J = e^*V/\hbar$. Using formal diagrammatic techniques we have justified this interpretation, and, for integer g, we have obtained exact answers for the form of the singularity in the equilibrium case.

One particularly striking result we obtained is that the form of the leading singularity at zero frequency ($\propto |\omega|$) is the same for strongly correlated Luttinger liquids as well as for non-interacting systems. The effects of correlations in the case of low-frequency noise is present only in the strength of the singularity, with a strong non-linear dependence on the applied voltage that is proportional to $V^{4(g-1)}$.

Although our Coulomb gas picture and the accompanying formalism has enabled us to calculate the form of the singularities to all orders in perturbation theory, beyond the order $|\Gamma|^4$ it is too cumbersome to find the strength (i.e. the coefficient in front) of these singularities. We would also like to point out that the structure of the noise far away from the frequencies $n\omega_J$, at higher orders in perturbation theory, is unknown; the information we are able to obtain is limited solely to frequencies near the singular points. One exception is the exactly solvable case of $g = 1$, where we find that the noise spectrum must have the form $a + b|\omega| + c|\omega \pm \omega_J|$, where a, b and c can be calculated from the non-equilibrium voltage and the transmission coefficient. Thus in this case we recover the results for non-interacting electrons. Indeed, the framework we presented can be used with $g = 1$ for studying coherence effects which appear in the noise for non-interacting electrons and are due to the Pauli principle, because the statistics enter in the formulation we use through the bosonization.

There are two points in this work that need further exploration. The first is the apparent fine point of better understanding the role of the short distance cutoff in our calculations. We need either to determine whether the non-equilibrium noise is sensitive to our choice of regulator or else to show that our choice of regulating the fermion-like propagators instead of the Coulomb gas is the physical one. The second, and more important, question is to understand non-perturbative effects. For

example, one expects that the position of finite voltage singularities should depend on Γ. In the case of tunneling between edge states, when we increase the current, the frequency should shift from $e\frac{V}{\hbar}$ to $\frac{e}{m}\frac{V}{\hbar}$ as we go from the configuration in Fig. 2-1b, where the electrons are tunneling, to the one in Fig. 2-1a, where the quasi-particles are tunneling. This is not reflected in our perturbative calculations. However, we have evidence that within our Coulomb gas picture this shift can be explained by non-perturbative effects, and we address this issue in the next chapter.

Chapter 4

Scattering Approach

4.1 Introduction

In the previous chapter, the noise spectrum of the tunneling current between edge states directly at the point contact was calculated perturbatively. To low orders in the tunneling amplitude, we found that there was a singularity at $\omega = 0$; for small ω the noise spectrum has the form $S_{SN} + S_{\text{sing}}(\omega)$, where S_{SN} is the zero-frequency shot noise and $S_{\text{sing}}(\omega) = c|\omega|$. The slope c of the $|\omega|$ singularity has a strong non-linear dependence on the applied voltage V ($c \propto (2g-1)^2 V^{4(g-1)}$), which is another signature of Luttinger liquid behavior (to be contrasted with the case of non-interacting electrons, $g = 1$, where the slope is independent of V). The exponent g characterizes the Luttinger liquid behavior. This low-frequency part of the spectrum is the one more easily accessible experimentally. Secondly, there is another singularity at $\omega = \omega_J$ where $\omega_J = e^*V/\hbar$ is the Josephson frequency of the electron ($e^* = e$) or quasiparticle ($e^* = \nu e$) that tunnels through the point contact. The shape of this singularity depends on g and goes as $|\omega \pm \omega_J|^{2g-1}$. Measurements of the location of this singularity would give the value e^* of the charge of the carriers of the current, which would be yet another way of observing fractional charge from noise measurements. The method originally suggested is to measure the shot noise, which for small tunneling amplitude is related to the tunneling current I_t by $S_{SN} = 2e^*I_t$ [38, 39, 40]. Lastly, for $g > 1$, we found that the singularities at both $\omega = 0$ and

$\omega = \omega_J$ should persist to all orders in perturbation theory.

These results present a puzzle which we describe below and address in this chapter. The case of $g = \nu < 1$ corresponds to a single quantum Hall droplet with a constriction. In this case, quasiparticles can tunnel across the constriction, from one edge to the other (see Fig. 2-1a). These quasiparticles have fractional charge e^*, given by νe. If the constriction is made narrower, the tunneling amplitude will increase. As the constriction is further narrowed, eventually the droplet will break into two disconnected pieces, and now only electrons will be able to tunnel from one edge to the other (see Fig. 2-1b). Their tunneling should once again behave like tunneling in a chiral Luttinger liquid, but with new exponent $\tilde{g} = 1/g$ and charge equal to e. This is the physical picture behind the duality seen in reference [24]; as the tunneling amplitude is increased (or the voltage is decreased) g goes to $1/g$. Similarly, if we start with the two quantum Hall droplets with exponent $\tilde{g}$ and increase the tunneling amplitude of the electron, eventually we will obtain the single droplet picture with exponent $g = 1/\tilde{g}$.

In light of this duality and the results of Chapter 3, the following question arises. If we start with the two disconnected droplets, we expect the singularity in the noise to occur at multiples of $\tilde{\omega}_J = eV/\hbar$, the Josephson frequency for the electron. As the tunneling amplitude is increased, at some point we expect the singularity at the Josephson frequency for the quasiparticle, $\omega_J = e^*V/\hbar$, to appear. However, according to the perturbative calculations, to all orders in the electron tunneling amplitude the quasiparticle singularity does not appear. This question is of interest because the location of the singularities tells us which particles are tunneling and, as mentioned above, should give a way to measure the fractional charge of the quasiparticles.

In this chapter we will address the question of what happens to this quasiparticle singularity and show how these two seemingly contradictory statements above are resolved in the special case of $g = 1/2$ and $\tilde{g} = 2$ [41]. The current in the $g = 1/2$ case is known to be exactly solvable [14, 24, 42, 43, 44]. Here we present an exact solution for the non-equilibrium noise spectrum. We find that for $g = 1/2$ the singularity at the quasiparticle Josephson frequency $\omega_J = e^*V/\hbar$ is destroyed by

non-perturbative effects, and exists only in the limit of zero quasiparticle tunneling amplitude Γ. The quasiparticle singularity that was obtained by perturbative calculations is instead smeared for finite tunneling strength: the noise spectrum is analytic near $\omega_J = e^*V/\hbar$, but it still has structure within a region of width $\Delta\omega \sim 4\pi|\Gamma|^2$. Thus, for zero coupling a "fake" singularity appears as this width vanishes. The results in this chapter, together with the previous perturbative results valid to all orders in the electron tunneling amplitude, suggest what may be happening at other values of g also. The quasiparticle singularity should only exist in the limit of vanishing quasiparticle tunneling amplitude, and it should acquire a finite width controlled by a non-zero tunneling amplitude. In physical terms, tunneling between edges destroys both the perfectly quantized Hall conductance and the quasiparticle singularity in the noise spectrum.

One of the tools we use in this chapter is the Landauer-Buttiker scattering approach. The geometry is illustrated in Figure 4-1. The choice of the Landauer-Buttiker approach is justified for a number of reasons. The chiral nature of the system under study naturally poses the problem in terms of incoming and outgoing scattering states to and from the point contact region. The incoming branches should be in equilibrium with their respective reservoirs of departure, and should be insensitive to the tunneling of charges in the tunneling region shown in Fig. 4-1. This is so because information on tunneling events cannot propagate in the direction opposite to the incoming branch chirality. Also, the Landauer-Buttiker approach and the chiral nature of the system suggest naturally a four-terminal geometry for experimental measurements, probing voltage fluctuations in the two incoming and two outgoing branches. The tunneling takes place in the point contact, or scattering region, which is not directly accessible by the probing leads. Auto-correlations of current and voltage fluctuations measured in the four terminals, as well as cross-correlations between different terminals, are the experimental probes that should allow the remote measurement of the tunneling events and noise spectrum.

The chapter is organized as follows. In section 4.2 we obtain the noise spectrum perturbatively for the four terminal geometry, using the Keldysh non-equilibrium for-

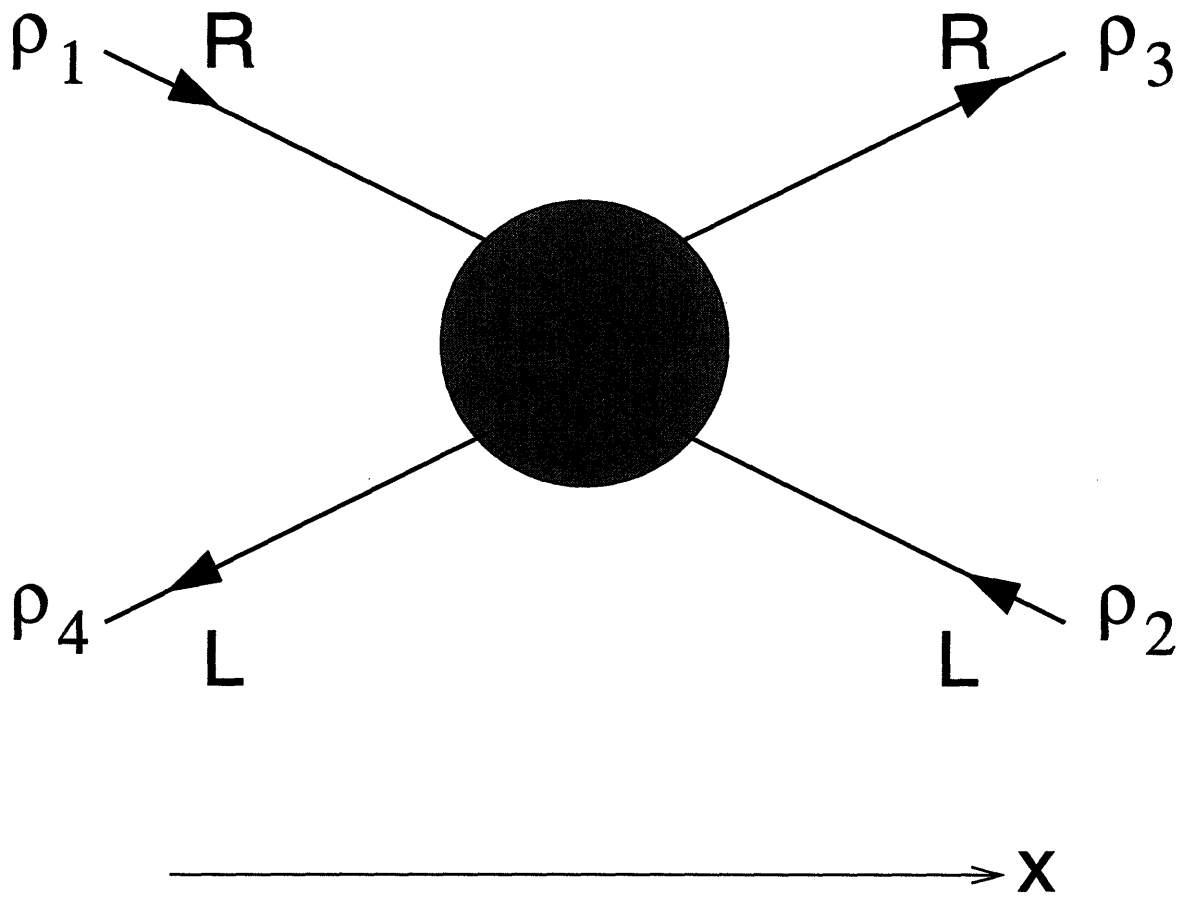

Figure 4-1: Four terminal geometry for the measurement of tunneling between edge states. The terminals 1 and 2 correspond to branches that are incoming to the scatterer, while terminals 3 and 4 correspond to outgoing ones. The arrows indicate the direction of propagation for a given branch. The incoming branches are in equilibrium with their reservoirs of origin, while the outgoing ones do get affected by the scatterer. Voltages and currents in the four probes are directly related to the densities ρ_i $(i = 1, 2, 3, 4)$. By measuring fluctuations in the voltages or currents at the four terminals (V_i or I_i, $i = 1, 2, 3, 4$), the auto-correlation spectra $S_{ij}(\omega)$, with $i = j$, and the cross-correlation spectra $S_{ij}(\omega)$, with $i \neq j$, can be obtained. These voltage and current fluctuations contain information on the fluctuations of the tunneling current.

malism. We show that only the noise spectrum for the outgoing branches is affected by the tunneling, whereas the incoming branches are completely insensitive to the charge transfer between the edges. This is consistent with the Landauer-Buttiker picture and the chirality of the system. The noise spectrum for the incoming branches can thus serve as reference level for the measurement of the excess noise on the outgoing branches due to tunneling. The noise spectrum obtained contains interesting structures both at low and high frequencies. The tunneling excess noise vanishes for frequencies above the Josephson frequency $\omega_J = e^*V/\hbar$. The issue of how the singularity moves from the quasiparticle frequency to the electron frequency is resolved in section 4.3, where we use the Landauer-Buttiker approach to solve exactly for the noise spectrum in the case of $g = 1/2$, for which the problem can be cast as a free fermion problem. We show that the singularity at the quasiparticle frequency is smeared for finite tunneling and is not a true singularity, whereas the singularity at the electron frequency survives for all non-zero coupling. In section 4.4 we discuss the duality when $g = 1/2$ goes to $\tilde{g} = 2$, which we show is not exact in the naive sense for the case of noise, in contrast to the case of conductance. We find that the noise spectrum of the current correlations on a single branch (auto-correlations) satisfies the duality relation, while current correlations between distinct branches (cross-correlations) do not satisfy the naive duality relation. We show that the correct dual Lagrangian to the $g = 1/2$ theory is the $g = 2$ theory plus a neutral density-density coupling, which has the same dimension as the tunneling operator. The effect of the neutral coupling appears in the noise, but not in the conductance.

4.2 Perturbative Approach

In this section we treat the tunneling between edge states perturbatively, and obtain the noise spectrum for the current and voltage fluctuations at the four leads as shown in Fig. 4-1. In the figure we separate the branches into their right and left moving components, as well as incident and scattered ones. Right and left branches are

incoming or outgoing depending on their position relative to the scatterer:

$$\begin{array}{lll} \text{Incident} & \phi_R(t, x < 0) \text{ and } & \phi_L(t, x > 0) \\ \text{Scattered} & \phi_R(t, x > 0) \text{ and } & \phi_L(t, x < 0) \ . \end{array} \tag{4.1}$$

Both the currents and the densities at the four terminals can be related to the fields $\phi_{R,L}$. The densities are simply given by $\rho_{R,L} = \frac{\sqrt{\nu}}{2\pi}\partial_x\phi_{R,L}$. Voltage measurements probe these densities. The currents at the four terminals can be trivially related to the densities at those same terminals through the continuity equation for $x \neq 0$. The currents are given by $j_{R,L} = \pm\frac{\sqrt{\nu}}{2\pi}\partial_x\phi_{R,L}$, with positive currents flowing to the right. By choosing the convention that positive currents flow in the direction of the arrows in Fig. 4-1, we can write new currents $\tilde{j}_{R,L} = \pm j_{R,L} = \rho_{R,L}$. It then becomes transparent that there is a tight relationship between current and voltage in the chiral branches. For example, measuring the noise in either the current or the voltage yields information about the other. This kind of relationship between voltage and current noise was obtained in Ref. [38]. We will thus focus on the calculation of density-density correlations, for these will give us information on both current and voltage noise.

We will label the densities at the four terminals shown in Fig. 4-1 by ρ_i, $i = 1, 2, 3, 4$. In terms of the right and left moving fields we have:

$$\begin{array}{ll} \rho_1(t) = \rho_R(t, x_1) & \rho_3(t) = \rho_R(t, x_3) \\ \rho_2(t) = \rho_L(t, x_2) & \rho_4(t) = \rho_L(t, x_4) \ , \end{array} \tag{4.2}$$

where $x_1, x_4 < 0$, $x_2, x_3 > 0$. The noise spectrum of the density fluctuations in terminals i, j is obtained from the correlations between the densities ρ_i, ρ_j:

$$S_{ij}(\omega) = S_{ji}(-\omega) = \int_{-\infty}^{\infty} dt \ e^{i\omega t}\langle\{\rho_i(t), \rho_j(0)\}\rangle \ . \tag{4.3}$$

These quantities are calculated perturbatively in Appendix A, using the techniques in the previous chapter. The components with $i \neq j$ are very sensitive to phases which

depend on the position of the probes x_i and x_j. These phases cancel in the case of auto-correlations, *i.e.*, when $i = j$. The quantities $S_{ii}(\omega)$, which correspond to the noise spectrum obtained entirely from one of the four probes for i=1 to 4, are thus the most robust measurements of fluctuations, because when they are extracted away from the junction they are independent of the position x_i where they are taken.

To second order in perturbation theory, S_{ii} is given by:

$$S_{11}(\omega) = S_{22}(\omega) = S^{(0)}(\omega) \tag{4.4}$$

$$S_{33}(\omega) = S_{44}(\omega) = S^{(0)}(\omega) + S^{(2)}(\omega) \ , \tag{4.5}$$

where

$$S^{(0)}(\omega) = \frac{\nu}{2\pi}|\omega| \ , \tag{4.6}$$

$$S^{(2)}(\omega) = \frac{4\pi\nu g}{\Gamma(2g)} \ |\Gamma|^2 \ \Big||\omega| - |\omega_J|\Big|^{2g-1} \ \theta(|\omega_J| - |\omega|) \ . \tag{4.7}$$

Substituting the perturbative result (to order $|\Gamma|^2$) for the tunneling current $I_t = \frac{2\pi}{\Gamma(2g)} e^* |\Gamma|^2 \omega_J^{2g-1}$ [13], $S^{(2)}(\omega)$ can be written as

$$S^{(2)}(\omega) = 2e^* I_t \ \Big|1 - \Big|\frac{\omega}{\omega_J}\Big|\Big|^{2g-1} \ \theta(|\omega_J| - |\omega|) \ . \tag{4.8}$$

Notice that the effects of tunneling are contained in $S^{(2)}(\omega)$, and only appear in the outgoing branches, terminals $i = 3, 4$. The incoming branches are insensitive to the tunneling between edges, due to the chiral nature of the system. Information about what goes on in the junction cannot propagate in the direction opposite to the chirality of the branch, and therefore the noise in the incoming branches is independent of the tunneling of charged particles between edges. This result of chirality is clear within the Landauer-Buttiker scattering approach. Another physical consequence closely related to this is the fact that the average voltage along the branches remains constant outside the scattering region. Also notice that the equilibrium noise ($\omega_J = e^* V/\hbar = 0$) in an outgoing branch ($S_{33}^{V=0}(\omega)$, for example) is simply the total noise in an incoming

branch ($S_{11}(\omega)$, for example); thus, the incoming branches can be used as the reference level for measurements of excess noise.

The second point to notice from Eq. (4.8) is that to order $|\Gamma|^2$ the noise in the outgoing branches that is in excess to the noise in the incoming branches has a singularity at the Josephson frequency ω_J, vanishing for $\omega > \omega_J$, as illustrated in Fig. 4-2. The non-equilibrium voltage V determines the frequency scale $\omega_J = e^*V/\hbar$, up to which there is structure in the excess noise due to tunneling. Such vanishing of the excess noise spectrum past a frequency set by the non-equilibrium voltage should be familiar to readers accustomed to noise in non-interacting systems ($g = 1$), in which the excess noise goes to zero linearly at the Josephson frequency [31]. This point will be illustrated further in the next section, when we will have at hand the exact solution for the noise spectrum in the case of $g = 1/2$. The strong coupling limit of the solution for $g = 1/2$ also gives us the solution for $g = 2$, which we shall use for comparison purposes.

The last, and most important, point about this high frequency singularity in the noise spectrum is in regard to the connection between the two dual pictures illustrated in Fig. 2-1. In the previous chapter it was pointed out that the singularity at the Josephson frequency remained to all orders in perturbation theory. However, the perturbative expansion for the geometries in Figs. 2-1a and 2-1b yields two distinct frequencies, namely the quasiparticle frequency $\omega_{qp} = \nu eV/\hbar$ when quasiparticles are the tunneling charges (Fig. 2-1a), and the electron frequency $\omega_{el} = eV/\hbar$, when electrons are the tunneling current carriers (Fig. 2-1b). These configurations are connected in the sense that one is the strong coupling limit of the other, and thus there should be a non-perturbative mechanism by which the singularity moves from one place to the other. This was the clearest open question in the previous chapter, and which we can answer by focusing on the exactly solvable case of $g = 1/2$. Another exactly solvable point is the trivial case $g = 1$, which unfortunately cannot be used to address this issue of the singularity in the noise spectrum because in this case the two frequencies ω_{el} and ω_{qp} coincide.

Before answering the question about the high frequency singularity, we will close

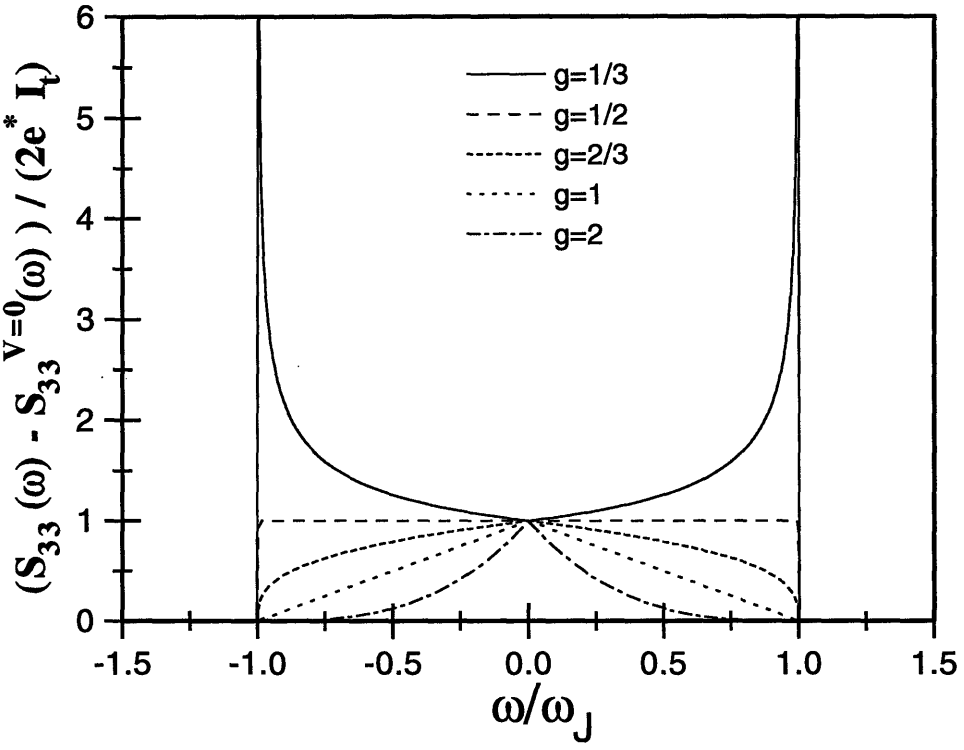

Figure 4-2: Plots of the excess noise of outgoing branches (probes 3 and 4 of Fig. 2) calculated to second order in perturbation theory (equation (4.8)). The excess noise in branch 3 is shown normalized to the zero-frequency shot noise level, and the frequency ω normalized to the Josephson frequency $\omega_J = e^*V/\hbar$ (*i.e.*, we show the plot of $(S_{33}(\omega) - S_{33}^{V=0}(\omega))/2e^*I_t$ *vs.* ω/ω_J). Different singularities are obtained at $\omega = \omega_J$ for different values of g: $\frac{1}{3}$, $\frac{1}{2}$, $\frac{2}{3}$, 1, and 2. One should keep in mind that, although the singularities all occur at $\omega = \omega_J$, the value of ω_J depends on the charge e^* of the current carrier, which in turn also depends on g. The results are exactly the same for the excess noise measured in branch 4.

this section with the implications of tunneling between edge states to the low frequency noise measured in the four terminal geometry. In Chapter 3, a correction to the low frequency shot noise spectrum was found, which corresponded to an $|\omega|$ singularity, or a cusp, in the noise spectrum. This correction was found to order $|\Gamma|^4$, while to order $|\Gamma|^2$ the low frequency corrections to the flat shot noise started as $\propto \omega^2$. In the four terminal geometry proposed in this chapter, what is probed is not the tunneling current in the junction area (as in the previous chapter and Ref. [39]), but its consequences in the current and voltage in the four terminals away from the scattering region. The four terminal measurement, as seen from Eq. (4.8), does have a correction $\propto |\omega|$ to order $|\Gamma|^2$. For $\omega \ll \omega_J$ we have, for example,

$$\begin{aligned} S_{33}(\omega) - S_{33}^{V=0}(\omega) &= S^{(2)}(\omega) = S_{33}(\omega) - S_{11}(\omega) \\ &= 2e^* I_t \left|1 - \left|\frac{\omega}{\omega_J}\right|\right|^{2g-1} \theta(|\omega_J| - |\omega|) \\ &\approx 2e^* I_t \left[1 - (2g-1)\left|\frac{\omega}{\omega_J}\right|\right] . \end{aligned} \tag{4.9}$$

One recovers the classical shot noise expression for $\omega = 0$. Notice that, since these results are valid only to order $|\Gamma|^2$, there is no correction to the classical shot noise expression for $\omega = 0$. Corrections appear at order $|\Gamma|^4$ (see Ref. [39]). Also notice that the non-zero ω corrections to the shot noise depend on whether g is larger or smaller then $1/2$. For $g > 1/2$, the difference between the outgoing and incoming spectra (the $S_{33}(\omega) - S_{11}(\omega)$ above, for example) decreases with ω, whereas for $g < 1/2$ it increases.

4.3 Scattering Approach for $g = 1/2$

In this section we will use the Landauer-Buttiker Scattering approach to obtain an exact solution for the noise when $g = 1/2$. In this approach, we use the quantum equations of motion derived from the Hamiltonian to solve for the scattering states. These scattering states describe free left movers and right movers that are incident on the impurity and then are reflected or scattered by the impurity. The solutions

for these states can be used to calculate the conductance and the noise in the various branches.

The advantage of focusing on $g = 1/2$ is that for this value of g the system can be described by free fermions [42, 44], making it straightforward to solve for the scattering states. However, already at $g = 1/2$, we expect to see singularities in the noise at $\omega_J = e^*V/\hbar$, corresponding to quasiparticle tunneling. As the tunneling amplitude Γ increases (or V decreases), we expect to obtain the dual picture at $g = 2$, with electrons tunneling and a singularity at $eV/\hbar$. Thus the full solution at $g = 1/2$ will show us what happens to the quasiparticle singularity as Γ is increased. The hope is that the qualitative behavior of these results will also apply for other values of g.

When $g = 1/2$, the Hamiltonian for the system is given by

$$H = H_R^0 + H_L^0 + \Gamma e^{-i\omega_0 t}\, e^{\frac{i}{\sqrt{2}}(\phi_R(t,0)+\phi_L(t,0))} + \Gamma^* e^{i\omega_0 t}\, e^{-\frac{i}{\sqrt{2}}(\phi_R(t,0)+\phi_L(t,0))} \tag{4.10}$$

where $H_{R,L}^0$ are the free Hamiltonians for the right and left moving fields, and $\omega_0 = e^*V/\hbar$, with $e^* = e/2$.

The Hamiltonian can be recast in terms of new chiral fields $\phi_\pm$ given by $\phi_\pm(t,x) = \frac{1}{\sqrt{2}}(\phi_R(t,x) \mp \phi_L(t,-x))$:

$$H = H_+^0 + H_-^0 + \Gamma e^{-i\omega_0 t}\, e^{i\phi_-(t,0)} + \Gamma^* e^{i\omega_0 t}\, e^{-i\phi_-(t,0)}\ . \tag{4.11}$$

The densities of the new fields $\rho_\pm = \frac{1}{2\pi}\partial_x\phi_\pm$ are related to the densities $\rho_{R,L} = \frac{\sqrt{1/2}}{2\pi}\partial_x\phi_{R,L}$ by $\rho_\pm(t,x) = \rho_R(t,x) \pm \rho_L(t,-x)$. Notice that the $\phi_\pm$ fields are decoupled in Eq.(4.11), and the Hamiltonian for ϕ_+ is simply the free H_+^0. The Hamiltonian for ϕ_- can be fermionized by defining $\eta(t,x) \equiv \frac{1}{\sqrt{2\pi}} : e^{i\phi_-(t,x)} :$. One can check that η defined as such satisfies the proper commutation relations $\{\eta(t,x)\ ,\ \eta^\dagger(t,y)\} = \delta(x-y)$ [45].

In terms of the fermionic fields $\eta, \eta^\dagger$, the Hamiltonian H_- is:

$$H_- = \int dx \left\{ \eta^\dagger(x) \left[-i\frac{\partial}{\partial x} - \omega_0 \right] \eta(x) + \sqrt{2\pi}\delta(x) \left[\Gamma\eta(x) + \Gamma^* \eta^\dagger(x) \right] \right\}, \qquad (4.12)$$

where we absorbed the oscillating phases $e^{i\omega_0 t}$ into a redefinition of the chemical potential. The Hamiltonian above contains terms linear in the fermionic fields η and $\eta^\dagger$, which prevent a direct calculation of the commutators that would give us the equations of motion for the fields. This problem can be circumvented by redefining the fermionic fields to be $\psi(t,x) = \eta(t,x)f$, with $f = C + C^\dagger$ and $\{C, C^\dagger\} = 1$, as in Ref. [44]. More formally, such a transformation can be constructed from the proper handling of the zero modes of the bosonic fields ϕ [5, 46], and one can identify f with $(-1)^F$, the fermion counting operator commonly used to switch from periodic to anti-periodic boundary conditions in fermionic conformal field theories.

The Hamiltonian we will use in the exact solution of the noise spectrum for the $g = 1/2$ case is the one written in terms of the $\psi, \psi^\dagger$ fields and f:

$$H_- = \int dx \left\{ \psi^\dagger(x) \left[-i\frac{\partial}{\partial x} - \omega_0 \right] \psi(x) + \sqrt{2\pi}\delta(x) \left[\Gamma\psi(x)f + \Gamma^* f \psi^\dagger(x) \right] \right\}, \qquad (4.13)$$

where the non-vanishing equal-time commutation relations between $\psi(x), \psi^\dagger(x)$ and f are

$$\{\psi(x), \psi^\dagger(x')\} = \delta(x - x') \ , \ \{\psi(x), f\} = 0 \ , \ \{f, f\} = 2 \ . \qquad (4.14)$$

The density ρ_- can be written in terms of the fields ψ and $\psi^\dagger$ as $\rho_-(x) = \psi^\dagger(x)\psi(x)$, so that all correlations between ρ_-'s can be derived from the correlations of the fermions. The fermionic model is solved using the equations of motion obtained by commuting the operators $\psi(x)$ and f with the Hamiltonian:

$$-i\partial_t \psi(x) = [H, \psi(x)] = (i\partial_x + \omega_0)\psi(x) + \sqrt{2\pi}\Gamma^* f \delta(x), \qquad (4.15)$$

$$-i\partial_t \psi^\dagger(x) = [H, \psi^\dagger(x)] = (i\partial_x - \omega_0)\psi^\dagger(x) - \sqrt{2\pi}\Gamma f \delta(x), \qquad (4.16)$$

and

$$-i\partial_t f = [H, f] = 2\sqrt{2\pi}\left[\Gamma\psi(0) - \Gamma^*\psi^\dagger(0)\right]. \tag{4.17}$$

According to these equations, for $x \neq 0$, the field ψ satisfies the free equation of motion for a rightmover with energy shifted by ω_0:

$$(i\partial_x + i\partial_t + \omega_0)\psi = 0. \tag{4.18}$$

At $x = 0$, it picks up a discontinuity because of the impurity. In order to preserve unitarity and obtain the proper commutation relations in the solutions of ψ, in equation (4.17) the field $\psi(0)$ must be given by $(1/2)(\psi(0^+) + \psi(0^-))$. With this definition, it is straightforward to solve the equations of motion. The solutions are given by

$$\psi(x) = \begin{cases} \sum_\omega A_\omega e^{i(\omega+\omega_0)x} e^{-i\omega t} & \text{for } x < 0 \\ \sum_\omega B_\omega e^{i(\omega+\omega_0)x} e^{-i\omega t} & \text{for } x > 0 \end{cases} \tag{4.19}$$

and

$$\psi^\dagger(x) = \begin{cases} \sum_\omega A^\dagger_{-\omega} e^{i(\omega-\omega_0)x} e^{-i\omega t} & \text{for } x < 0 \\ \sum_\omega B^\dagger_{-\omega} e^{i(\omega-\omega_0)x} e^{-i\omega t} & \text{for } x > 0, \end{cases} \tag{4.20}$$

where

$$B_\omega = \frac{(1 + e^{i\phi(\omega)})A_\omega + (1 - e^{i\phi(\omega)})A^\dagger_{-\omega}}{2}, \tag{4.21}$$

and

$$e^{i\phi(\omega)} = \frac{i\omega + 4\pi|\Gamma|^2}{i\omega - 4\pi|\Gamma|^2}. \tag{4.22}$$

Given the commutation relation for ψ, the A_ω satisfy the following commutation relation:

$$\{A_{\omega_1}, A^\dagger_{\omega_2}\} = \delta_{\omega_1,\omega_2}. \tag{4.23}$$

These solutions can be interpreted as having an incident particle at energy ω that scatters into a particle with energy ω and a hole with energy $-\omega$ (see Fig. 4-3). Both the particle and hole scattering involve an energy dependent phase shift.

The reservoir is located to the left of the impurity, for some $x < 0$. To obtain the scattering state $|\Phi\rangle$, we assume that the states leaving the reservoir are in equilibrium

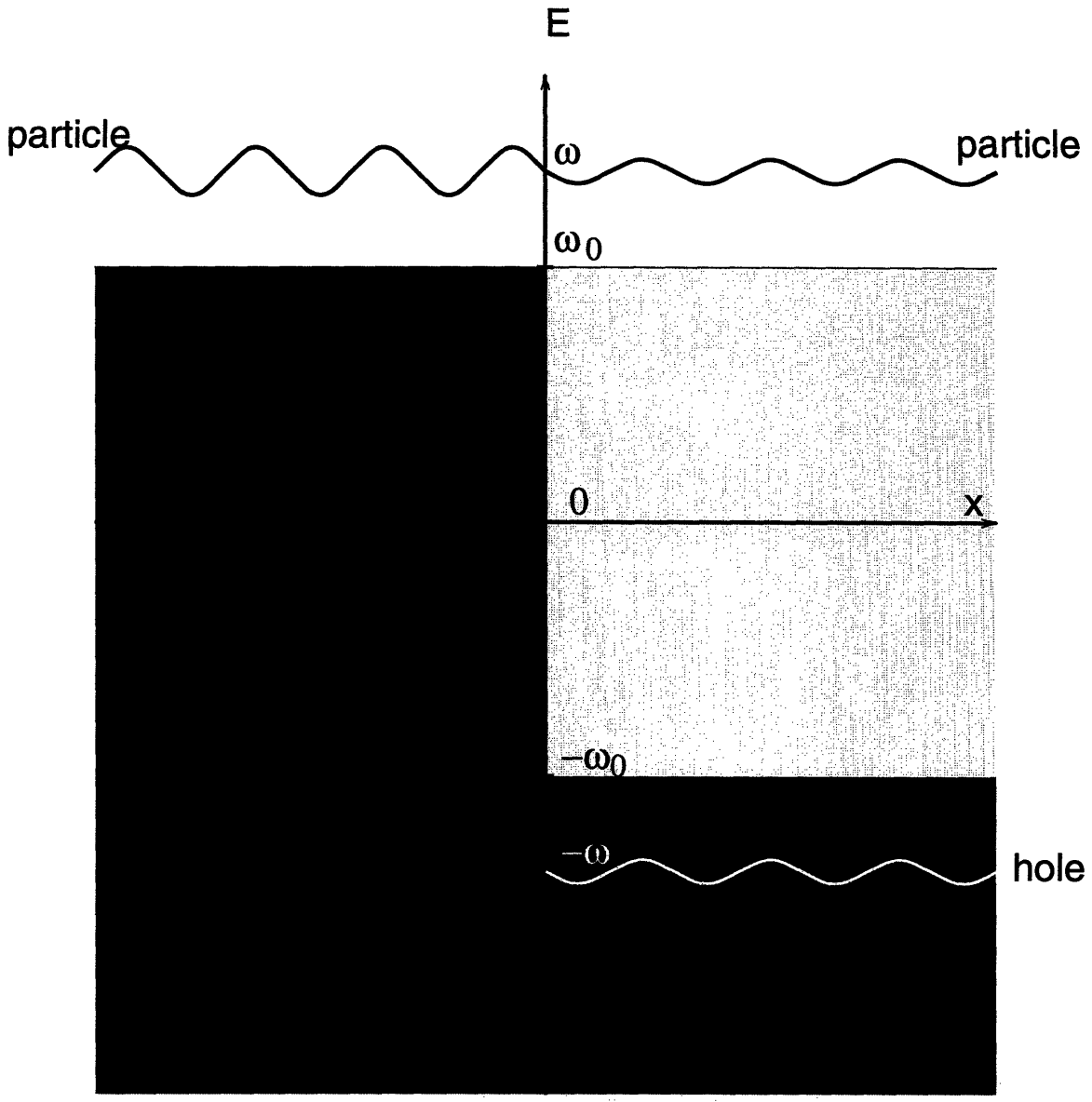

Figure 4-3: A particle (plane wave) incoming from the left ($x < 0$) with energy ω scatters off the impurity at $x = 0$ into a superposition of a particle at energy ω and a hole at energy $-\omega$ on the right side of the impurity ($x > 0$). In the case where the incoming state is a filled Fermi sea up to the energy ω_0, the scattered state on the right side of the impurity will be completely filled up to energy $-\omega_0$, and partially filled between $-\omega_0$ and ω_0. It is this partially filled energy range from $-\omega_0$ and ω_0 which is responsible for the non-equilibrium properties of the system.

with the reservoir, which has energy ω_0. Thus, for $x < 0$, at zero temperature all the states with $\omega \leq \omega_0$ are filled. This means that

$$A_\omega^\dagger |\Phi\rangle = 0 \qquad \text{for} \quad \omega < \omega_0, \tag{4.24}$$

and

$$A_\omega |\Phi\rangle = 0 \qquad \text{for} \quad \omega > \omega_0. \tag{4.25}$$

Using the commutation relations for A in equation (4.23), we then find that

$$\langle\Phi| A_{\omega_1} A_{\omega_2} |\Phi\rangle = 0, \tag{4.26}$$

and

$$\langle\Phi| A_{\omega_1}^\dagger A_{\omega_2} |\Phi\rangle = n_{\omega_1} \delta_{\omega_1,\omega_2}, \tag{4.27}$$

where

$$n_\omega = \begin{cases} 1 & \text{for } \omega < \omega_0 \\ 0 & \text{for } \omega > \omega_0. \end{cases} \tag{4.28}$$

In this chapter, we will just concentrate on the case when $T = 0$. However, we can obtain the finite temperature results by replacing n_ω with

$$n_\omega = \frac{1}{e^{\beta(\omega-\omega_0)} + 1}. \tag{4.29}$$

It is easy to show that these solutions reproduce the exact results for both the equilibrium [14, 44] and non-equilibrium [24] tunneling current.

We can now use the solutions for ψ and the scattering state to solve for the noise in both incoming and outgoing channels. Our calculations will closely follow those by Buttiker in reference [29]. The noise is given by

$$S(\omega; x_1, x_2) = \int_{-\infty}^{\infty} dt \; e^{i\omega t} \langle \{\rho_-(t, x_1), \rho_-(0, x_2)\} \rangle, \tag{4.30}$$

where we take only the connected part of the correlation function, and x_1 and x_2 are positive or negative depending on whether the current is evaluated in the incoming

or outgoing channel.

4.3.1 Calculation of Auto-correlations

We will begin by calculating the noise when $x_1 = x_2$. In this case, both of the currents are evaluated on the same side of the impurity. Because of the time translational invariance of the correlators, the expression for the noise simplifies to

$$S(\omega; x_1, x_1) = \int_{-\infty}^{\infty} dt \left(e^{i\omega t} + e^{-i\omega t}\right) \langle \rho_-(t, x_1)\rho_-(0, x_1)\rangle. \tag{4.31}$$

To find the noise in the incoming channel, we must evaluate the expectation value

$$\langle \rho_-(t, x_-)\rho_-(0, x_-)\rangle = \langle \psi^\dagger(t, x_-)\psi(t, x_-)\psi^\dagger(0, x_-)\psi(0, x_-)\rangle, \tag{4.32}$$

with $x_- < 0$. Using the solutions (4.19) and (4.20) for ψ and $\psi^\dagger$, we find

$$\langle \rho_-(t, x_-)\rho_-(0, x_-)\rangle = \sum_{\omega_1,\omega_2,\omega_3,\omega_4} e^{-i(\omega_1+\omega_2)t} \langle \Phi | A^\dagger_{-\omega_1} A_{\omega_2} A^\dagger_{-\omega_3} A_{\omega_4} | \Phi \rangle e^{i(\omega_1+\omega_2+\omega_3+\omega_4)x_-}. \tag{4.33}$$

This expectation value, and the resulting integrals for $S(\omega; x_-, x_-)$ are evaluated in Appendix C, with the result,

$$S(\omega; x_-, x_-) = \frac{1}{2\pi}|\omega|. \tag{4.34}$$

If we want to calculate the noise in one of the two original R and L incoming branches, we must use the relations

$$\rho_R(x) = \frac{1}{2}(\rho_+(x) + \rho_-(x)) \qquad \text{and} \qquad \rho_L(x) = \frac{1}{2}(\rho_+(-x) - \rho_-(-x)). \tag{4.35}$$

Then the density-density correlations can be evaluated as follows:

$$\langle \rho_{R,L}\rho_{R,L}\rangle = \frac{1}{4}\langle (\rho_+ \pm \rho_-)(\rho_+ \pm \rho_-)\rangle = \frac{1}{4}\langle \rho_-\rho_-\rangle + \frac{1}{4}\langle \rho_+\rho_+\rangle, \tag{4.36}$$

where the last equality follows from the fact that ρ_+ and ρ_- are decoupled. Recall that ρ_+ is a free field, so that the contribution to the noise from ρ_+ is simply $\frac{1}{2\pi}|\omega|$. We find that the noise in each of the two incoming R and L branches is given by

$$\begin{aligned} S_{11}(\omega) = S_{22}(\omega) &= \frac{1}{4}S(\omega; x_-, x_-) + \frac{1}{4}\frac{|\omega|}{2\pi} \\ &= \frac{1}{4\pi}|\omega|, \end{aligned} \tag{4.37}$$

just as we found in the perturbative calculation with $\nu = 1/2$ in Eqs. (4.4) to (4.7). Using this scattering approach, it is clear that for these two incoming probes the noise is the same as for a free system, because in these two channels the densities have not yet reached the impurity.

Next, we will calculate the noise in the outgoing current. This time we must evaluate the correlator

$$\langle \rho_-(t, x_+)\rho_-(0, x_+)\rangle = \langle \psi^\dagger(t, x_+)\psi(t, x_+)\psi^\dagger(0, x_+)\psi(0, x_+)\rangle, \tag{4.38}$$

with $x_+ > 0$. According to equations (4.19) and (4.20), this is equal to

$$\langle \rho_-(t, x_+)\rho_-(0, x_+)\rangle = \sum_{\omega_1,\omega_2,\omega_3,\omega_4} e^{-i(\omega_1+\omega_2)t}\langle\Phi|B^\dagger_{-\omega_1}B_{\omega_2}B^\dagger_{-\omega_3}B_{\omega_4}|\Phi\rangle e^{i(\omega_1+\omega_2+\omega_3+\omega_4)x_+}. \tag{4.39}$$

When we expand the B's in terms of the A's, we will obtain two different types of processes (see Fig. 4-4). In the first, at time 0 one particle is created while another is destroyed, and then at time t the first particle is destroyed and another is created. In terms of the original tunneling picture, this describes the process where both at time t and at time 0 one quasiparticle tunnels from the left branch to the right branch and another tunnels in the opposite direction. In the second process, at time 0 two particles are created and then at time t they are destroyed (or *vice versa*). In the original tunneling picture, this corresponds to two quasiparticles tunneling in one direction at time 0 and two quasiparticles tunneling in the opposite direction at time t. As shown in Appendix C, this second process is responsible for the electron

singularity at $\tilde{\omega}_0 = 2\omega_0$. In Appendix C, the expectation values in Eq.(4.39) and the integrals for $S(\omega; x_+, x_+)$ are evaluated. We find that the noise on the outgoing side of the impurity is

$$S(\omega; x_+, x_+) = \frac{1}{2\pi}|\omega| + \theta(|2\omega_0| - |\omega|)\Bigg\{4|\Gamma|^2\left[\tan^{-1}\left(\frac{|\omega_0|}{4\pi|\Gamma|^2}\right) + \tan^{-1}\left(\frac{|\omega_0| - |\omega|}{4\pi|\Gamma|^2}\right)\right] + \frac{16\pi|\Gamma|^4}{|\omega|}\left[\ln\left((4\pi|\Gamma|^2)^2 + (|\omega| - |\omega_0|)^2\right) - \ln\left((4\pi|\Gamma|^2)^2 + \omega_0^2\right)\right]\Bigg\}. \quad (4.40)$$

In the limit $\omega \to 0$, this reduces to the non-equilibrium zero frequency noise found in reference [43] using a different approach. This agreement provides further support for our choice of regulation of the $\psi(0)$ operator across the impurity.

To compare with our perturbative calculation for the noise in the original four probe geometry, we again make use of equation (4.36). Thus, the noise in the two outgoing branches is related to $S(\omega; x_+, x_+)$ as follows:

$$S_{33}(\omega) = S_{44}(\omega) = \frac{1}{4}S(\omega; x_+, x_+) + \frac{1}{4}\frac{|\omega|}{2\pi}. \quad (4.41)$$

4.3.2 Discussion of Auto-correlations

The first striking feature to note in equation (4.40) is that the noise due to the tunneling vanishes identically for $|\omega| > |2\omega_0|$. This means that whenever $|\omega|$ is larger than the electron frequency, the noise shows no sign of the impurity; it is the same as for the incoming branch. This is also what happens for the free electron case, with $g = 1$. To second order in perturbation theory, this is indeed the case for any g, as seen in the previous section. The strength of the results presented here is that for *any value* of the coupling Γ the noise vanishes above the electron frequency when $g = 1/2, 1$ and 2. (The last case, $g = 2$, is obtained by resorting to the strong coupling limit of the $g = 1/2$ case.) It is not clear whether this will happen for the other values of g beyond second order in perturbation theory.

Next, we can expand $S(\omega; x_+, x_+)$ out for small and large $|\Gamma|$ to compare with the

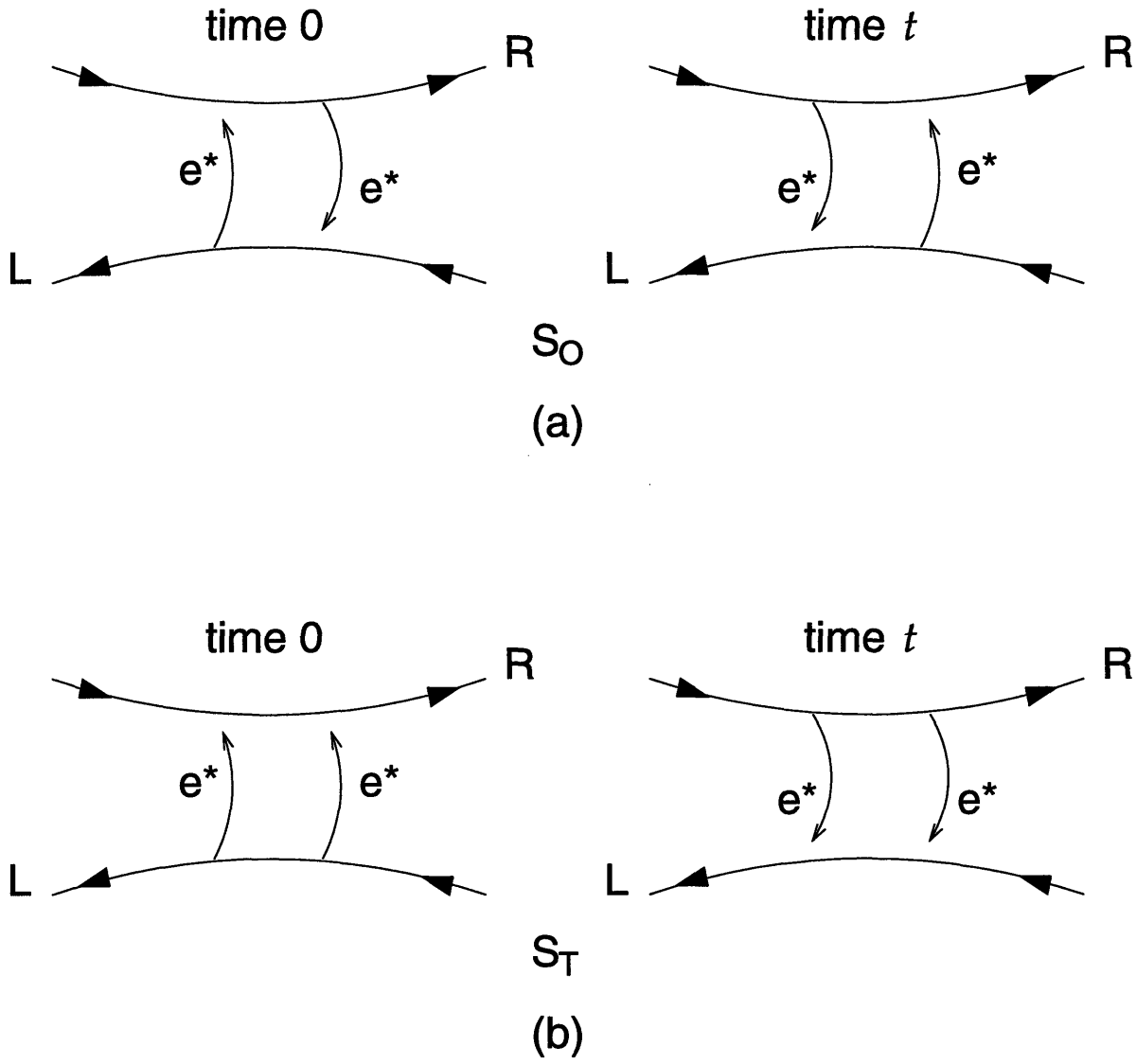

Figure 4-4: The tunneling processes s_0 (a) and s_t (b). In the process s_0, both at time 0 and t, a quasiparticle tunnels from the left branch to the right branch, and another quasiparticle tunnels in the opposite direction. In the s_t process, at time 0 two quasiparticles tunnel from, say, the left to the right branch, and at time t the two quasiparticles tunnel back in the opposite direction. The process s_t is responsible for the singularity at the electron frequency $\tilde{\omega}_0 = 2\omega_0$.

perturbative results. As $|\Gamma|$ goes to zero, the noise becomes

$$S_{33}(\omega) = S_{44}(\omega) = \frac{1}{4\pi}|\omega| + \pi|\Gamma|^2\theta(|\omega_0| - |\omega|). \tag{4.42}$$

This agrees with the perturbative result for $g = 1/2$. We note that the quasiparticle singularity arises because we took the $|\Gamma| \to 0$ limit of the arctangents. In addition, because this step function is already zero for $|\omega| > |\omega_0|$, the electron singularity at $|\omega| = |2\omega_0|$ drops out. Thus, to this order we only have the quasiparticle singularity. However, for any finite value of $|\Gamma|$ the quasiparticle singularity becomes smoothed out and the electron singularity appears. As we shall see later, though, the "smoothed out" quasiparticle singularity is still a more distinctive feature in the plots of the full noise than is the electron singularity.

Next, for $|\Gamma| \to \infty$, the noise becomes

$$S_{33}(\omega) = S_{44}(\omega) = \frac{1}{4\pi}|\omega| + \frac{1}{384\pi^3|\Gamma|^4}\theta\left(|2\omega_0| - |\omega|\right)\left(|2\omega_0| - |\omega|\right)^3 + O(1/|\Gamma|^8). \tag{4.43}$$

If we make the identification that $\Gamma_{\frac{1}{2}}$, the tunneling amplitude for $g = 1/2$, is related to Γ_2, the tunneling amplitude for $g = 2$, by

$$|\Gamma_2| = \frac{1}{16\pi^2|\Gamma_{\frac{1}{2}}|^2}, \tag{4.44}$$

then this answer agrees with the perturbative result for $g = 2$. (To make the comparison, we must recall that the ω_0 in this equation corresponds to the Josephson frequency for the quasiparticle, whereas the ω_J in the perturbative calculation Eqs. (4.4) to (4.7) is the Josephson frequency for the electron, which is twice as large.) In addition, the expansion in $\frac{1}{|\Gamma|}$ of the scattering solution only contains powers of $\frac{1}{|\Gamma|^4} = |\Gamma_2|^2$, and at every order in $|\Gamma_2|^2$ the electron singularity at $|\omega| = |2\omega_0|$ remains. These two properties also agree with the perturbative results found in the previous chapter.

Lastly, we can make use of the scaling properties of the noise to write $\tilde{S} = S/2|\Gamma|^2$

as a function only of $\tilde{\omega} = \frac{\omega}{4\pi|\Gamma|^2}$ and $\tilde{\omega}_0 = \frac{\omega_0}{4\pi|\Gamma|^2}$. The noise is then given by

$$\begin{aligned}\tilde{S}_{33}(\tilde{\omega}) &= \tilde{S}_{44}(\tilde{\omega}) \\ &= \frac{1}{2}|\tilde{\omega}| + \theta(|2\tilde{\omega}_0| - |\tilde{\omega}|)\Big\{\frac{1}{2}\left[\tan^{-1}(|\tilde{\omega}_0|) + \tan^{-1}(|\tilde{\omega}_0| - |\tilde{\omega}|)\right] \\ &\quad + \frac{1}{2|\tilde{\omega}|}\left[\ln\left(1 + (|\tilde{\omega}| - |\tilde{\omega}_0|)^2\right) - \ln\left(1 + \tilde{\omega}_0^2\right)\right]\Big\}. \qquad (4.45)\end{aligned}$$

In Figure 4-5a, the excess noise $\tilde{S} - \tilde{S}^{\tilde{\omega}_0=0}$ is plotted against $\tilde{\omega}/\tilde{\omega}_0$ for different values of $\tilde{\omega}_0$. As $\tilde{\omega}_0$ becomes large, the excess noise approaches the step function in Eq. (4.42). Recall that $\tilde{\omega}_0 = \tilde{\omega}/(4\pi|\Gamma|^2)$, so this limit is equal to the weak coupling limit with $|\Gamma| \to 0$. To see the strong coupling limit, in Fig. 4-5b we plot the excess noise divided by $\tilde{\omega}_0^3$ (in order to fit in the same scale). As $\tilde{\omega}_0$ becomes small, this clearly has the cubic behavior in Eq. (4.43). Finally, the full noise, divided by $\tilde{\omega}_0$, is plotted in Fig. 4-5c. The cubic singularity at $\tilde{\omega} = 2\tilde{\omega}_0$ decays too quickly to appear in the full noise. However, for $\tilde{\omega}_0 = 100$ and $\tilde{\omega}_0 = 10$, there is clearly a "blip" in the plot of the noise, which shows the "smoothed out" quasiparticle singularity. We note that the width of the "smoothed out" quasiparticle singularity is $\sim 4\pi|\Gamma|^2$. This width can be interpreted as the inverse lifetime of the quasiparticles. Thus, for non-zero values of the tunneling amplitude, the quasiparticles appear to have a finite lifetime.

4.3.3 Calculation of Cross-correlations

For completeness, we will conclude this section by giving the result for the noise $S(\omega; x_+, x_-)$ between incoming and outgoing currents. By comparing this with the perturbative calculations of the cross-correlations, we will see to what extent the duality symmetry holds. In addition, once we have $S(\omega; x_+, x_-)$, $S(\omega; x_+, x_+)$ and $S(\omega; x_-, x_-)$, we can calculate the noise in the Hall current and the tunneling current. The Hall current is the total current running down the sample, given by $I_H = j_L(x) + j_R(x) = \rho_R(x) - \rho_L(x)$ and the tunneling current is the current that tunnels across the sample, which is given by $I_t = \rho_R(x_+) - \rho_R(x_-) = \rho_L(x_-) - \rho_L(x_+)$.

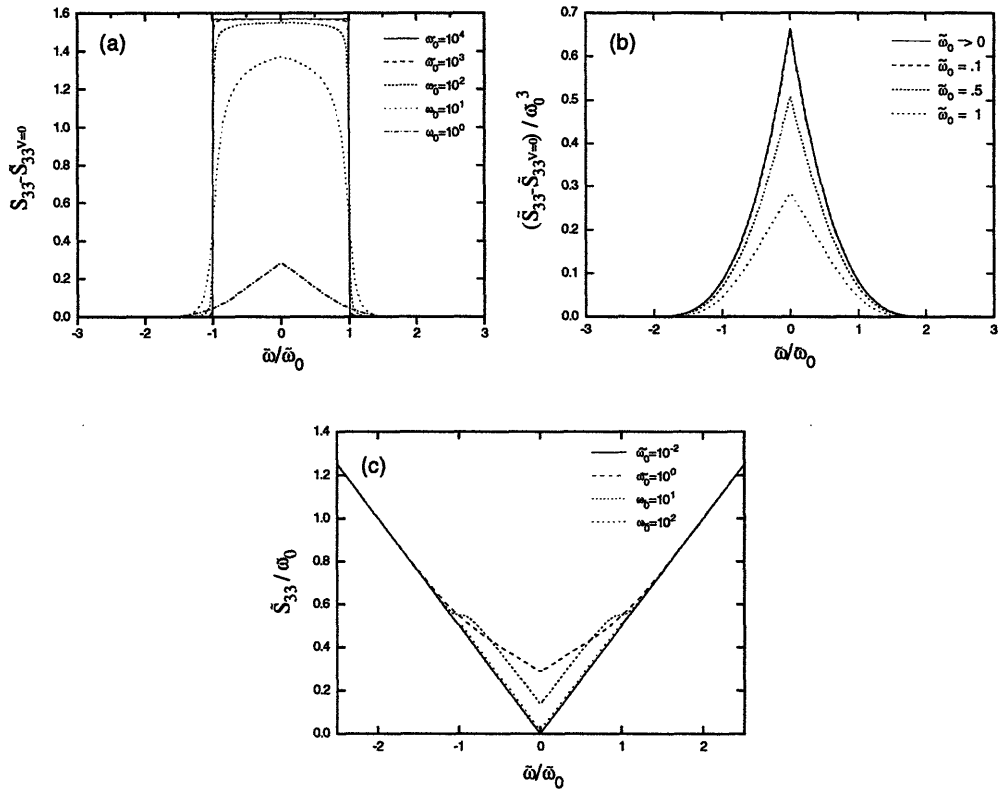

Figure 4-5: Plots for the renormalized noise in one of the outgoing branches (probe 3 in Fig. 2), $\tilde{S}_{33}$ *vs.* $\tilde{\omega}/\tilde{\omega}_0$. $\tilde{S}_{33}$, $\tilde{\omega}$ and $\tilde{\omega}_0$ are the renormalized noise and frequencies, using the coupling constant as the scaling factor ($\tilde{S}_{33} = \frac{S_{33}}{2|\Gamma|^2}$, $\tilde{\omega} = \frac{\omega}{4\pi|\Gamma|^2}$ and $\tilde{\omega}_0 = \frac{\omega_0}{4\pi|\Gamma|^2}$, where $\omega_0 = e^*V/\hbar$). In (a) the excess noise $\tilde{S}_{33} - \tilde{S}_{33}^{V=0}$ is plotted for large values of $\tilde{\omega}_0$, which illustrates the weak coupling ($|\Gamma| \to 0$) limit. The rescaled excess noise $(\tilde{S}_{33} - \tilde{S}_{33}^{V=0})/\tilde{\omega}_0^3$ is plotted in (b). It shows the strong coupling limit ($|\Gamma| \to \infty$) as $\tilde{\omega}_0 \to 0$. The full noise $\tilde{S}_{33}/\tilde{\omega}_0$ is plotted in figure (c). For the larger values of $\tilde{\omega}_0$, notice that the singularity at $\tilde{\omega} = 2\tilde{\omega}_0$ is hidden in the full noise. Meanwhile, some reminiscent signs of the quasiparticle singularity appear near $\tilde{\omega} = \tilde{\omega}_0$. The results for the noise in the other outgoing branch (probe 4) are exactly the same.

The expression for the $S(\omega; x_+, x_-)$ noise is

$$S(\omega; x_+, x_-) = \int_{-\infty}^{\infty} dt\ e^{i\omega t} \langle \{\rho_-(t, x_+), \rho_-(0, x_-)\} \rangle, \tag{4.46}$$

where $x_- < 0$ and $x_+ > 0$. Again, we can expand the $\rho_-(x_+)$ and $\rho_-(x_-)$ in terms of the A_ω's and B_ω's in the solution for ψ. After evaluating the expectation values and performing the integrals over ω_i and t, we find

$$\begin{aligned} S(\omega; x_+, x_-) = \Bigg\{ & \frac{|\omega|}{2\pi} - 2|\Gamma|^2 \left[\tan^{-1}\left(\frac{|\omega| - \omega_0}{4\pi|\Gamma|^2} \right) + \tan^{-1}\left(\frac{|\omega| + \omega_0}{4\pi|\Gamma|^2} \right) \right] \\ + \ & i|\Gamma|^2 \mathrm{sign}(\omega) \Big[2\ln\left(\omega_0^2 + (4\pi|\Gamma|^2)^2 \right) - \ln\left((\omega + \omega_0)^2 + (4\pi|\Gamma|^2)^2 \right) \\ & - \ln\left((\omega - \omega_0)^2 + (4\pi|\Gamma|^2)^2 \right) \Big] \Bigg\} e^{i\omega(x_+ - x_-)}. \end{aligned} \tag{4.47}$$

We can again use equation (4.36) to obtain the expression for the cross-correlations of the currents in the original four reservoirs. We find, for example,

$$S_{31}(\omega) = \frac{1}{4} S(\omega; x_+, x_-) + \frac{1}{4} \frac{|\omega|}{2\pi} e^{i\omega(x_+ - x_-)}. \tag{4.48}$$

and

$$S_{41}(\omega) = -\frac{1}{4} S(\omega; x_+, x_-) + \frac{1}{4} \frac{|\omega|}{2\pi} e^{i\omega(x_+ - x_-)}. \tag{4.49}$$

The other cross-correlations, namely S_{32} and S_{42}, can be calculated similarly. For small $|\Gamma|$, the noise is

$$\begin{aligned} S_{31}(\omega) = \Bigg[& \frac{|\omega|}{4\pi} - \frac{\pi}{4}|\Gamma|^2 \left(\mathrm{sign}(|\omega| + \omega_0) + \mathrm{sign}(|\omega| - \omega_0) \right) \\ & - i\frac{1}{2}|\Gamma|^2 \ln\left(\left| \frac{\omega^2 - \omega_0^2}{{\omega_0}^2} \right| \right) \Bigg] e^{i\omega(x_+ - x_-)}, \end{aligned} \tag{4.50}$$

and when $|\Gamma|$ is large, the noise becomes

$$\begin{aligned} S_{41}(\omega) = \Bigg\{ & \frac{|\omega|}{4\pi} + i\frac{1}{32\pi^2}\frac{1}{|\Gamma|^2}\omega^2 \mathrm{sign}(\omega) \\ & - \frac{1}{384\pi^3}\frac{1}{|\Gamma|^4}\left[(|\omega| + \omega_0)^3 + (|\omega| - \omega_0)^3 \right] \Bigg\} e^{i\omega(x_+ - x_-)}. \end{aligned} \tag{4.51}$$

In the following section, we will compare these results with the perturbative calculation. We will find that for $g = 1/2$ they agree, but they differ for $g = 2$. In Section 4.4, we will also discuss this apparent breakdown of the duality transformation.

4.4 Discussion of the Duality Symmetry

As we have seen in the previous sections, we expect this system to exhibit a duality symmetry. In this section, we will first describe this duality symmetry more fully, and then compare the results from the perturbative and scattering calculation to see how consistent they are with this symmetry.

For $g = 1/2$, the original picture of this system is a single quantum Hall droplet with "filling fraction" $\nu = 1/2$. Quasiparticles can tunnel from one branch to the other, and they have charge $e^* = \nu e$, tunneling amplitude Γ_q, and Josephson frequency $\omega_0 = e^*V/\hbar$. The Lagrangian describing this system can be written as

$$\mathcal{L} = \frac{1}{8\pi}\left[(\partial_t\phi)^2 - v^2(\partial_x\phi)^2\right] - \Gamma_q e^{-i\omega_0 t}\delta(x)e^{i\sqrt{g}\phi(t,0)} + H.c., \tag{4.52}$$

with $g = 1/2$ and $\phi = \phi_R(x)+\phi_L(-x)$. If we use the four probe geometry to study this system, then Eq. (4.2) gives the relation between the densities in the four probes, ρ_1, ρ_2, ρ_3, and ρ_4, and the densities of the leftmovers and rightmovers. They are shown in Fig. 4-6a.

Once Γ is increased (or V is decreased), the droplet should split into two. Each of the two new droplets is still characterized by filling fraction ν. However, now only electrons can tunnel across the gap from one branch to the other. For $g = 1/2$, the electron is made up of two quasiparticles, so the tunneling operator for the electron should be

$$\Gamma_e\left(e^{i\sqrt{1/2}\phi(t,0)}\right)^2 = \Gamma_e e^{i\sqrt{2}\phi(t,0)}; \tag{4.53}$$

the charge is e, and the Josephson frequency is $\tilde{\omega}_0 = 2\omega_0$. Thus, when Γ_q in equation

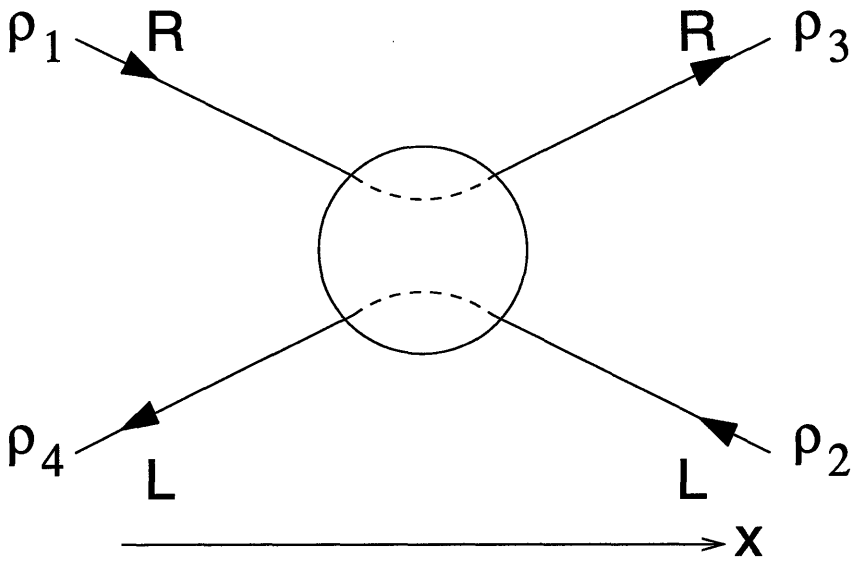

(a)

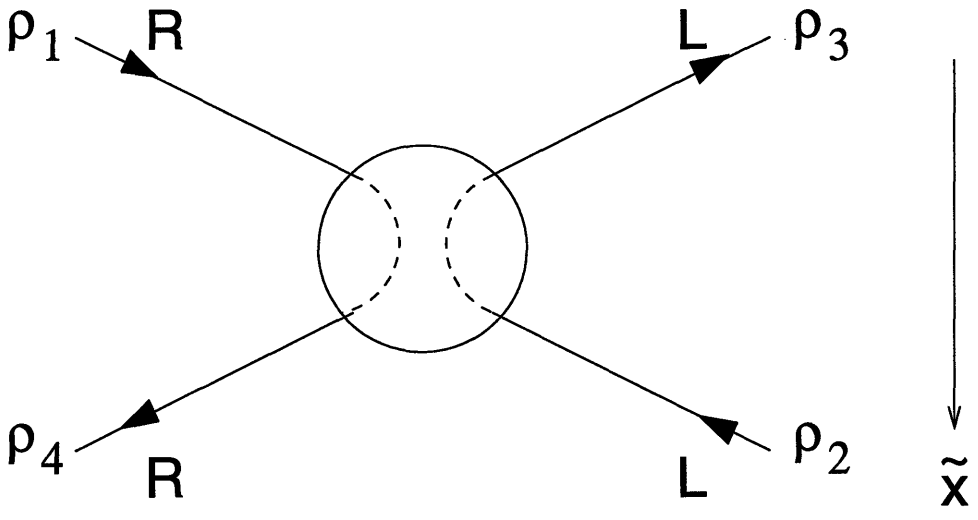

(b)

Figure 4-6: The association of the four densities ρ_i $(i = 1, 2, 3, 4)$ to the left and right moving branches for the dual pictures corresponding to (a) $g = \nu$ and (b) $g = \nu^{-1}$ (compare to Figs. 1a and 1b). Notice that ρ_3 and ρ_4 change chirality under duality, and that the space coordinates (the x and $\tilde{x}$ axis) should also be redefined under the duality transformation.

4.52 becomes large, this system can *also* be described by the Lagrangian density

$$\mathcal{L} = \frac{1}{8\pi}\left[(\partial_t\phi)^2 - v^2(\partial_x\phi)^2\right] - \Gamma_e e^{-i\tilde{\omega}_0 t}\delta(x)e^{i\sqrt{\tilde{g}}\phi(t,0)} + H.c., \tag{4.54}$$

where $\tilde{g} = 2$ and Γ_e is small. However, in this geometry with the two droplets, we must be careful when we write the densities in the four probes in terms of the left-moving and right-moving densities. According to Fig. 4-6b, this relation is given by

$$\begin{aligned}
\rho_1(t) &= \rho_R(t,\tilde{x}) \quad \text{for} \quad \tilde{x} < 0 \\
\rho_2(t) &= \rho_L(t,\tilde{x}) \quad \text{for} \quad \tilde{x} > 0 \\
\rho_3(t) &= \rho_L(t,\tilde{x}) \quad \text{for} \quad \tilde{x} < 0 \\
\rho_4(t) &= \rho_R(t,\tilde{x}) \quad \text{for} \quad \tilde{x} > 0.
\end{aligned} \tag{4.55}$$

With these identifications, $S_{31}(\omega)$ in the four probe geometry equals $S_{LR}(\omega;\tilde{x}_-,\tilde{x}_-)$ in the two-droplet geometry, and similarly, $S_{41}(\omega)$ is given by $S_{RR}(\omega;\tilde{x}_+,\tilde{x}_-)$, where $\tilde{x}_- < 0$ and $\tilde{x}_+ > 0$. Also, we see that the Hall current in the single droplet, $\rho_R(t,x) - \rho_L(t,x)$ is dual to the tunneling current in the two droplets, $\rho_R(t,\tilde{x}_-) - \rho_R(t,\tilde{x}_+)$, because both are equivalent to $\rho_1(t) - \rho_4(t)$.

We will first verify that the scattering and perturbative calculations agree for $g = 1/2$. We have already found that when the noise is evaluated on only one side of the junction, then both the scattering and perturbative results agree. If one probe is in an incoming channel and the other probe is in an outgoing channel, then according to Appendix A the perturbative result for the noise is

$$\begin{aligned}
S_{31}(\omega;x_+,x_-) = e^{i\omega(x_+-x_-)}\Bigg\{ & \frac{|\omega|}{4\pi} \\
& - \frac{|\Gamma_q|^2}{8}\left[i4\text{sign}(\omega)\ln\left(\left|\frac{\omega^2-\omega_0^2}{\omega_0^2}\right|\right) + 2\pi\left[(1+\text{sign}\left(|\omega|-|\omega_0|\right))\right]\right]\Bigg\},
\end{aligned} \tag{4.56}$$

where we have set $g = \nu = 1/2$ in Eq. (A.20). On comparing this with the expansion

of the scattering calculation for small Γ in Eq. (4.50), we find that also in this case the scattering and perturbative results agree.

Next, to check the duality transformation, we must compare the scattering calculation as $\Gamma \to \infty$ with the perturbative calculation at $g = 2$. Again we found that if both probes are in the same branch then the two calculations agree. This is rather remarkable, because when $g = 2$ the system can be sensitive to short distance behavior, which means that it could depend on the detailed structure of the junction and on how it is regulated. However, here we found that the weak-coupling perturbative calculation and the strong-coupling limit of the scattering calculation are the same, even though they treat the junction very differently. We conclude that, at least to the order in perturbation theory that we have calculated, the noise extracted from a single channel is not affected by the short-distance properties of the impurity.

To complete the comparison, we need the results for the noise between the incoming and outgoing channels. Using Eq. (4.44) to relate the quasiparticle tunneling amplitude to the electron tunneling amplitude, we find that the expansion for $\Gamma \to \infty$ of the scattering calculation becomes

$$S_{41}(\omega; x_+, x_-) = \left\{ \frac{1}{4\pi}|\omega| + \frac{i}{2}|\Gamma_e|\omega^2 \mathrm{sign}(\omega) - \frac{2\pi}{3}|\Gamma_e|^2 \left[(|\omega| + \omega_0)^3 + (|\omega| - \omega_0)^3 \right] \right\} e^{i\omega(x_+ - x_-)}. \tag{4.57}$$

This must be compared with the perturbative calculation of $S_{RR}(\omega; \tilde{x}_+, \tilde{x}_-)$. To obtain this perturbative result, we set $\nu = 1/2$, $g = 2$ and replace ω_0 by $2\omega_0$ in Eq. (A.20). Then the perturbative calculation of the noise across the junction yields

$$S^{RR}(\omega; \tilde{x}_+, \tilde{x}_-) = \left\{ \frac{1}{4\pi}|\omega| - |\Gamma_e|^2 \left[\frac{\pi}{6} \left((|\omega| + |2\omega_0|)^3 + (|\omega| - |2\omega_0|)^3 \right) + \frac{2i\omega^2}{3\delta} \right] \right\} e^{i\omega(x_+ - x_-)}. \tag{4.58}$$

We first note that this expression for the noise contains a linear divergence in the cutoff δ. Thus this perturbative calculation is regulator dependent, which is not surprising because the tunneling operator at $g = 2$ has dimension 2 and should be an

irrelevant operator. In spite of this, both calculations do agree to order ω (which is all that the derivations of the duality transformation in reference [25] would predict); it is only the higher order terms in ω that disagree. This suggests that we are on the right track with the perturbative calculation, but we just need to add in the appropriate counter terms.

To see which counter term we should add, we begin by recalling that we used the most relevant tunneling operator to describe the system. However, for $g = 2$ the operators $(\rho_L)^2 + (\rho_R)^2$ and $\rho_L \rho_R$ are just as relevant as the tunneling operator, so we must consider their effects also. In fact, $(\rho_R(0) - \rho_L(0))^2$ also encourages tunneling because it tries to equalize the density of right movers and left movers. Another way to look at it is that we cannot have quasiparticles tunneling between the droplets, but density fluctuations on one side may affect the other side.

In Appendix B, we found that when the interaction

$$\mathcal{L}_{\text{int}} = \gamma \left(\rho_R(t,0) - \rho_L(t,0)\right)^2 \delta(x) \tag{4.59}$$

is included in the Lagrangian, it gives the following contribution to the noise

$$S^{RR}_{\rho\rho}(x_1, x_2) = \tag{4.60}$$
$$\theta(-x_1 x_2)\left\{ \frac{i\gamma}{8\pi^2}\omega^2 \text{sign}(\omega x_1) - \frac{\gamma^2}{16\pi^3}\left[|\omega|^3 - 2i\text{“}\delta(0)''\omega^2 \text{sign}(\omega x_1)\right] \right\} e^{i\omega(x_1 - x_2)}.$$

First, we note that the density-density coupling does not affect the noise evaluated on only one side of the impurity (i.e. when $x_1 x_2 > 0$.) According to equations (4.4) to (4.7), (4.43), and (4.44), this is necessary for the scattering and the perturbative calculations to agree. It is reasonable that the noise evaluated on only one side of the junction should be less affected by the counter terms and the regulator than the noise between probes on either side of the junction, because even though in both cases all the measurements are done far from the junction, in the second case the information must travel from one side of the junction to the other.

Second, we note that when $x_1 x_2 < 0$, equation (4.60) contains the linear term in γ,

which also appears in the scattering calculation, but not in the original perturbative calculation. We find that the only density-density interaction that gives the same linear term as in the scattering result for *all* of the cross-correlations is the one given in equation (4.59), with $\gamma = 1/(4\Gamma_q^2)$. When we add the density-density term with this choice for γ to the original perturbative calculation, we obtain

$$S^{RR}_{\rm pert}(\omega; x_+, x_-) = \left\{ \frac{1}{4\pi}|\omega| \;+\; \frac{i}{2}|\Gamma_e|\omega^2 {\rm sign}(\omega) - \frac{2\pi}{3}|\Gamma_e|^2 \left[(|\omega|+\omega_0)^3 + (|\omega|-\omega_0)^3\right] \right.$$
$$\left. +\; 2i|\Gamma_e|^2\omega^2 {\rm sign}(\omega)\left(\pi \text{“}\delta(0)'' - \frac{1}{3\delta}\right)\right\} e^{i\omega(x_+ - x_-)}. \quad (4.61)$$

Thus, (except for the divergent part), this perturbative result agrees with the scattering result.

To cancel the divergent part, we must regulate the delta-function properly and adjust the counterterm accordingly. Then the two results will agree in the limit as x_+ and $x_- \to \pm\infty$. Another approach, which may be more appropriate, is to "smooth out" the density-density interaction. This is accomplished by replacing the interaction in equation (4.59) by the following expression

$$\mathcal{L}_{\rm int} = \gamma \left(\rho_R(t,0) - \rho_L(t,0)\right)^2 f_\epsilon(x), \quad (4.62)$$

where $f_\epsilon(x) \to \delta(x)$ as $\epsilon \to 0$. This new interaction does not change the finite part of Eq. (4.61), and the function f can be chosen so that the divergence cancels. As a result, even though the duality symmetry is not exactly obeyed for the cross-correlations, it is possible to add in counter terms to bring the strong-coupling limit of one picture into agreement with the weak-coupling limit of the dual picture.

To summarize, to the order in Γ we have calculated, the action for $g = 1/2$ is dual to the renormalized action for $g = 2$, given by

$$\mathcal{L} \;=\; \frac{1}{8\pi}\left[(\partial_t\phi)^2 - v^2(\partial_x\phi)^2\right] - \Gamma_e e^{-i2\omega_0 t}\delta(x)e^{\sqrt{2}\phi(t,0)} + H.c.$$
$$+\; 4\pi^2\Gamma_e\delta(x)\left(\rho_R(t,0) - \rho_L(t,0)\right)^2; \quad (4.63)$$

and if we only want to calculate the noise in one particular channel, then it is not necessary to include the $\rho\rho$ interaction to obtain the dual picture. As explained above, this action can be interpreted as containing two different terms that induce or encourage tunneling. We can also use the relation

$$\rho_R(0) - \rho_L(0) = \frac{1}{2\sqrt{2\pi}}\partial_x\phi(0) \tag{4.64}$$

to write the action as

$$\mathcal{L} = \frac{1}{8\pi}\left[(\partial_t\phi)^2 - \tilde{v}^2(\partial_x\phi)^2\right] - \Gamma_e e^{-i2\omega_0 t}\delta(x)e^{\sqrt{2}\phi(t,0)} + H.c., \tag{4.65}$$

where $\tilde{v}^2 = v^2 + 4\pi\delta(x)\Gamma_e^2$ is the "renormalized" velocity. In this case, the velocity remains the same everywhere but right at the junction. If, instead, we use Eq. (4.62) for the density interaction, then the velocity is renormalized in a region around the junction.

4.5 Conclusion

In this chapter we studied the four terminal tunneling noise spectrum for chiral Luttinger liquids characterized by an exponent g. Perturbative results are obtained for arbitrary g. Perturbative calculations for quasiparticle tunneling reveal a singularity at the quasiparticle Josephson frequency $\nu eV/\hbar$, while perturbative calculations for electron tunneling only produce a singularity at the electron Josephson frequency $eV/\hbar$. This appears to be inconsistent with the duality picture that quasiparticle and electron tunneling describe the same tunneling junction in two different limits. To understand how the quasiparticle tunneling picture can smoothly connect to the electron tunneling picture, we calculated the exact noise spectrum for $g = 1/2$ (or $g = 2$ due to duality). We find that the singularity at the quasiparticle Josephson frequency $\frac{1}{2}eV/\hbar$ is smeared for finite tunneling and is not a true singularity, while the singularity at the electron Josephson frequency $eV/\hbar$ survives in the exact result. Thus, for all non-zero values of Γ, the electron singularity coexists with a smoothed

out quasiparticle singularity, and only in the limit of the quasiparticle tunneling going to zero is there a "transition" where the quasiparticle singularity appears. An interpretation of this is that at finite tunneling the quasiparticles can acquire a finite lifetime, so there is no sharp quasiparticle singularity. This is consistent with the calculations of the Hall current, which is no longer at its quantized value once the quasiparticles can tunnel. In light of our perturbative calculations, we expect that this qualitative picture will also apply for other values of $g \leq 1/2$. It would be interesting to check this picture by direct calculation for some $g < 1/2$. It does not appear that the thermal Bethe ansatz techniques of reference [24] will be applicable because they do not give information about the excited states. However, it might be possible to use a leading-log calculation, perhaps along the lines of reference [22], to solve for values around $g = 1/2$.

From the exact result we also find that the noise spectrum of the current correlations on a single branch (auto-correlations) satisfies the duality relation, while current correlations between distinct branches (cross-correlations) do not satisfy the naive duality relation.

Chapter 5

Open questions

Although we have learned much on the problem of tunneling in Luttinger liquids, most notably on noise in these strongly correlated states, there are (as usual) many open questions. Here I will list some of the interesting problems that are left open in the study of noise and transport in chiral Luttinger liquids.

First, there is the question on whether one can treat the problem exactly for other values of g. For transport and the DC noise ($\omega = 0$) that is the case, as shown in Refs. [23, 24, 40]. However, the thermodynamic Bethe Ansatz does not gives information on excited states, or put differently, on dynamical correlation functions. That means that one would not be able to obtain the noise spectrum at *finite* frequencies using those techniques.

In the $g = 1/2$ case, we could solve for the correlation functions because we could redefine the problem in terms of free chiral fermions with a boundary interaction. The other solvable case is $g = 1$, which corresponds to free fermions to begin with. From the strong-weak coupling duality $g \leftrightarrow g^{-1}$, we can obtain the $g = 2$ case as the dual of the $g = 1/2$ one. We thus have three points for which we can obtain dynamical correlation functions, and consequently the noise spectrum at finite frequencies.

It is hard to resist trying to make a connection to integrable random matrix models, which have three exactly solvable points characterized by $\beta = 1, 2, 4$ corresponding respectively to the orthogonal, unitary and simpletic ensembles. The association of β and $2g$ can be more than a coincidence. This connection may be the deeper rea-

son for the exactly solvability for the g's treated in this thesis. If this speculation is correct, there is hope in trying to solve for the noise spectrum for the case $g = p/q$, p, q integers. The noise spectrum depends on the two-point correlations of density operators, and these correlations have been calculated in the $1/r^2$ interaction models for rational β.

Second, it would be extremely important to obtain results for multiple impurity scatterers. The motivation here is to gain a better understanding on the effects of weaker or stronger disorder in the tunneling current. So far, there is only one experiment that has observed the characteristic nonlinear dependence of the tunneling conductance on temperature [18]. The hope is that by learning the effects of impurities will help the design of further experimental tests.

Third, one should observe quantum interference between edge modes by considering two point contacts separated by a distance d. One can think of the region between the two point contacts as a Fabri-Perot interferometer. The distance d sets the time scale $\tau = d/v$, where v is the edge velocity. Oscillations in the conductance should occur at source-drain voltages V such that $\omega_J = e^*V/\hbar = 2\pi n/\tau$. The amplitude of the oscillations should have a nonlinear dependence on V, which is yet another manifestation of Luttinger liquid behavior [47].

Fourth, experiments probing quantum dots or artificial atoms usually focus on interaction effects inside the dots. The "leads' are usually thought to be Fermi liquids that serve the purpose of particle reservoirs for the dots. At high magnetic fields the "leads" form FQH states, and the reservoirs will be the edges of the FQH liquids, which are chiral Luttinger liquids. There will then be correlation effects that arise not from the dots but from the leads. An important issue is how to separate the two effects, so as to be able to study quantum dots at high magnetic field [48].

These are only a few of the many interesting directions that are ahead of us in the study of the strongly correlated chiral Luttinger liquids. The ideas and techniques developed in the course of the work presented in this thesis, hopefully, will be useful in addressing some of these questions.

Appendix A

Perturbative Calculation

In order to obtain the noise spectrum of density-density correlations on given leads, we start by writing the correlations between density operators as follows:

$$\langle \rho_a(t, x_1)\rho_b(0, x_2)\rangle \ , \tag{A.1}$$

where a, b take the values $+1$ for R moving branches and -1 for L moving ones. Such compressed notation makes it simpler to identify incoming and outgoing branches in a unified way for both left and right movers: $\rho_a(t, x_1)$, for example, is the density in an incoming or outgoing branch if $ax_1 < 0$ or $ax_1 > 0$, respectively.

The densities are related to the fields $\phi_{R,L}$ through $\rho_{R,L} = \frac{\sqrt{\nu}}{2\pi}\partial_x\phi_{R,L}$, so that we can write

$$\langle \rho_a(t, x_1)\rho_b(t', x_2)\rangle = \frac{\nu}{(2\pi)^2}\ \partial_{x_1}\partial_{x_2}\langle \phi_a(t, x_1)\phi_b(t', x_2)\rangle \ , \tag{A.2}$$

where it is convenient to use

$$\langle \phi_a(t, x_1)\phi_b(t', x_2)\rangle = \frac{d}{d\lambda_1}\frac{d}{d\lambda_2}\langle e^{i\lambda_1\phi_a(t,x_1)}\ e^{-i\lambda_2\phi_b(t',x_2)}\rangle|_{\lambda_1,\lambda_2=0} \ . \tag{A.3}$$

The last correlation function is easy to calculate perturbatively using

$$\langle T_c(e^{i\lambda_1\phi_a(t,x_1)}\ e^{-i\lambda_2\phi_b(t',x_2)})\rangle = \langle 0|\ T_c(S(-\infty,-\infty)\ e^{i\lambda_1\phi_a(t,x_1)}\ e^{-i\lambda_2\phi_b(t',x_2)})\ |0\rangle \ , \tag{A.4}$$

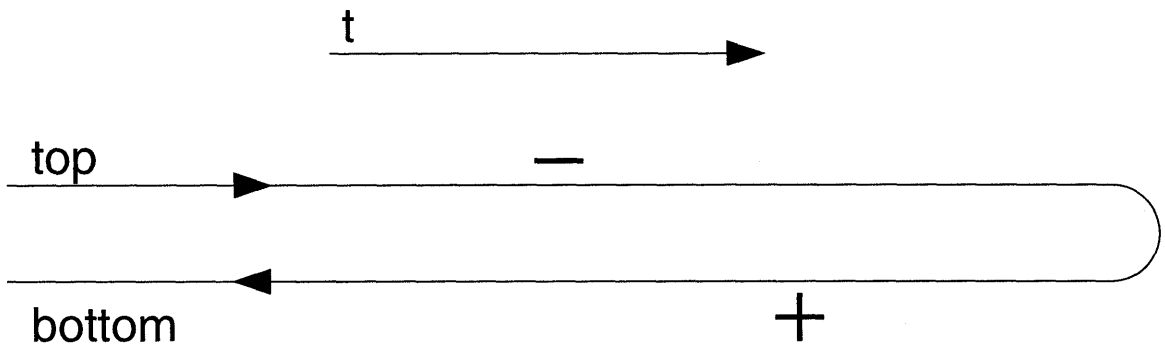

Figure A-1: An insertion of an operator $e^{+iq\phi(t)}$ corresponds to the insertion of a charge + on the contour at time t. Similarly, an insertion of an operator $e^{-iq\phi(t)}$ corresponds to an insertion of a charge − at time t. The time t is ordered along the contour shown, and there is a distinction between charges placed on the top and bottom branches. In the illustration, we consider the particular case when the − charge is inserted on the top contour, and the + charge is inserted on the bottom contour.

where $|0\rangle$ is the unperturbed ground state, and T_c is the ordering along the Keldysh contour (Fig. A-1). The scattering operator $S(-\infty,-\infty)$ takes the initial state, evolves it from $t=-\infty$ to $t=\infty$ and back to $t=-\infty$. The use of the Keldysh contour is necessary in the treatment of non- equilibrium problems, such as the one we have in hand. A more detailed description of the method in the context treated here can be found in Chapter 3.

In order to proceed we expand $S(-\infty,-\infty)$ to second order in perturbation theory. In terms of the Coulomb gas of Chapter 3, we have an insertion of two charges of opposite sign:

$$\begin{aligned} &\langle\, T_c\left(e^{i\lambda_1\phi_a(t,x_1)}\; e^{-i\lambda_2\phi_b(t',x_2)}\right)\,\rangle_{|\Gamma|^2} = \\ &(i\Gamma)(i\Gamma^*)\oint_c dt_+ \oint_c dt_-\; e^{i\omega_0 t_+}\; e^{-i\omega_0 t_-} \\ &\qquad\qquad \langle 0|\; T_c(\; e^{iq\phi(t_+,0)}\; e^{-iq\phi(t_-,0)}\; e^{i\lambda_1\phi_a(t,x_1)}\; e^{-i\lambda_2\phi_b(t',x_2)})\;|0\rangle\;, \end{aligned} \tag{A.5}$$

where $q=\sqrt{g}$, and ϕ without subscript stands for the sum $\phi_R+\phi_L$. The expression above is simplified using

$$\langle 0|T_c(\prod_j e^{iq_j\phi(t_j,x_j)})|0\rangle = e^{-\sum_{i>j} q_i q_j \langle 0|T_c(\phi(t_i,x_i)\phi(t_j,x_j))|0\rangle}\;. \tag{A.6}$$

Substituting it into Eq. (A.3) we obtain

$$\begin{aligned}\langle T_c(\phi_a(t,x_1)\phi_b(t',x_2))\rangle_{|\Gamma|^2} = \qquad\qquad (A.7)\\ |\Gamma|^2 \oint dt_+ \oint dt_- e^{q^2\langle 0|T_c(\phi(t_+,0)\phi(t_-,0))|0\rangle} e^{i\omega_0(t_+-t_-)}\\ \times\Big\{q^2\Big[\langle 0|T_c(\phi(t_+,0)\phi_a(t,x_1))|0\rangle - \langle 0|T_c(\phi(t_-,0)\phi_a(t,x_1))|0\rangle\Big]\\ \times\Big[\langle 0|T_c(\phi(t_+,0)\phi_b(t',x_2))|0\rangle - \langle 0|T_c(\phi(t_-,0)\phi_b(t',x_2))|0\rangle\Big]\\ + \langle 0|T_c(\phi_a(t,x_1)\phi_b(t',x_2))|0\rangle\Big\}\ .\end{aligned}$$

The last term in the expression above, the one proportional to the correlation function $\langle 0|T_c(\phi_a(t,x_1)\phi_b(t',x_2))|0\rangle$, vanishes. The reason why this happens is very simple: the factor in front of it is the term of order $|\Gamma|^2$ in the expansion of $Z = \langle 0|S(-\infty,-\infty)|0\rangle$; since $Z \equiv 1$, the correction at any order in Γ must vanish.

In order to carry out the calculations, we introduce notation that keeps track of the position of the two inserted charges along the contour, *i.e.*, whether they are in the forward (or top) branch, or in the return (or bottom) branch (see Fig. A-1). The position of the charges is important for the computation of the contour-ordered correlation function, given by $\langle 0|T_c(\phi_{R,L}(t_1,x_1)\phi_{R,L}(t_2,x_2))|0\rangle$

$$= \begin{cases} -\ln(\delta + i\ \mathrm{sign}(t_1-t_2)[(t_1-t_2) \mp (x_1-x_2)], & t_1 \text{ and } t_2 \text{ in the top branch} \\ -\ln(\delta - i\ \mathrm{sign}(t_1-t_2)[(t_1-t_2) \mp (x_1-x_2)], & t_1 \text{ and } t_2 \text{ in the bottom branch} \\ -\ln(\delta - i[(t_1-t_2) \mp (x_1-x_2)]), & t_1 \text{ in the top, } t_2 \text{ in the bottom} \\ -\ln(\delta + i[(t_1-t_2) \mp (x_1-x_2)]), & t_1 \text{ in the bottom, } t_2 \text{ in the top.} \end{cases}$$

The compact notation consists of giving indices to the times which contain the information about which branch of the Keldysh contour they are on, so that t^μ is on the top branch for $\mu = +1$, and on the bottom for $\mu = -1$. In this way, we can compress the correlations to a compact form:

$$\begin{aligned} G^{ab}_{\mu\nu}(t_1,x_1;t_2,x_2) = G^{ab}_{\mu\nu}(t_1-t_2,x_1-x_2) = \langle 0|T_c(\phi_a(t_1^\mu,x_1)\phi_b(t_2^\nu,x_2))|0\rangle \\ = -\delta_{a,b}\ \ln(\delta + i\ K_{\mu\nu}(t_1-t_2)[(t_1-t_2) - a(x_1-x_2)])\ , \qquad (A.8)\end{aligned}$$

where

$$K_{\mu\nu}(t) = \theta(\mu\nu)\ \mathrm{sign}(\nu t) + \theta(-\mu\nu)\ \mathrm{sign}(\nu)\ . \tag{A.9}$$

Again, we have used $a, b = \pm 1$ for R and L fields, respectively. The correlation in Eq. (A.7) can be written, using this compressed notation, as

$$\langle T_c(\phi_a(t,x_1)\phi_b(t',x_2))\rangle_{|\Gamma|^2} = \tag{A.10}$$

$$\begin{aligned} &|\Gamma|^2 q^2 \sum_{\mu\nu} \mathrm{sign}(\mu\nu) \int_{-\infty}^{\infty} dt_+ \int_{-\infty}^{\infty} dt_-\ e^{i\omega_0(t_+ - t_-)} P_{\mu\nu}(t_+ - t_-) \\ &\times [G^{aa}_{+\mu}(t - t_+, x_1) - G^{aa}_{+\nu}(t - t_-, x_1)] \\ &\times [G^{bb}_{+\mu}(t' - t_+, x_2) - G^{bb}_{+\nu}(t' - t_-, x_2)]\ , \end{aligned} \tag{A.11}$$

where $P_{\mu\nu}(t_+ - t_-) = e^{q^2[G^{++}_{\mu\nu}(t_+ - t_-,0) + G^{--}_{\mu\nu}(t_+ - t_-,0)]}$, or explicitly:

$$P_{\pm\pm}(t) = \frac{1}{(\delta \pm i|t|)^{2g}}\ ,\ P_{\pm\mp}(t) = \frac{1}{(\delta \mp it)^{2g}}\ . \tag{A.12}$$

The factor $\mathrm{sign}(\mu\nu)$ simply keeps track of the sign coming from the integration of the times $t_\pm$ along the contour. Notice that the times t and t' are taken to be on the top branch.

Now, let

$$\begin{aligned} F_{ab}(\omega; x_1, x_2) &= \int_{-\infty}^{\infty} dt\ e^{i\omega t}\ \langle T_c(\rho_a(t,x_1)\rho_b(0,x_2))\rangle_{|\Gamma|^2} \\ &= \frac{\nu}{(2\pi)^2}\ \partial_{x_1}\partial_{x_2} \int_{-\infty}^{\infty} dt\ e^{i\omega t}\ \langle T_c(\phi_a(t,x_1)\phi_b(0,x_2))\rangle_{|\Gamma|^2}\ , \end{aligned} \tag{A.13}$$

which can be easily shown, using Eq. (A.11), to yield

$$\begin{aligned} F_{ab}(\omega; x_1, x_2) &= |\Gamma|^2 \frac{\nu q^2}{(2\pi)^2} \sum_{\mu\nu} \mathrm{sign}(\mu\nu) \\ &\times \Big[\tilde{P}_{\mu\nu}(\omega_0) \left(g^{aa}_{+\mu}(\omega, x_1) g^{bb}_{+\mu}(-\omega, x_2) + g^{aa}_{+\nu}(\omega, x_1) g^{bb}_{+\nu}(-\omega, x_2) \right) \\ &\quad - \tilde{P}_{\mu\nu}(\omega_0 - \omega)\ g^{bb}_{+\mu}(-\omega, x_2) g^{aa}_{+\nu}(\omega, x_1) \\ &\quad - \tilde{P}_{\mu\nu}(\omega_0 + \omega)\ g^{aa}_{+\mu}(\omega, x_1) g^{bb}_{+\nu}(-\omega, x_2) \Big]\ . \end{aligned} \tag{A.14}$$

In this equation, g is given by $g^{aa}_{+\mu}(\omega,x) = \partial_x \tilde{G}^{aa}_{+\mu}(\omega,x)$ and can be obtained from Eqs. (A.8) and (A.9):

$$g^{ab}_{\mu\nu}(\omega,x) = \delta_{a,b} \times \begin{cases} \pi i a\, e^{i\omega a x}\ (\mathrm{sign}(\omega) + \mathrm{sign}(ax)) & , \mu = +1, \nu = +1 \\ \pi i a\, e^{i\omega a x}\ (\mathrm{sign}(\omega) - \mathrm{sign}(ax)) & , \mu = -1, \nu = -1 \\ -2\pi i a\, e^{i\omega a x}\ \theta(-\omega) & , \mu = +1, \nu = -1 \\ 2\pi i a\, e^{i\omega a x}\ \theta(\omega) & , \mu = -1, \nu = +1 \end{cases}$$

The spectrum to second order can be obtained from $F_{ab}(\omega, x_1, x_2)$ as follows:

$$\begin{aligned} S^{(2)}_{ab}(\omega; x_1, x_2) &= S^{(2)}_{ba}(-\omega; x_2, x_1) = \int_{-\infty}^{\infty} dt\ e^{i\omega t} \langle \{\rho_a(t, x_1), \rho_b(0, x_2)\} \rangle_{|\Gamma|^2} \\ &= F_{ab}(\omega; x_1, x_2) + F^*_{ab}(-\omega; x_1, x_2)\ . \end{aligned} \tag{A.15}$$

The only ingredients remaining to be calculated are the $\tilde{P}(\omega)'s$, which are given by:

$$\begin{aligned} \tilde{P}_{++}(\omega) &= t(-\omega) = \int_{-\infty}^{\infty} dp \frac{e^{i\omega p}}{(\delta + i|p|)^{2g}} \\ \tilde{P}_{--}(\omega) &= b(-\omega) = \int_{-\infty}^{\infty} dp \frac{e^{i\omega p}}{(\delta - i|p|)^{2g}} \\ \tilde{P}_{\pm\mp}(\omega) &= c_{\pm}(-\omega) = \int_{-\infty}^{\infty} dp \frac{e^{i\omega p}}{(\delta \mp ip)^{2g}}\ . \end{aligned} \tag{A.16}$$

The $t, b, c_{\pm}$ are the same as in Chapter 3. One can easily check that $t(\omega) + b(\omega) = c_+(\omega) + c_-(\omega)$, and that the $c_{\pm}$ are given by

$$c_{\pm}(\omega) = \int_{-\infty}^{\infty} dp \frac{e^{-i\omega p}}{(\delta \mp ip)^{2g}} = \frac{2\pi}{\Gamma(2g)} |\omega|^{2g-1} e^{-|\omega|\delta}\ \theta(\pm\omega)\ . \tag{A.17}$$

Now, we have the tools we need in order to obtain all correlations. In particular, correlations within the same branch and taken at the same point, *i.e.*, $a = b$ and $x_1 = x_2$, can be shown to yield:

$$S^{(2)}_{aa}(\omega; x_1, x_1) = \frac{4\pi\nu g}{\Gamma(2g)}\ |\Gamma|^2\ \theta(a x_1)\ \Big||\omega| - |\omega_0|\Big|^{2g-1}\ \theta(|\omega_0| - |\omega|)\ . \tag{A.18}$$

The zero order term in Γ is trivially obtained from the unperturbed density-density correlation functions:

$$\begin{aligned} S^{(0)}_{ab}(\omega; x_1, x_2) &= S^{(0)}_{ba}(-\omega; x_2, x_1) = \int_{-\infty}^{\infty} dt\ e^{i\omega t} \langle 0 | \{\rho_a(t, x_1), \rho_b(0, x_2)\} | 0 \rangle \\ &= \frac{\nu}{2\pi} |\omega|\ \delta_{a,b}\ e^{i\omega a(x_1 - x_2)}\ , \end{aligned} \tag{A.19}$$

so that, in particular, $S^{(0)}_{aa}(\omega; x_1, x_1) = \frac{\nu}{2\pi}|\omega|$.

Combining the zeroth and second order results, we obtain the results used in section 4.2 for the noise in incoming ($ax_1 < 0$) and outgoing ($ax_1 > 0$) branches, namely:

$$S(\omega) = \begin{cases} \frac{\nu}{2\pi}|\omega|, & \text{incoming branches} \\ \frac{\nu}{2\pi}|\omega| + \frac{4\pi\nu g}{\Gamma(2g)}\ |\Gamma|^2\ \left||\omega| - |\omega_0|\right|^{2g-1}\ \theta(|\omega_0| - |\omega|), & \text{outgoing branches} \end{cases}$$

It is straightforward to show that the noise in the incoming branch remains equal to $\frac{\nu}{2\pi}|\omega|$ to all orders in perturbation theory.

Next, we will obtain correlations between densities of an incoming and an outgoing branch (the cross-correlations). Without loss of generatity, we will focus on the correlations between two R branches ($a = 1$), one outgoing ($x_1 > 0$), and another incoming ($x_2 < 0$). The results for other combinations of branches are trivially obtained from the case we consider. We have, again, all the tools at hand, namely Eqs. (A.14) and (A.15), as well as our expressions for $g^{ab}_{\mu\nu}(\omega, x)$ and $\tilde{P}_{\mu\nu}(\omega)$. We find

$$\begin{aligned} S^{(2)}_{RR}(\omega; x_1 > 0, x_2 < 0) &= \int_{-\infty}^{\infty} dt\ e^{i\omega t} \langle \{\rho_R(t, x_1 > 0), \rho_R(0, x_2 < 0)\} \rangle_{|\Gamma|^2} \\ &= e^{i\omega(x_1 - x_2)}\ \frac{|\Gamma|^2 g\nu}{2} \Bigg\{ \mathrm{sign}(\omega) H_g(\omega) \\ &\quad - \frac{2\pi}{\Gamma(2g)} \left[(|\omega| + |\omega_0|)^{2g-1} + \left||\omega| - |\omega_0|\right|^{2g-1} \mathrm{sign}(|\omega| - |\omega_0|) \right] \Bigg\}\ , \end{aligned} \tag{A.20}$$

where the function $H_g(\omega)$ is defined as

$$H_g(\omega) = 2[t(\omega_0) - b(\omega_0)] - [t(\omega_0 - \omega) - b(\omega_0 - \omega)] - [t(\omega_0 + \omega) - b(\omega_0 + \omega)]$$

$$= 8\int_0^\infty dt\ \cos(\omega_0 t)\sin^2(\omega t/2)\left[\frac{1}{(\delta+it)^{2g}} - \frac{1}{(\delta-it)^{2g}}\right] . \qquad \text{(A.21)}$$

One can show particularly that $H_{1/2}(\omega) = -4i\ln(|\frac{\omega^2-\omega_0^2}{\omega_0^2}|)$, $H_1(\omega) = 0$, and $H_2(\omega) = -\frac{4i\omega^2}{3\delta} \to \infty$ as $\delta \to 0$.

The zero order contribution to the cross-correlations can be read directly from Eq.(A.19): $S^{(0)}_{RR}(\omega; x_1 > 0, x_2 < 0) = \frac{\nu}{2\pi}|\omega|\ e^{i\omega(x_1-x_2)}$.

Appendix B

Perturbative Calculation for the Density-density Coupling

Here we consider the neutral coupling $L_{\rm int} = \gamma(\rho_R(t,0) - \rho_L(t,0))^2$, and show that it contributes to the correlations between incoming and outgoing branches, although it does not contribute to correlations between two incoming or two outgoing ones. The calculations are simpler than the ones in Appendix A. We will demonstrate the point by calculating the correlation $\langle T_c(\rho_R(t,x_1)\rho_R(0,x_2))\rangle$ to first and second order in γ. Other correlations can be calculated in a very similar way.

As in Appendix A, contour integrals are simplified by keeping track of insertions in the top and bottom branches with indices $\mu, \nu = \pm 1$. It is useful to define

$$\begin{aligned} h^{ab}_{\mu\nu}(t_1,x_1;t_2,x_2) &= h^{ab}_{\mu\nu}(t_1-t_2,x_1-x_2) = \langle 0|T_c(\rho_a(t_1^\mu,x_1)\rho_b(t_2^\nu,x_2))|0\rangle \\ &= \frac{\nu}{(2\pi)^2}\partial_{x_1}\partial_{x_2}\langle 0|T_c(\phi_a(t_1^\mu,x_1)\phi_b(t_2^\nu,x_2))|0\rangle \qquad \text{(B.1)} \\ &= \frac{\nu}{(2\pi)^2}\partial_{x_1}\partial_{x_2}G^{ab}_{\mu\nu}(t_1-t_2,x_1-x_2)\ , \end{aligned}$$

(B.2)

where a and b, as in Appendix A, take the values $+1$ for R moving branches and -1 for L moving ones. It follows from the calculations of Appendix A that $\tilde{h}^{ab}_{\mu\nu}(\omega,x) =$

$-\frac{\nu}{(2\pi)^2}\partial_x^2\tilde{G}^{ab}_{\mu\nu}(\omega,x) = -\frac{\nu}{(2\pi)^2}\partial_x g^{ab}_{\mu\nu}(\omega,x)$, which gives

$$\tilde{h}^{ab}_{\mu\nu}(\omega,x) = \frac{\nu}{(2\pi)^2}\delta_{a,b} \times \begin{cases} 2\pi|\omega|\ \theta(a\omega x)\ e^{i\omega a x} - 2\pi i\delta(x), & \mu=+1,\nu=+1 \\ 2\pi|\omega|\ \theta(-a\omega x)\ e^{i\omega a x} + 2\pi i\delta(x), & \mu=-1,\nu=-1 \\ 2\pi|\omega|\ \theta(-\omega)\ e^{i\omega a x}, & \mu=+1,\nu=-1 \\ 2\pi|\omega|\ \theta(\omega)\ e^{i\omega a x}, & \mu=-1,\nu=+1 \end{cases}$$

The perturbative results can be easily written in terms of these $\tilde{h}$'s.

Notice that the only term in the interaction $\rho_-^2 = \rho_R^2 - 2\rho_R\rho_L + \rho_L^2$ that contributes to $\langle T_c(\rho_R(t,x_1)\rho_R(0,x_2))\rangle$ to order γ is the ρ_R^2 term. The first order in γ correction to the correlation function can be written as

$$\begin{aligned} \langle\ T_c\ & (\rho_R(t,x_1)\rho_R(0,x_2))\rangle_\gamma \\ &= i\gamma\oint_c dt_1\ \langle 0|\ T_c(\rho_R(t,x_1)\rho_R(0,x_2)\rho_R(t_1,0)\rho_R(t_1,0))\ |0\rangle \\ &= 2i\gamma\oint_c dt_1\ \langle 0|\ T_c(\rho_R(t,x_1)\rho_R(t_1,0))\ |0\rangle \times \langle 0|\ T_c(\rho_R(0,x_2)\rho_R(t_1,0))\ |0\rangle \end{aligned} \quad \text{(B.3)}$$

The Fourier transform $F^{(1)}_{RR}(\omega;x_1,x_2)$ of the expression in Eq.(B.3) is simply

$$F^{(1)}_{RR}(\omega;x_1,x_2) = 2i\gamma\sum_\mu \mathrm{sgn}(\mu)\ \tilde{h}^{++}_{+\mu}(\omega,x_1)\tilde{h}^{++}_{+\mu}(-\omega,x_2)\ , \quad \text{(B.4)}$$

and thus to first order in γ the cross-correlation spectrum is given by

$$\begin{aligned} S^{(1)}_{RR}(\omega;x_1,x_2) &= S^{(1)}_{RR}(-\omega;x_2,x_1) = \int_{-\infty}^{\infty} dt\ e^{i\omega t}\langle\{\rho_R(t,x_1),\rho_R(0,x_2)\}\rangle_\gamma \\ &= F^{(1)}_{RR}(\omega;x_1,x_2) + F^{(1)^*}_{RR}(-\omega;x_1,x_2) \\ &= \frac{i\gamma\nu^2}{2\pi^2}\ \theta(-x_1x_2)\ \omega^2\ \mathrm{sign}(\omega x_1)\ e^{i\omega(x_1-x_2)}\ . \end{aligned} \quad \text{(B.5)}$$

Turning now to second order in the perturbation expansion, both the ρ_R^2 and the $\rho_R\rho_L$ terms in the interaction $\rho_-^2 = \rho_R^2 - 2\rho_R\rho_L + \rho_L^2$ can contribute to the order γ^2 correction to $\langle T_c(\rho_R(t,x_1)\rho_R(0,x_2))\rangle$. Consider the $\gamma\rho_R^2$ coupling, so that to second

order we have

$$\begin{aligned}
\langle\ T_c\ & (\rho_R(t,x_1)\rho_R(0,x_2))\rangle_{(\gamma\rho_R^2)^2} \\
&= \frac{(i\gamma)^2}{2!}\oint_c dt_1 \oint_c dt_2 \langle 0|\ T_c(\rho_R(t,x_1)\rho_R(0,x_2)\rho_R(t_1,0)\rho_R(t_1,0)\rho_R(t_2,0)\rho_R(t_2,0))\ |0\rangle \\
&= 8\frac{(i\gamma)^2}{2!}\oint_c dt_1 \oint_c dt_2\ \ \langle 0|\ T_c(\rho_R(t,x_1)\rho_R(t_1,0))\ |0\rangle \\
&\qquad\qquad \times\langle 0|\ T_c(\rho_R(0,x_2)\rho_R(t_2,0))\ |0\rangle \\
&\qquad\qquad \times\langle 0|\ T_c(\rho_R(t_1,0)\rho_R(t_2,0))\ |0\rangle\ . \qquad \text{(B.6)}
\end{aligned}$$

The effect of the $\gamma 2\rho_R\rho_L$ coupling can be calculated likewise. The Fourier transform of these two contributions combined give

$$F^{(2)}_{RR}(\omega;x_1,x_2) = -4\gamma^2\sum_{\mu\nu}\mathrm{sign}(\mu\nu)\tilde{h}^{++}_{+\mu}(\omega,x_1)\tilde{h}^{++}_{+\nu}(-\omega,x_2)\left[\tilde{h}^{++}_{\mu\nu}(\omega,0)+\tilde{h}^{--}_{\mu\nu}(\omega,0)\right]\ , \qquad \text{(B.7)}$$

so that the cross-correlation spectrum to second order is

$$\begin{aligned}
S^{(2)}_{RR}(\omega;x_1,x_2) &= S^{(2)}_{RR}(-\omega;x_2,x_1) = \int_{-\infty}^{\infty} dt\ e^{i\omega t}\langle\{\rho_R(t,x_1),\rho_R(0,x_2)\}\rangle_{\gamma^2} \qquad \text{(B.8)} \\
&= F^{(2)}_{RR}(\omega;x_1,x_2) + F^{(2)*}_{RR}(-\omega;x_1,x_2) \\
&= -\frac{\gamma^2\nu^3}{2\pi^3}\,\theta(-x_1x_2)\ e^{i\omega(x_1-x_2)}\left[|\omega|^3 - 2i\ \text{“}\delta(0)\text{”}\ \omega^2\ \mathrm{sign}(\omega x_1)\right]\ ,
\end{aligned}$$

where “$\delta(0)$” is a regulation dependent divergent term.

Notice that, both to first and second order in γ, the correlations on the same side of the junction, *i.e.*, $x_1x_2 > 0$, do not feel the density-density coupling, whereas correlations across the junction ($x_1x_2 < 0$) do feel the coupling. More generally, when one considers all possible correlations involving R and L branches, only those which contain an incoming and an outgoing branch will have a non-zero correction due to the density-density coupling. Correlations between two incoming or two outgoing branches will be zero.

Appendix C

Scattering Calculation

In this appendix, we evaluate the expectation values and integrals used for calculating the noise in section 4.3. The methods of calculation are very similar to those in [29]

First, we will evaluate the noise in the incoming reservoir, which is given by

$$S(\omega; x_-, x_-) = \int_{-\infty}^{\infty} dt \left(e^{i\omega t} + e^{-i\omega t}\right) \langle \rho_-(t, x_-)\rho_-(0, x_-)\rangle. \tag{C.1}$$

The expectation value we must calculate is given by

$$\langle \rho_-(t, x_-)\rho_-(0, x_-)\rangle = \langle \psi^\dagger(t, x_-)\psi(t, x_-)\psi^\dagger(0, x_-)\psi(0, x_-)\rangle, \tag{C.2}$$

with $x_- < 0$. Using the solutions in Eqs. (4.19) and (4.20) for ψ and $\psi^\dagger$, we find

$$\langle \rho_-(t, x_-)\rho_-(0, x_-)\rangle = \sum_{\omega_1,\omega_2,\omega_3,\omega_4} e^{-i(\omega_1+\omega_2)t} \langle \Phi | A^\dagger_{-\omega_1} A_{\omega_2} A^\dagger_{-\omega_3} A_{\omega_4} | \Phi \rangle e^{i(\omega_1+\omega_2+\omega_3+\omega_4)x_-}. \tag{C.3}$$

The connected part of $\langle A^\dagger_{-\omega_1} A_{\omega_2} A^\dagger_{-\omega_3} A_{\omega_4}\rangle$ has $A^\dagger_{-\omega_1}$ paired with A_{ω_4} and A_{ω_2} paired with $A^\dagger_{-\omega_3}$ and is given by

$$\langle \Phi | A^\dagger_{-\omega_1} A_{\omega_2} A^\dagger_{-\omega_3} A_{\omega_4} | \Phi \rangle_{\text{con}} = \langle \Phi | A^\dagger_{-\omega_1} A_{\omega_4} | \Phi \rangle \langle \Phi | A_{\omega_2} A^\dagger_{-\omega_3} | \Phi \rangle. \tag{C.4}$$

Evaluating these correlations using equations (4.23) and (4.27), we find that the

current-current correlation reduces to

$$\langle \rho_-(t, x_-)\rho_-(0, x_-)\rangle = \sum_{\omega_1,\omega_2} e^{-i(\omega_1+\omega_2)t} n_{-\omega_1}(1 - n_{\omega_2}). \tag{C.5}$$

Substituting this expression back into equation (4.31) for the noise, and performing the integrals over t and ω_1, we obtain

$$S(\omega; x_-, x_-)(\omega) = \int_{-\infty}^{\infty} \frac{d\omega_2}{2\pi}\, n_{\omega_2-\omega}(1 - n_{\omega_2}) + \int_{-\infty}^{\infty} \frac{d\omega_2}{2\pi} n_{\omega_2+\omega}(1 - n_{\omega_2}). \tag{C.6}$$

At zero temperature, the integrands are given by

$$n_{\omega_2\mp\omega}(1 - n_{\omega_2}) = \begin{cases} 1 & \text{for } \pm\omega > 0 \text{ and } \omega_0 \le \omega_2 \le \omega_0 \pm \omega \\ 0 & \text{otherwise.} \end{cases} \tag{C.7}$$

Performing the integral, we obtain the desired result:

$$S(\omega; x_-, x_-)(\omega) = \frac{1}{2\pi}|\omega|. \tag{C.8}$$

Next, we will calculate the noise in the outgoing current, which is given by

$$S(\omega; x_+, x_+) = \int_{-\infty}^{\infty} dt \left(e^{i\omega t} + e^{-i\omega t}\right) \langle \rho_-(t, x_+)\rho_-(0, x_+)\rangle, \tag{C.9}$$

where $x_+ > 0$. This time we must evaluate the expectation value

$$\langle \rho_-(t, x_+)\rho_-(0, x_+)\rangle = \langle \psi^\dagger(t, x_+)\psi(t, x_+)\psi^\dagger(0, x_+)\psi(0, x_+)\rangle, \tag{C.10}$$

According to equations (4.19) and (4.20), this is equal to

$$\langle \rho_-(t, x_+)\rho_-(0, x_+)\rangle = \sum_{\omega_1,\omega_2,\omega_3,\omega_4} e^{-i(\omega_1+\omega_2)t} \langle \Phi | B^\dagger_{-\omega_1} B_{\omega_2} B^\dagger_{-\omega_3} B_{\omega_4} | \Phi\rangle e^{i(\omega_1+\omega_2+\omega_3+\omega_4)x_+}. \tag{C.11}$$

Because the scattering states are defined in terms of the operator A_ω, we will use

equation (4.21) to rewrite all the B's in terms of the A's, with the result

$$\langle B^\dagger_{-\omega_1} B_{\omega_2} B^\dagger_{-\omega_3} B_{\omega_4} \rangle = s_o + s_t. \tag{C.12}$$

In this equation, s_o describes events where at both time 0 and at time t one particle is destroyed and another is created. The second term, s_t, describes events where at one time two particles are created, and at the other time two are destroyed. All the other terms in the correlation function of the four B's will vanish. s_o and s_t are given by

$$\begin{aligned} s_o = \frac{1}{16} \Big[& \; c_{\omega_1} c_{\omega_2} c_{\omega_3} c_{\omega_4} \langle A^\dagger_{-\omega_1} A_{\omega_2} A^\dagger_{-\omega_3} A_{\omega_4} \rangle \\ & + \; c_{\omega_1} c_{\omega_2} d_{\omega_3} d_{\omega_4} \langle A^\dagger_{-\omega_1} A_{\omega_2} A_{\omega_3} A^\dagger_{-\omega_4} \rangle \\ & + \; d_{\omega_1} d_{\omega_2} c_{\omega_3} c_{\omega_4} \langle A_{\omega_1} A^\dagger_{-\omega_2} A^\dagger_{-\omega_3} A_{\omega_4} \rangle \\ & + \; d_{\omega_1} d_{\omega_2} d_{\omega_3} d_{\omega_4} \langle A_{\omega_1} A^\dagger_{-\omega_2} A_{\omega_3} A^\dagger_{-\omega_4} \rangle \Big], \end{aligned} \tag{C.13}$$

and

$$\begin{aligned} s_t = \frac{1}{16} \Big[& \; d_{\omega_1} c_{\omega_2} c_{\omega_3} d_{\omega_4} \langle A_{\omega_1} A_{\omega_2} A^\dagger_{-\omega_3} A^\dagger_{-\omega_4} \rangle \\ & + \; c_{\omega_1} d_{\omega_2} d_{\omega_3} c_{\omega_4} \langle A^\dagger_{-\omega_1} A^\dagger_{-\omega_2} A_{\omega_3} A_{\omega_4} \rangle \Big]. \end{aligned} \tag{C.14}$$

In these equations, c_ω and d_ω are given by

$$c_\omega = 1 + e^{i\phi(\omega)} \qquad \text{and} \qquad d_\omega = 1 - e^{i\phi(\omega)}, \tag{C.15}$$

with $\phi(\omega)$ defined in Eq. (4.22). The correlations of the four A's can be evaluated using Eqs. (4.23) and (4.27). If we interchange ω_1 with ω_2 in the second two lines of s_o, and perform the sums over ω_3 and ω_4, we obtain

$$\begin{aligned} \sum_{\omega_3,\omega_4} s_o \, e^{i(\omega_1+\omega_2+\omega_3+\omega_4)x_+} = \frac{1}{16} \Big[& \; c_{\omega_1} c_{\omega_2} c_{-\omega_1} c_{-\omega_2} - c_{\omega_1} c_{\omega_2} d_{-\omega_1} d_{-\omega_2} \\ & - \; d_{\omega_1} d_{\omega_2} c_{-\omega_1} c_{-\omega_2} + d_{\omega_1} d_{\omega_2} d_{-\omega_1} d_{-\omega_2} \Big] \end{aligned}$$

$$\times \quad n_{-\omega_1}(1-n_{\omega_2}). \tag{C.16}$$

In this equation, the expression containing the number operators is the same as for the noise in the incoming current, so we will obtain the same limits of integration as in equation (C.7). Next, we can expand out the c_ω's and d_ω's in terms of ω and substitute this back into equation (4.31) for the noise. After performing the integrals over t and ω_1, we find that the contribution to the noise due to s_o has the form

$$S_o(\omega; x_+, x_+) = \int_{\omega_0}^{\omega_0 \pm \omega} \frac{d\omega_2}{2\pi} \frac{\left((4\pi|\Gamma|^2)^2 - \omega_2(\omega_2 \mp \omega_1)\right)^2}{\left((\omega_2 \mp \omega)^2 + (4\pi|\Gamma|^2)^2\right)\left(\omega_2^2 + (4\pi|\Gamma|^2)^2\right)} \theta(\pm\omega), \tag{C.17}$$

where we sum over the two different signs in front of ω. Upon performing the ω_2 integral, we obtain

$$\begin{aligned} S_o(\omega; x_+, x_+) = \frac{|\omega|}{2\pi} \quad &- \quad 2|\Gamma|^2 \left[\tan^{-1}\left(\frac{|\omega| - \omega_0}{4\pi|\Gamma|^2}\right) + \tan^{-1}\left(\frac{|\omega| + \omega_0}{4\pi|\Gamma|^2}\right)\right] \\ &- \quad 8\pi\frac{|\Gamma|^4}{|\omega|}\Big[2\ln\left(\omega_0^2 + (4\pi|\Gamma|^2)^2\right) - \ln\left((\omega+\omega_0)^2 + (4\pi|\Gamma|^2)^2\right) \\ &\qquad - \ln\left((\omega-\omega_0)^2 + (4\pi|\Gamma|^2)^2\right)\Big]. \end{aligned} \tag{C.18}$$

Next, we will calculate the contribution to the noise due to s_t. The two expectation values we must evaluate are $\langle A_{\omega_1} A_{\omega_2} A^\dagger_{-\omega_3} A^\dagger_{-\omega_4}\rangle$ and $\langle A^\dagger_{-\omega_1} A^\dagger_{-\omega_2} A_{\omega_3} A_{\omega_4}\rangle$. In both cases, either ω_1 is paired with ω_3 and ω_2 is paired with ω_4, or ω_1 is paired with ω_4 and ω_2 with ω_3. Thus we have

$$\langle A_{\omega_1} A_{\omega_2} A^\dagger_{-\omega_3} A^\dagger_{-\omega_4}\rangle = (1-n_{\omega_1})(1-n_{\omega_2})(\delta_{\omega_1,-\omega_4}\delta_{\omega_2,-\omega_3} - \delta_{\omega_1,-\omega_3}\delta_{\omega_2,-\omega_4}), \tag{C.19}$$

and

$$\langle A^\dagger_{-\omega_1} A^\dagger_{-\omega_2} A_{\omega_3} A_{\omega_4}\rangle = n_{-\omega_1} n_{-\omega_2}(\delta_{-\omega_1,\omega_4}\delta_{-\omega_2,\omega_3} - \delta_{-\omega_1,\omega_3}\delta_{-\omega_2,\omega_4}). \tag{C.20}$$

Substituting these expressions into the equation for s_t and performing the integrals

over ω_3 and ω_4, we obtain

$$\sum_{\omega_3,\omega_4} s_t\, e^{i(\omega_1+\omega_2+\omega_3+\omega_4)x_+} = \frac{1}{16} \quad [d_{\omega_1} d_{-\omega_1} c_{\omega_2} c_{-\omega_2} - d_{\omega_1} c_{-\omega_1} c_{\omega_2} d_{-\omega_2}] \times [(1-n_{\omega_1})(1-n_{\omega_2}) + n_{-\omega_1} n_{-\omega_2}]. \quad \text{(C.21)}$$

When we expand the c's and d's in terms of ω and perform the integral over t, we find that the contribution to the noise due to s_t is given by

$$S_t(\omega; x_+, x_+) = \int \frac{d\omega_1}{2\pi}\frac{d\omega_2}{2\pi} \frac{(4\pi|\Gamma|^2)^2(\omega_2^2 - \omega_1\omega_2)}{(\omega_1^2 + (4\pi|\Gamma|^2)^2)(\omega_2^2 + (4\pi|\Gamma|^2)^2)} \times \delta(\omega_1 + \omega_2 \pm \omega)\left[(1-n_{\omega_1})(1-n_{\omega_2}) + n_{-\omega_1} n_{-\omega_2}\right], \quad \text{(C.22)}$$

where again it is understood that we sum the two integrands with the different sign in front of ω. After the integration over ω_1 is performed, the expression in square brackets becomes

$$(1-n_{-\omega_2\mp\omega})(1-n_{\omega_2}) + n_{\omega_2\pm\omega} n_{-\omega_2} = \begin{cases} 1 & \omega_0 < \omega_2 < \mp\omega - \omega_0 \text{ and } \mp\omega - 2\omega_0 > 0 \\ 1 & -\omega_0 < \omega_2 < \mp\omega + \omega_0 \text{ and } \mp\omega + 2\omega_0 > 0 \\ 0 & \text{otherwise.} \end{cases} \quad \text{(C.23)}$$

We note that this time the limits of integration determined by the factors of n impose cutoffs at $\omega = \pm 2\omega_0$. These are the origins of the singularities at $\omega = 2\omega_0$, which, as we shall see shortly, persist for all $|\Gamma| \neq 0$. After equation (C.23) is substituted into the equation for $S_t(\omega; x_+, x_+)$, the noise becomes

$$S_t(\omega; x_+, x_+) = \sum_{a,b=\pm 1} \theta(a\omega + b2\omega_0) \int_{-b\omega_0}^{b\omega_0 - a\omega} \frac{d\omega_2}{2\pi} \frac{(4\pi|\Gamma|^2)^2\,(\omega_2^2 + \omega_2(\omega_2 + a\omega))}{((\omega_2 + a\omega)^2 + (4\pi|\Gamma|^2)^2)\,(\omega_2^2 + (4\pi|\Gamma|^2)^2)}. \quad \text{(C.24)}$$

The integration over ω_2 yields

$$S_t(\omega; x_+, x_+) = \sum_{a,b=\pm 1} \theta(a\omega + b2\omega_0)\left\{2|\Gamma|^2\left[\tan^{-1}\left(\frac{b\omega_0}{4\pi|\Gamma|^2}\right) + \tan^{-1}\left(\frac{a\omega + b\omega_0}{4\pi|\Gamma|^2}\right)\right] + \frac{8\pi|\Gamma|^4}{a\omega}\left[\ln\left((4\pi|\Gamma|^2)^2 + \omega_0^2\right) - \ln\left((4\pi|\Gamma|^2)^2 + (a\omega + b\omega_0)^2\right)\right]\right\}. \quad \text{(C.25)}$$

We note that this contribution to the noise has the step function which provides a "sharp" singularity at $|\omega| = |2\omega_0|$, for any non-zero value of $|\Gamma|$. This is the electron singularity. However, for $|\Gamma| \to 0$, the arctangents provide a singularity at $|\omega| = |\omega_0|$, which is the quasiparticle singularity.

When we add the two contributions to the noise together, we find that the noise on the outgoing side of the impurity is

$$S(\omega; x_+, x_+) = \frac{|\omega|}{2\pi} + \theta(2|\omega_0| - |\omega|)\Bigg\{4|\Gamma|^2\left[\tan^{-1}\left(\frac{|\omega_0|}{4\pi|\Gamma|^2}\right) + \tan^{-1}\left(\frac{|\omega_0| - |\omega|}{4\pi|\Gamma|^2}\right)\right] + 16\pi\frac{|\Gamma|^4}{|\omega|}\left[\ln\left((4\pi|\Gamma|^2)^2 + (|\omega| - |\omega_0|)^2\right) - \ln\left((4\pi|\Gamma|^2)^2 + \omega_0^2\right)\right]\Bigg\}. \quad \text{(C.26)}$$

Finally, the noise between the currents on either side of the impurity can be calculated similarly, so we will omit the details here.

Bibliography

[1] F. D. M. Haldane, J. Phys. C. **14**, 2585 (1981); Phys. Rev. Lett. **47**, 1840 (1981).

[2] J. M. Luttinger, J. Math. Phys. **4** 609 (1963).

[3] D. C. Mattis and E. H. Lieb, J. Math. Phys. **6** 304 (1965).

[4] Xiao-Gang Wen, Phys. Rev. B **43**, 11025 (1991).

[5] X. G. Wen, Phys. Rev. B **41**, 12838 (1990).

[6] X. G. Wen, Mod. Phys. Lett. B **5**, 39 (1991).

[7] D. H. Lee and X. G. Wen, Phys. Rev. Lett. **66**, 1765 (1991).

[8] X. G. Wen, Phys. Rev. Lett. **66**, 802 (1991).

[9] Xiao-Gang Wen, Intl. J. of Mod. Phys. B **6**, 1711 (1992).

[10] For a review, see D. V. Averin and K. K. Likharev, in *Mesoscopic Phenomena in Solids*, edited by B. L. Altshuler, P. A. Lee, and R. A. Webb (Elsevier, Amsterdam, 1990).

[11] Tai Kai Ng and Patrick A. Lee, Phys. Rev. Lett. **61**, 1768 (1988).

[12] Y. Meir, N. S. Wingreen, and P. A. Lee, Phys. Rev. Lett. **66**, 3048 (1991).

[13] X. G. Wen, Phys. Rev. B **44**, 5708 (1991).

[14] C. L. Kane and Matthew P. A. Fisher, Phys. Rev. Lett. **68**, 1220 (1992); Phys. Rev. B **46**, 15233 (1992); Phys. Rev. Lett. **72**, 724 (1994).

[15] Akira Furusaki and Naoto Nagaosa, Phys. Rev. B **47**, 3827 (1993); Phys. Rev. B **47**, 3827 (1993).

[16] C. de C. Chamon and X. G. Wen, Phys. Rev. Lett. **70**, 2605 (1993).

[17] R. Shankar, J. Mod. Phys. B **4**, 2371 (1990).

[18] F. P. Milliken, C. P. Umbach and R. A. Webb, Solid State Comm. **97**, 309 (1995).

[19] K. Moon, H. Yi, C. L. Kane, S. M. Girvin, and Matthew P. A. Fisher, Phys. Rev. Lett. **71**, 4381 (1993).

[20] F. Guinea, G. Gomez-Santos, M. Sassetti, and U. Ueda, cond-mat/9411130.

[21] C. H. Mak, Reinhold Egger, Maura Sassetti, and Ulrich Weiss, preprint.

[22] R. Egger, M. Sassetti and U. Weiss, cond-mat/9504040.

[23] P. Fendley, A. W. W. Ludwig, and H. Saleur, Phys. Rev. Lett. **74**, 3005 (1995).

[24] P. Fendley, A. W. W. Ludwig, and H. Saleur, cond-mat/9503172.

[25] A. Schmid, Phys. Rev. Lett. **51** (1983) 1506; M. P. A. Fisher and W. Zwerger, Phys. Rev. B **32** (1985) 6190; C. G. Callan and D. E. Freed, Nucl. Phys. B **374** (1992), 543.

[26] J. B. Johnson, Phys. Rev. **29**, 367 (1927).

[27] H. Nyquist, Phys. Rev. **32**, 110 (1928).

[28] G. B. Lesovik, JETP Lett. **49**, 594 (1989).

[29] M. Buttiker, Phys. Rev. Lett. **65**, 2901 (1990); Phys. Rev. B **46**, 12485 (1992) and references therein.

[30] G. B. Lesovik and L. S. Levitov, Phys. Rev. Lett. **72**, 538 (1994); JETP Lett. **58**, 231 (1993).

[31] S.-R. Eric Yang, Solid State Comm. **81**, 375 (1992).

[32] L. V. Keldysh, Soviet Phys. JETP **20**, 1018 (1965).

[33] Sudip Chakravarty and Anthony J. Leggett, Phys. Rev. Lett. **52**, 5 (1984).

[34] Matthew P. A. Fisher and Wilhelm Zwerger, Phys. Rev. B **32**, 6190 (1985).

[35] Rolf Landauer, Physica D **38**, 226 (1989).

[36] Denise. E. Freed, Nucl. Phys. B **409**, 565 (1993).

[37] T. Muir, *A treatise on the Theory of Determinants*, Longmens, Green and Co, New York, 1933.

[38] C. L. Kane and Matthew P. A. Fisher, Phys. Rev. Lett. **72**, 724 (1994).

[39] C. de C. Chamon, D. E. Freed, and X. G. Wen, Phys. Rev. B **51**, 2363 (1995).

[40] P. Fendley, A. W. W. Ludwig, and H. Saleur, cond-mat/9505031.

[41] C. de C. Chamon, D. E. Freed, and X. G. Wen, Phys. Rev. B **53**, 4033 (1996).

[42] F. Guinea, Phys. Rev. B **32**, 7518 (1985).

[43] Maura Sassetti, Manfried Milch, and Ulrich Weiss, Phys. Rev. A **46**, 4615 (1992).

[44] K. A. Matveev, Phys. Rev. B **51**, 1743 (1995); A. Furusaki and K. A. Matveev, cond-mat/9505035.

[45] R. Floreanini and R. Jackiw, Phys. Rev. Lett. **59**, 1873 (1987).

[46] M. B. Green, J. H. Schwartz and E. Witten, *Superstring theory*, volume I, Cambridge University Press, Cambridge, 1988.

[47] D. E. Freed, C. de C. Chamon, S. Sondhi, and X. G. Wen, in preparation

[48] Claudio Chamon and Xiao-Gang Wen, in preparation